UNIVERSITY OF WEST BOHEMIA
FACULTY OF MECHANICAL ENGINEERING

Study Program: N2301 Mechanical Engineering
Field of Study: Design of Power Machines and Equipment

MASTER THESIS

A study of reciprocating compressor valve dynamics

Author: **Bc. Michal VOLF**
Supervisor: **Doc. Ing. Petr ERET, Ph.D.**

Academic year 2016/2017

ZÁPADOČESKÁ UNIVERZITA V PLZNI
Fakulta strojní
Akademický rok: **2016/2017**

ZADÁNÍ DIPLOMOVÉ PRÁCE

(PROJEKTU, UMĚLECKÉHO DÍLA, UMĚLECKÉHO VÝKONU)

Jméno a příjmení: **Bc. Michal VOLF**
Osobní číslo: **S15N0067P**
Studijní program: **N2301 Strojní inženýrství**
Studijní obor: **Stavba energetických strojů a zařízení**
Název tématu: **A study of reciprocating compressor valve dynamics**
Zadávající katedra: **Katedra energetických strojů a zařízení**

Zásady pro vypracování:

Tasks:

- To justify the necessity of understanding valve dynamics (see References).
- To present a dynamic model of reciprocating compressor valve including the fluid-structure interaction (see References).
- To simulate a valve motion based on specified system parameters.
- To perform a parametric study of valve dynamics for modified design parameters.

Skills required:

1. Single degree of freedom system dynamics.
2. Basics of Matlab software - equations of motion simulation.
3. Upper intermediate English (B2) - literature study.

Rozsah grafických prací:	**dle potřeby**
Rozsah kvalifikační práce:	**50 - 70 stran**
Forma zpracování diplomové práce:	**tištěná/elektronická**
Jazyk zpracování diplomové práce:	**Angličtina**

Seznam odborné literatury:

- **Habing R. A., Peters M. C. A. M, 2006: An Experimental Method for Validating Compressor Valve Vibration Theory, Journal of Fluids and Structures 22, 683 - 697**
- **Habing R. A., 2005: Flow and Plate Motion in Compressor Valves, Ph.D. Thesis, University of Twente, Enschede, The Netherlands**
- **Touber S., 1976: A Contribution to the Improvement of Compressor Valve Design. Ph.D. Thesis, Delft Univesity, The Netherlands**

Vedoucí diplomové práce:	**Doc. Ing. Petr Eret, Ph.D.** Katedra energetických strojů a zařízení
Konzultant diplomové práce:	**Doc. Ing. Petr Eret, Ph.D.** Katedra energetických strojů a zařízení

Datum zadání diplomové práce:	**17. října 2016**
Termín odevzdání diplomové práce:	**2. června 2017**

Doc. Ing. Milan Edl, Ph.D.
děkan

Západočeská univerzita v Plzni
Fakulta strojní
L.S.

Dr. Ing. Jaroslav Synáč
vedoucí katedry

V Plzni dne 3. října 2016

Declaration

I hereby declare that this master thesis is entirely my own work and that I only used the cited sources.

Pilsen, June 2, 2017

_____

Acknowledgement

I would like to express my very profound gratitude to my supervisor, Petr Eret for the useful comments, remarks and engagement from the beginning to the very end of my master thesis. I truly appreciate his helpful advice and generous help.

Furthermore, my deepest and sincere gratitude goes to my family for their unflagging and unparalleled love, help and support throughout my life and my studies.

Finally, I would like to thank Richard Pisinger for correcting the English language of this thesis.

ANOTAČNÍ LIST DIPLOMOVÉ PRÁCE

AUTOR	**Příjmení** Bc. Volf	**Jméno** Michal	
STUDIJNÍ OBOR	N2301 Strojní inženýrství		
VEDOUCÍ PRÁCE	**Příjmení** Doc. Ing. Eret, Ph.D.	**Jméno** Petr	
PRACOVIŠTĚ	ZČU – FST – KKE		
DRUH PRÁCE	**DIPLOMOVÁ**	~~**BAKALÁŘSKÁ**~~	**Nehodící se škrtněte**
NÁZEV PRÁCE	Studie dynamiky ventilu u pístového kompresoru		

FAKULTA	strojní		**KATEDRA**	KKE		**ROK ODEVZDÁNÍ**	2017

POČET STRAN (A4 a ekvivalentů A4)

CELKEM	103		**TEXTOVÁ ČÁST**	82		**GRAFICKÁ ČÁST**	0

STRUČNÝ POPIS	Diplomová práce se zaměřuje na jednodimenzionální studium dynamického chování ventilu pístového kompresoru. Za tímto účelem byl vytvořen program, pomocí nějž jsou kvalitativně hodnoceny jednotlivé projevy dynamického chování a jejich vzájemný vliv. Matematický model, jenž je v tomto programu implementován, je v práci rovněž detailně popsán.
KLÍČOVÁ SLOVA	pístový kompresor, dynamika ventilu, interakce těleso-tekutina, proudění vzduchu, jednodimenzionální model

SUMMARY OF DIPLOMA SHEET

AUTHOR	**Surname** Bc. Volf	**Name** Michal	
FIELD OF STUDY	N2301 Mechanical Engineering		
SUPERVISOR	**Surname** Doc. Ing. Eret, Ph.D.	**Name** Petr	
INSTITUTION	ZČU - FST - KKE		
TYPE OF WORK	**DIPLOMA**	~~**BACHELOR**~~	**Delete when not applicable**
TITLE OF THE WORK	A study of reciprocating compressor valve dynamics		

FACULTY	Mechanical Engineering		**DEPARTMENT**	KKE		**SUBMITTED IN**	2017

NUMBER OF PAGES (A4 and eq. A4)

TOTALLY	103		**TEXT PART**	82		**GRAPHICAL PART**	0

BRIEF DESCRIPTION	This master thesis is focused on one-dimensional study of reciprocating compressor valve dynamics. For this purpose, a tool was developed, which is used to qualitatively evaluate the individual aspects of valve dynamics as well as their interaction. A mathematical model, which is implemented in the tool, is described in detail in this thesis.
KEY WORDS	reciprocating compressor, valve dynamics, flow-structure interaction, gas flow, one-dimensional model

Table of Contents

Table of Figures

Table of Tables

List of Abbreviations

Acronym	Definition
BDC	bottom dead center
CFD	computational fluid dynamics
CV	control volume
LES	large eddy simulation
ODE	ordinary differential equation
OOP	object-oriented programming
TDC	top dead center

List of Frequently Used Symbols

Symbol	Unit	Property
α	$[-]$	flow coefficient
β	$[°]$	meniscus contact angle
γ_{LG}	$[Nm^{-1}]$	surface tension
ϵ	$[-]$	expansion coefficient
Θ_{cd}	$[kg\ s^{-1}]$	mass flow in discharge valve
Θ_{cs}	$[kg\ s^{-1}]$	mass flow in suction valve
Θ_{d}	$[kg\ s^{-1}]$	mass flow in discharge pipe
Θ_{s}	$[kg\ s^{-1}]$	mass flow in suction pipe
κ	$[-]$	heat capacity ratio (Poisson constant)
ξ	$[-]$	loss coefficient in pipe
ρ_c	$[kg\ m^{-3}]$	density of gas inside cylinder
ρ_d	$[kg\ m^{-3}]$	density of gas inside discharge chamber
ρ_s	$[kg\ m^{-3}]$	density of gas inside suction chamber
ϕ	$[°]$	crank angle
ω	$[rad\ s^{-1}]$	angular velocity of crankshaft
A_c	$[m^2]$	cross-sectional area of cylinder
A_o	$[m^2]$	flow area
A_p	$[m^2]$	valve port cross-sectional area
A_v	$[m^2]$	valve plate area
c_f	$[Nsm^{-1}]$	friction coefficient
c_p	$[Jkg^{-1}K^{-1}]$	heat capacity at constant pressure
c_r	$[-]$	coefficient of restitution
c_v	$[Jkg^{-1}K^{-1}]$	heat capacity at constant volume
D_c	$[m]$	cylinder diameter
D_p	$[m]$	valve port diameter
D_v	$[m]$	valve plate diameter
E_{CV}	$[J]$	energy of fluid inside control volume
F_{adh}	$[N]$	adhesion force
F_f	$[N]$	fluid friction force
F_g	$[N]$	gas force

F_s	$[N]$	spring force
h	$[m]$	maximum valve plate lift
h_{film}	$[m]$	oil film thickness
k	$[Nm^{-1}]$	spring stiffness
L	$[m]$	connecting rod length
m	$[kg]$	mass of valve plate with equivalent mass of spring
m_c	$[kg]$	mass of gas inside cylinder
m_{plate}	$[kg]$	valve plate mass
m_{spring}	$[kg]$	spring mass
p_c	$[Pa]$	pressure in cylinder
p_d	$[Pa]$	pressure in discharge chamber
p_s	$[Pa]$	pressure in suction chamber
$\dot{Q}$	$[W]$	rate of total heat transfer
r	$[Jkg^{-1}K^{-1}]$	specific ideal gas constant
R	$[m]$	radius of crankshaft
Re	$[-]$	Reynolds number
t	$[s]$	time
T_c	$[K]$	temperature of gas in cylinder
T_d	$[K]$	temperature of gas in discharge chamber
T_s	$[K]$	temperature of gas in suction chamber
u	$[Jkg^{-1}]$	specific internal energy
v_c	$[m^3kg^{-1}]$	specific volume of gas inside cylinder
v_d	$[m^3kg^{-1}]$	specific volume of gas inside discharge chamber
v_s	$[m^3kg^{-1}]$	specific volume of gas inside suction chamber
W	$[J]$	work
w_z	$[ms^{-1}]$	piston velocity
x	$[m]$	valve plate lift
x_0	$[m]$	spring preload deflection
z	$[m]$	piston displacement
z_0	$[m]$	smallest distance between cylinder and piston (derived from clearance volume)

Introduction

Reciprocating compressors are among the most used types of compressors. They can be found in highly diverse fields of application, such as in the oil and gas industry or chemical industry, where these compressors are used mainly for their ability to deliver high-pressure gas. Basically, piston compressors are vital part in any process they are employed in; therefore their reliability has garnered widespread interest.

As the limiting elements in the design of the reciprocating compressor, the compressor valves can be considered. They are often described as the heart of the compressor, due to the fact that should they fail, it would lead to the shutdown of the compressor and to costly downtimes. A compressor running at even moderate speeds such as 700 rpm requires for each valve to open and close over one million times a day. It follows that valve design must bear in mind that it needs to be highly reliable and operate efficiently even in adverse conditions, such as in applications where there are liquids and debris in the gas stream.

The fundamental challenge in the design of a compressor valve lies in the opening and closing phase of the valve, where an effort is made to allow for the most desirable dynamic behavior as possible. For instance, lowering the pressure loss across the valve by increasing the flow area leads to a higher possibility of unsuitable dynamic behavior and thus decreases its lifetime.

This thesis is devoted to a theoretical study of reciprocating compressor valve dynamics. For this purpose, a tool for the prediction of valve plate motion is developed. The main reason in developing this tool is to qualitatively assess the factors influencing the dynamic behavior. To validate the precision of this tool, the results are compared to freely accessible experimental data found in literature. However, the main goal of this study is not aimed at a quantitative estimation, since an experiment would be inevitable for the precise evaluation of the theoretical results.

This thesis consists of five parts. The first part deals with the motivation and the purpose of this research, whereas the second part is meant to provide the general overview of compressor valves used today. The third part describes the physical model of the reciprocating compressor and its valves. Based on this, simplifications are introduced and a mathematical model is proposed. The fourth part is concerned with the implementation of the mathematical model in the proprietary software MATLAB. In the fifth part, the results of the developed tool are discussed. The analysis of the influence of the valve parameters on its dynamic behavior is also present in this chapter.

1 Research Outline

1.1 Motivation of Research

A reciprocating or piston compressor (Figure 1) is a compressor that is piston-driven by a crankshaft in order to deliver high-pressure gas. The compressor captures a volume of gas from a suction port and transfers it into a cylinder, where it is trapped and compressed by a piston that reduces its volume. Thereafter, the compressed gas is discharged through the exhaust port into the discharge pipe. The flow of the gas through the cylinder is controlled by valves.

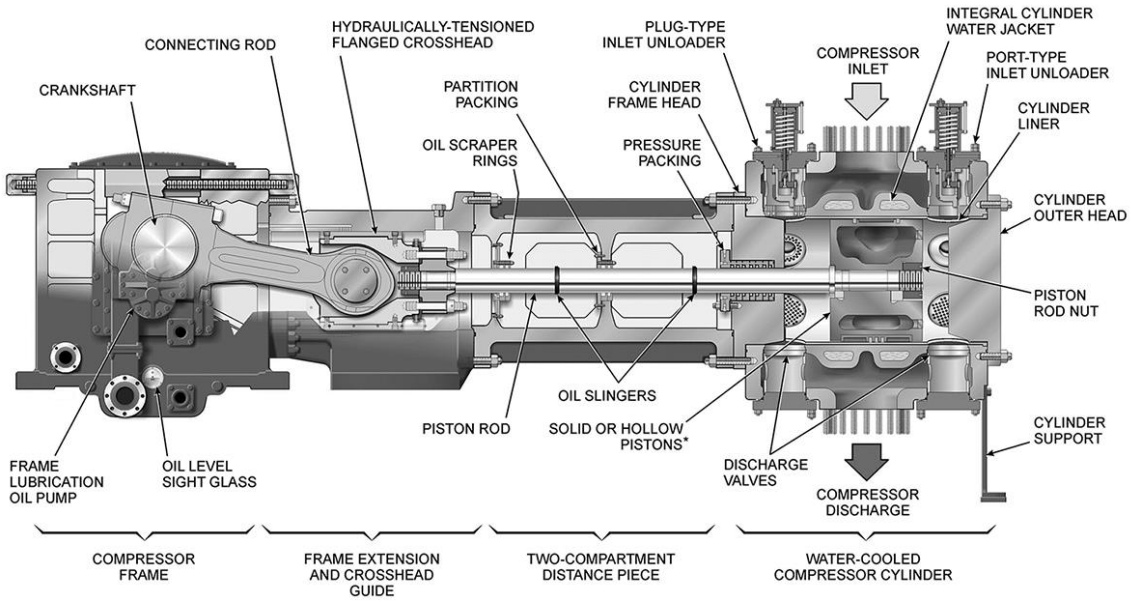

Figure 1 Sketch of a single-acting reciprocating compressor [41]

Piston compressors are widely employed in several industry and transportation branches as well as for domestic purposes. Even though they are not able to deliver the compressed gas continuously, which can be considered as one of their main drawbacks, since it leads to pressure pulsations in the suction and discharge pipes, their main advantage is the ability to achieve high pressure ratios (up to 2 500 [1]) and can therefore deliver gases at very high pressures. According to Ninković [2], an example of such an application involves compressing ethylene to pressures over 300 MPa to produce LDPE (low-density-polyethylene). Other typical applications include the compression of gases contaminated with particles, or gases with very low suction temperatures (down to -150 °C) in the field of liquefied gas transport and storage.

From the above, it can be freely stated that some of the applications would hardly be possible without this type of compressor. We can consider the compressor to be the heart of an installation, as its reliability determines the safety and availability of the entire plant. Despite there being a requirement of trouble-free operations for several years of operation,

compressors are very complex machines, a consequence of which is that unscheduled costly shutdowns can happen. An industrial investigation to identify and evaluate the factors of these shutdowns was conducted by the company Dresser-Rand [3]. The summary of these results is shown in Figure 2.

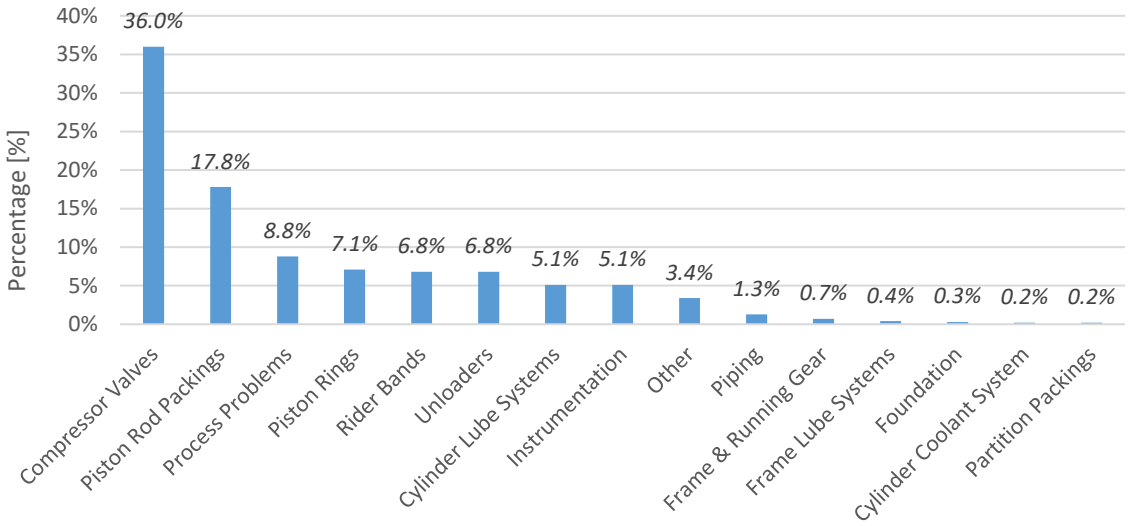

Figure 2 Causes of unscheduled compressor shutdowns [3]

Even though the investigation only shows the reliability of an operating piston compressor and does not take into account a human error, the results clearly identify compressor valves as the main cause of unscheduled shutdowns, with a relative rate of 36%. As Ninković [2] points out, in view of the fact that the second-major cause of compressor failure, the piston rod packing, is only present in compound and crosshead machines, one may surmise that valves are responsible for an even larger percentage of failure in small compressors. This underscores the idea outlined in the introduction that valves really are the heart of the compressor and proper care in their design is not only desired, but it is decidedly obligatory.

Dresser-Rand [3] states that among the most common causes of valve failures are high impact velocities, wear, corrosion, and application conditions. Below, we will proceed to outline how valve dynamics is involved in these causes of failure.

The moving element of the valve is limited in its motion by a seat and a guard. Every time the valve opens or closes, the moving element strikes the seat or guard. A rebound may occur if the velocity at the moment of impact is sufficiently high. This behavior is undesirable, for it leads to a higher dynamic stress of valve parts, resulting in chipping and cracks on the outer edge of the moving element as well as on the seat and guard (an example is given in Figure 3).

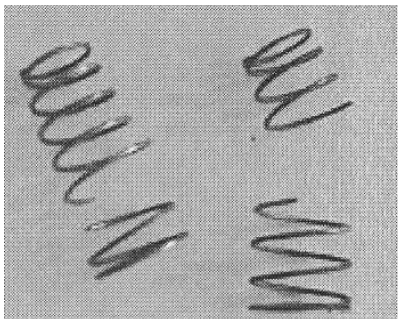

Figure 4 Spring failure due to abrasive wear [5]

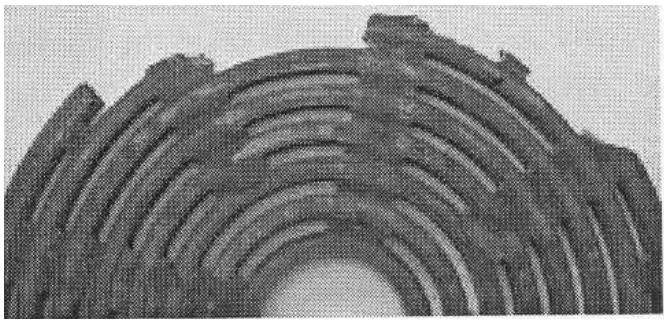

Figure 3 Impact failure of valve plate caused by stiction [5]

Figure 5 Valve ring subject to heavy wear due to the deposition of coke particles at the valve seats [42]

Since moving parts of the valve impact and slide against one another, a certain amount of wear is inevitable (examples are given in Figure 4 and Figure 5). Nevertheless, the wear rate does not solely depend on proper maintenance e.g. lubrication, but it also depends on the dynamic behavior of the valves. Moreover, there are pressure pulsations in the suction and discharge chambers as well as the flutter of the moving element, which can increase the wear rate and therefore decrease the time until failure.

If the corrosive elements are present in the compressed gas, they might bring about the corrosion of the valve parts. This is especially dangerous to the springs as they can fail prematurely due to the corrosion-related fatigue. However, if the gas composition is known during the design process, suitable corrosive resistant materials can be chosen and therefore the effects of the corrosion can be limited.

The application conditions refer mostly to the quality of the compressed gas. The presence of dirt or debris will accelerate wear, can limit opening and closing of the valve, and in extreme conditions, the valves can become blocked.

In view of the foregoing, it is obvious that rebound, stiction and other effects of valve dynamics play a vital role in the manner of their failure that can lead to the costly downtime of the entire plant. The study and deeper understanding of valve dynamics is necessary so as to further improve the design of the valve and thus the reliability of the compressor.

It should be also emphasized that the economic effect of valve design improvement can be very significant. According to Howes [4], a comparison of two valves with different valve lifts shows that for the lower lift version, the revenue[1] is higher, while operations and maintenance costs are slightly lower. Under the given circumstances of the calculation, he concluded that by optimizing the valve, the net profit could be increased by over half a million dollars per year.

1.2 Survey of Literature

Despite the long history of piston compressors dating back to 1777, when James Watt constructed a steam-driven air compressor, valve design was hardly mentioned in literature until the very beginning of the 20th century. However, the first attempts to describe valve behavior were purely empirical, even though experimental methods for recording the valve behavior, e.g. measuring its lift as a function of time, hardly existed. The evolution of the design methods for compressor valves was traced in detail by Habing [5]. An illustrative expression of this evolution, delineating the main milestones, is presented on a timeline in Figure 6.

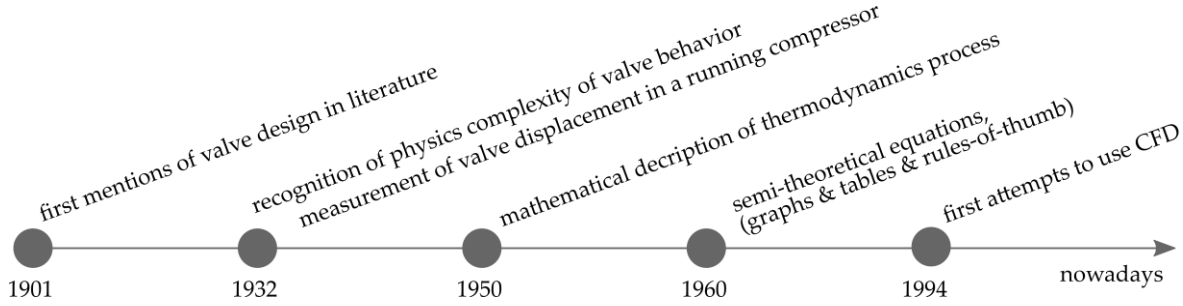

Figure 6 Timeline of evolution of valve design methods

The very first attempt to shift from purely empirical methods to the characterization of valve behavior based on theoretical assumptions can be found in a book from 1901 written by Stetefeld [6]. Nonetheless, the proposed model here was very simple since it was solely based on Newton's second law and Bernoulli's equation for incompressible fluid only. In 1932, Hirsh [7] published a book, in which he recognized the complexity of the physical situation regarding valve behavior, which is influenced by a variety of factors. Later in the same year, Lanzendörfer [8] recorded valve displacement in a running compressor by adapting the mechanical (pressure) indicator. This breakthrough in experimental measuring allowed engineers to start focusing on developing semi-theoretical models containing empirical coefficients (however, this method was formerly a privilege of a few investigators at first; the broadening of the semi-theoretical approach reaches back to 1960), instead of making purely theoretical models for predicting valve dynamics. It was not until 1950, when the first clear study encompassing a full mathematical explanation of gas flow

[1] $revenue\ (\$/yr.) = P * Q * (365 - t * f)$, *where* P *means gas selling price,* Q *denotes the capacity,* t *stands for the number of days lost due to the valve change and* f *means the frequency of repairs per year*

through the valves and of the thermodynamic process in a compressor cylinder appeared in a book by Costagliola [9]. Since 1994, computational fluid dynamics (CFD) has been used as a valuable tool for the analysis of compressor valves.

Our research of the recent literature on valve design shows that there is a rapidly growing number of literature these days, but mainly in the form of conference proceedings, namely from:

- International Compressor Engineering Conference at Purdue University
- International Conference on Compressors and their Systems of IMechE and City University in London
- European Forum for Reciprocating compressors

Somewhat surprising is the fact that, despite the compressor manufacturers' financial sponsorship of these conferences, much of the proceedings come from scientific researchers in universities. Furthermore, in view of the fact that only a few of these proceedings clearly state that the research was made in cooperation with a compressor manufacturer, one can conclude that compressor manufacturers likely follow the public progress in valve design, while keeping their own research results as valuable know-how. We mention this so as to emphasize the difficulty of comparing theoretical research results with commercial valves unless an experiment is carried out.

Regarding the specialization of conference proceedings, in most cases they analyze in great detail just one phenomenon, such as a report by Pereira [10] discussing the numerical analysis of heat transfer inside the cylinder of a reciprocating compressor, or a report by Lin [11] discussing the effective flow area of a compressor plate valve. Unfortunately, to the best of our knowledge, there are not many books that emphasize the fluid dynamical aspects, instead of treating the valve simply as a mechanical device. Moreover, just a few of them take into account the influence on the whole compression cycle on valve behavior, from the suction to the discharge.

Specifically, recent books about extensive valve dynamics can be referenced; a book by Touber [12], by Habing [5] and by Böswirth [13]. Touber presents a clear overview of valve dynamics and valve design. Besides the theoretical approach, he built a test stand to examine valve dynamics experimentally. However, the pitfall of his theoretical prediction of valve lift proved to be the use of an analog and hybrid computer. Habing, in his book, treats valve dynamics theoretically in two dimensions with computational fluid dynamics and then presents measurements to verify the results. Böswirth has been one of the most prolific authors recently. His books address, both theoretically and experimentally, the issues of unsteady gas flow in valves, valve flutter, etc.

1.3 Purpose of Research

As can be concluded from the aforementioned, when we strive for an improvement of a piston compressor, our efforts should in first order be directed to the valves. Besides justifying the necessity of compressor valves and their dynamic behavior, which was the first task of this thesis, in the preceding paragraphs we also discussed the evolution of the literature concerning this topic, its strengths as well as its weak points. In this subchapter, the main purpose of this thesis and its application are formulated.

This thesis is devoted to the study of the valve dynamics of the reciprocating compressor. To achieve this, we first introduce a one-dimensional mathematical model of the valve, including the fluid-structure interaction as well as the influence of the whole compression cycle, i.e. the process in the cylinder, suction chamber, and discharge chamber, etc. This specific kind of mathematical model is known as a complete model in relevant literature. Our approach to this mathematical model, notwithstanding the fact that we will be applying a complete model, which is still rarely found in literature, will differ also in its versatility as well as easy customizability. More on this can be found in chapter 3.

After a mathematical model is proposed, it will be implemented into a tool in the commercially available software MATLAB (version 2016b). For the purposes of examining the valve dynamics, the tool shall be written in compliance with the universality and complexity of the mathematical model. For this purpose, object-oriented programming will be utilized, instead of unstructured programming, the use of which could lead, in our belief, to a so-called *"spaghetti code"*. More on this can be found in chapter 4.

Afterwards, the developed tool will be used to examine the individual phenomena of valve dynamics and the parameters which influence them, which is the last task of this thesis. It shall be emphasized that we are focused on the qualitative assessment of the factors influencing the dynamic behavior of the valve.

We are aware that this thesis may be limited in its scope in two ways. The first is the restriction of the valve model to one-dimension. This forbids us from examining the phenomena that might occur in a real valve, e.g. non-parallel collisions of the valve plate. However, a reader who is interested can be referred to a recent study by Habing [5], utilizing computational fluid dynamics for the purpose of examining these relatively insignificant behaviors of the valve. As a second drawback, one might consider the lack of experimental validation of the results obtained from the developed tool, which is not, however, the subject of this thesis. To mitigate this limitation, we will draw a comparison of our results with experimental data available in literature.

Regarding the practical use of this thesis, let us first focus on the process of designing a compressor valve. As Tuhovcak [14] suggests, there are basically three different approaches employed in the development process; an experiment, computational fluid dynamics and

a simplified (analytical) model. The expensive and time-consuming nature of experiments limits their use to the final stages of valve development only.

Utilizing CFD to analyze the turbulent flow through the valves, the thermodynamic processes in the cylinder, etc. can provide us with rather accurate results even in three-dimensions; however, not even this approach in studying valve behavior can be satisfactorily utilized in the very early stages of development. This is mainly due to the rather lengthy process of preparation, i.e. geometry preparation and its discretization, before running the simulation itself. Although, this process is only done once for a given geometry of the valve and thus it can be utilized for simulation with different operating conditions, even for two-dimensional models the computational processing time needed to achieve a convergent solution is excessive for design purposes, as Howes [15] states. Naturally, it is necessary that the detailed valve geometry is already worked out, which usually presents a problem at the beginning of the design process and thus it further intensifies the need for a fast but extensive tool.

In those initial stages, it is very useful to have a tool that can help predict the influence of general parameters, such as valve mass, spring type, maximum valve lift, the area through the gas flows, etc. on valve behavior. We believe that in these cases, our developed tool has the potential to be employed thanks to its key features such as low computational time, user-friendliness, or simple and fast modifiability, which permits the user to implement a different mathematical model, if needed.

As Howes [15] points out, another benefit of the simulation lies in its help to overcome issues resulting from the fact that some quantities such as impact velocities are very difficult to measure in an operating compressor. Moreover, it is often impossible to measure results over the wide range of operating conditions. It follows that the utilization of such a tool for simulating valve behavior is kindly welcomed.

2 Compressor Valves

In this chapter, we will clarify the significance of automatic valves, which are the subject of this study. Hereafter, we will briefly describe the commonly used valves in present-day reciprocating compressors, and at the end of this chapter, we will discuss the valve design terminology that will be used in the rest of this thesis.

2.1 Self-acting and Mechanically Operated Valves

Depending on the principle of compressor valves, two main types can be distinguished, either automatic (self-acting) or mechanically operated valves. Automatic valves are actuated by the pressure difference in front of and behind the valve, whereas the motion of the latter is linked to the motion of the piston. This substantial difference gives rise to the automatic valves being more beneficial in comparison to the mechanically operated ones.

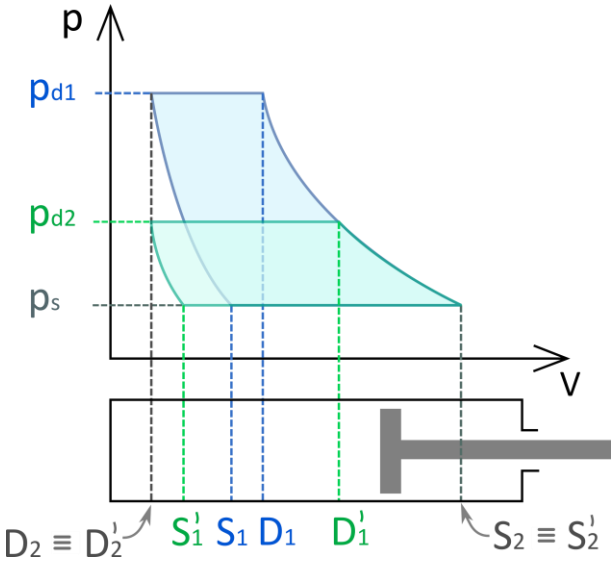

Figure 7 The influence of pressure ratio on compressor cycle

Assuming an ideal compression cycle (Figure 7) with a suction pressure p_s and a discharge pressure p_{d1}, when the pressure in the cylinder during compression reaches the discharge pressure p_{d1}, the discharge valve opens. Likewise, if the pressure in the cylinder during expansion decreases so that it is equal to the suction pressure p_s, the suction valve opens. A certain piston position corresponds to the points of both the opening (S_1, D_1) and the closing (S_2, D_2) of the valves. If we now reduce the discharge pressure to the value of p_{d2} so that $p_{d2} < p_{d1}$, the points of the opening (S_1', D_1') will change and will thus correspond to the new position of the piston.

These changes to the moment, when the valve is either opening or closing, are influenced by a variable pressure ratio and do not pose problems for automatic valves since they can adapt to them. For mechanically operated valves, this does not apply due to their fixed points of opening and closing. In addition to the external pressure ratio, these fixed points

of operation give rise to another pressure ratio, which is known as *"built-in compression ratio"*. Bloch [16] considers this to be the main disadvantage of mechanically controlled valves because every time the external pressure ratio changes such so that it is not equal to the built-in ratio, the energy conversion by the compressor will not be optimal.

As an advantage of mechanically controlled valves, one can consider the independence of their motion on forces originating from a gas flow, which ensures a full valve opening under any operating conditions. Nevertheless, their use these days is very limited due to the prevailing drawbacks, such as higher weight, which limits the speed at which a compressor can operate or the necessity of an actuating mechanism, which increases acquisition costs. Therefore, the vast majority of compressors nowadays are fitted with automatic valves, the common design of which is discussed in the next subchapter.

2.2 Automatic Valve Types

Conceptually, an automatic valve consists of a movable sealing element, a means for limiting the lift of the movable element for when the valve is fully open, a means to generate a force acting on the movable element to close it and then to press it against the seat, for when the valve is closed.

Even though there are a variety of valve designs available, only a few main types are predominant. Tierean [17] states that among the widespread and most used valve configurations these days are poppet valves, plate valves and ring valves. The choice of which valve type to select is made with special emphasis on work conditions (see Table 1).

	Differential Pressure	***Discharge Pressure***	***Revolutions***
Poppet Valve	$up\ to\ 15\ MPa$	$up\ to\ 30\ MPa$	$600\ rpm$
Plate Valve	$up\ to\ 20\ MPa$	$up\ to\ 40\ MPa$	$1800\ rpm$
Ring Valve	$up\ to\ 30\ MPa$	$up\ to\ 60\ MPa$	$600\ rpm$

Table 1 Operating conditions for different valve types [18]

2.2.1 Poppet Valve

The characterizing feature of the poppet valve (Figure 8) is the variety of same-sized ports through which the gas flows. Each port has its own sealing element, called the poppet. One of the main advantages of this valve is its high efficiency due to the streamlined shape of the poppets and their high lift[2]. According to Bloch [16], this makes for an ideal valve for applications with low compression ratios, or applications where high-density gas is compressed, because in the latter case, valve losses are very important. Another advantage of the poppet valve is its simplicity in maintenance as it can be done on-the-spot and without specially-trained people [19].

[2] According to Bloch [16], values of .250" (approximately 6.3 mm) or higher are common

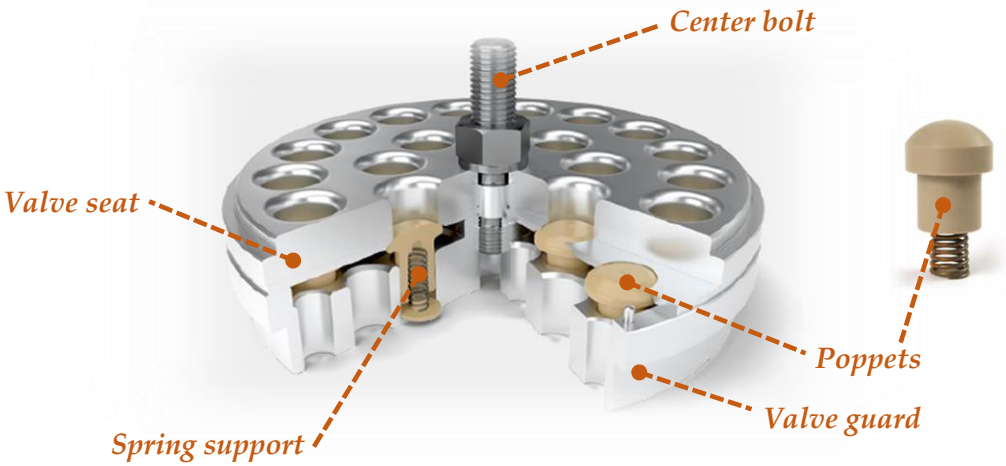

Figure 8 Poppet valve [40]

2.2.2 Ring Valve

The movable elements in the ring valve (Figure 9) are concentrically arranged narrow rings around the center axis of the valve. The independent rings make maintaining uniform flow control somewhat difficult, but they do have the advantage of low-stress levels due to the lack of stress concentration points [18]. The latter permits the use of these valves for the highest discharge and differential pressures, as seen in Table 1.

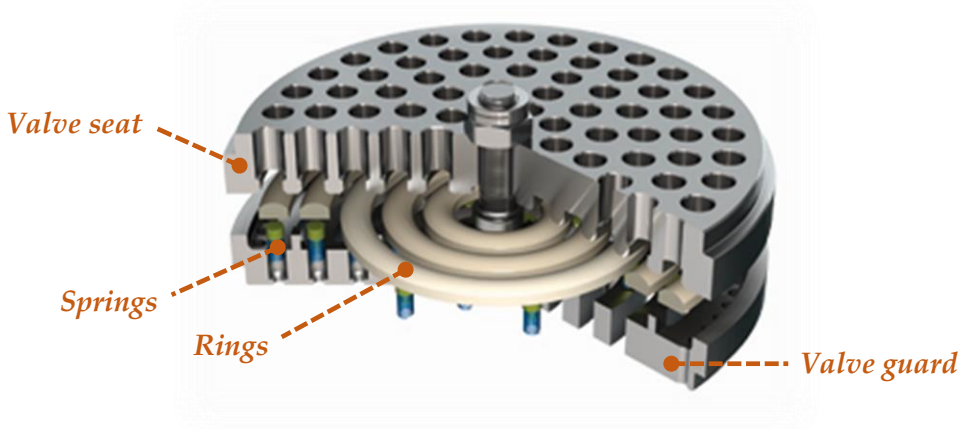

Figure 9 Ring valve [40]

2.2.3 Plate Valve

The plate valve design (Figure 10) is similar to the previous one, except that the rings are joined into a single movable element. This design adjustment of the sealing element permits the installation of a second, non-sealing, dampening disc.

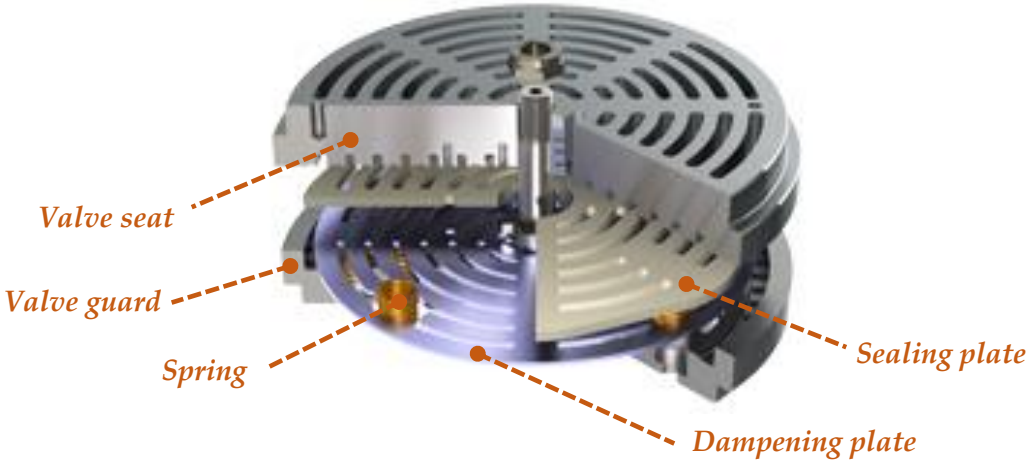

Figure 10 Plate valve [40]

The dampening disc is designed to be lightly spring-loaded between the valve body and the main movable disc. Its function is to decelerate the sealing element en route towards the valve guard and thus to mitigate the brunt of the impact.

Since a dampening plate is normally not installed in either valves with a non-metallic sealing element, or in valves with a metallic sealing plate for small air compressors, the discussion from now on shall be limited to valves without the addition of a dampening plate.

2.3 Valve Design Terminology

As previously mentioned in the topic concerning the design of automatic valves, one can conclude that the valves may differ considerably in construction details from one other. However, in principle, all valve types, except for the ones with a dampening plate, can be simplified to a model with a single sealing element, as depicted in Figure 11. To avoid misunderstandings, this subchapter will henceforth clarify the reference words for the valve elements used in the thesis.

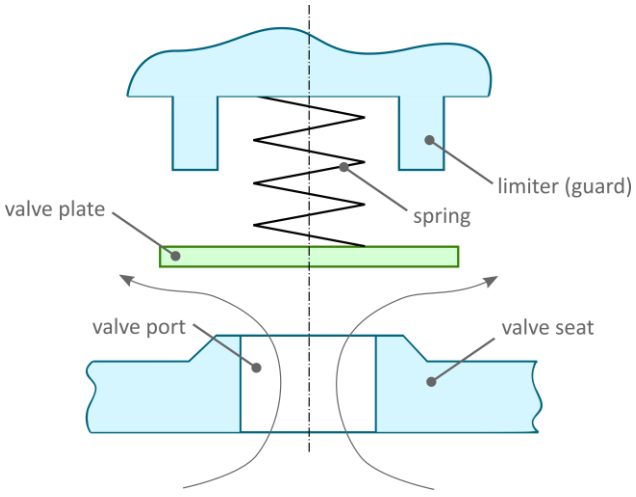

Figure 11 Generic model of a valve assembly

The channel through which the gas flows and which shall be opened and closed periodically, is called a **valve port**. The movable sealing element, which opens and closes the valve port, is called a **valve plate**. When the valve is closed, the valve plate is pressed against the **valve seat** by a **spring**. In the generic model, the spring is used as the means of generating the force acting on the valve plate. When the valve is in the process of opening, the valve plate lifts but is limited in its motion by a **limiter** or a **valve guard**, which the valve plate touches in a fully-open state. As a whole, these elements form a **valve assembly**, which is often simply abbreviated to a **valve**. For completeness, it shall be added that the expression "**valving system**" will be used when referring to all valve assemblies fitted in the piston compressor.

3 The Model

In order to theoretically examine the behavior of the valve, it is crucial to draft a model, in which real-life events can be reproduced with the goal of obtaining information about them. In this chapter, we will first discuss in short order to clarify the meaning of valve dynamics that shall be simulated in the compressor model; the structure of such a model and its general simplifying assumptions. Then we will go into each part of this model so as to analyze the physical process, then simplify it based on the assumptions and afterwards derive the mathematical description of this process. At the end of the chapter, we will present a tabular summary of the equations describing the entire compressor model.

3.1 Overview of the Model

3.1.1 Processes and Effects to be Simulated

Before we proceed to the layout of the compressor model, in which the valve dynamics is examined, let us briefly discuss what is meant by valve dynamics and what parts of the compressor the model shall include. In Figure 12a, one can see an example of an ideal valve plate lift during the (ideal) compressor cycle, which is the desired end goal of the design of the valve. However, the real valve behaves differently, as can be seen in Figure 12b.

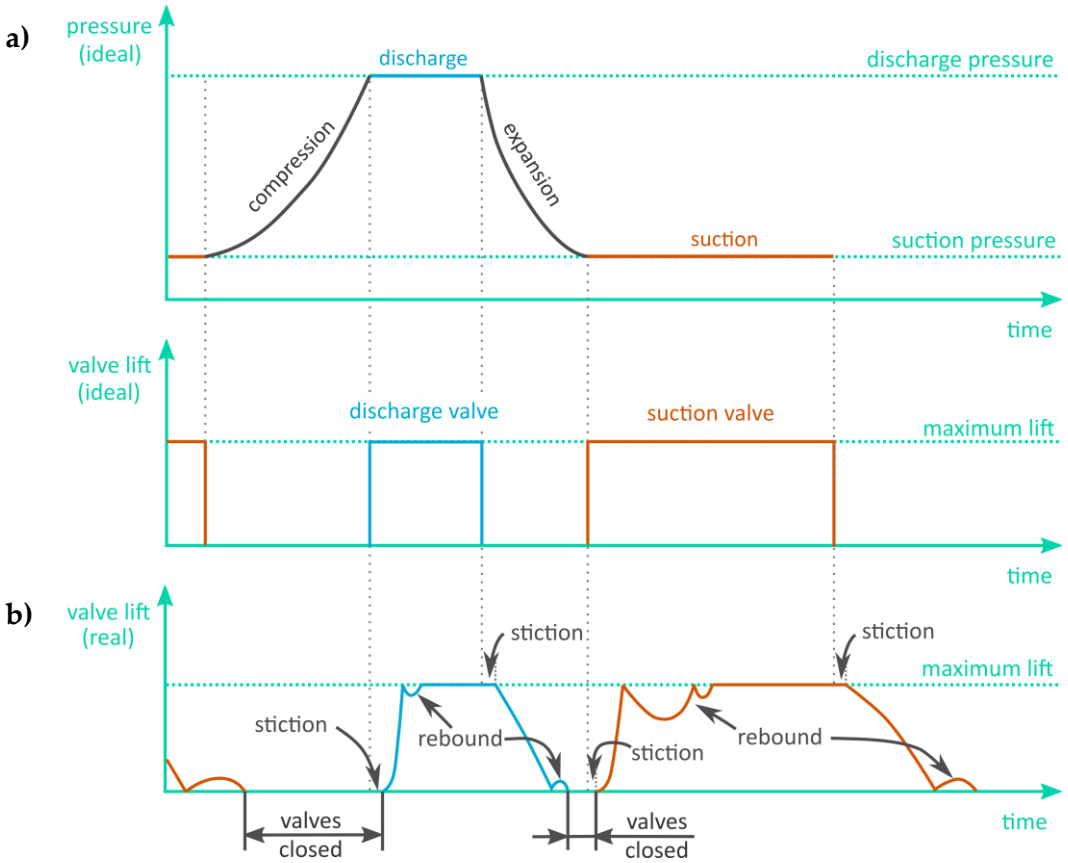

Figure 12 Ideal and real valve plate lift

From the comparison of the two figures above one can clearly observe a significant difference lying in the valve plate lift over a period of time, which can be attributed to a variety of effects of valve dynamics such as rebound or stiction, the former of which occurs when the valve plate strikes against the guard or the limiter, the latter case is the cause of delayed valve opening or closing. Among the most notable phenomena one should include the pressure pulsations in the piping system as well as the change in pressure in the cylinder. Since this thesis is devoted to automatic compressor valves, the latter two can significantly influence the valve plate lift.

When one is to go about studying valve dynamics, i.e. the motion of the valve plate under the action of external forces, these effects need to be considered in order to arrive at a valve design with ideal behavior. It follows that the valve plate lift is the essential quantity when evaluating valve dynamics.

Regarding the desired output quantities, we can distinguish *time-dependent quantities* and so called *"periodical" quantities*, which contain information about the whole compression cycle. Included in the former are the valve plate lift, its velocity, pressure in the cylinder, etc. It is important to note that these variables are strictly required from the perspective of valve designer [17]. Regarding the latter, i.e. the periodical quantities, examples are volumetric efficiency, indicated work etc., however, these quantities are not granted much attention in this thesis, as in addition to the effects of valve dynamics, processes such as heat transfer through the cylinder wall etc. can also influence them. Since these processes, discussed individually in relevant chapters, do not considerably influence valve dynamics, they are not covered in the compressor model and so the accuracy of the periodical results would be subject to debate.

3.1.2 The Model Structure

In view of the fact that the reciprocating compressor is composed of distinct components, e.g. a cylinder, a crank mechanism, a suction or discharge system etc., there is no reason to treat the developed model in a different way. Thus, the drafted model (Figure 13) consists of several components interacting with each other. The first essential element is a **cylinder**, within which the piston moves in a repetitive back-and-forth linear motion. The piston is driven by a **crank mechanism** and that as a whole constitutes the second element of the model. The third and fourth components respectively are formed by the **suction and discharge** spring loaded **valve,** the model of which has already been drafted in chapter 2.3. The last two elements of the model, are the **suction and discharge system** of similar structure.

This model configuration, in which the valve dynamics is examined, is known as the complete model and it allows for the extensive analysis of the aspects influencing valve motion since it includes all the components that a real-life reciprocating compressor is composed of.

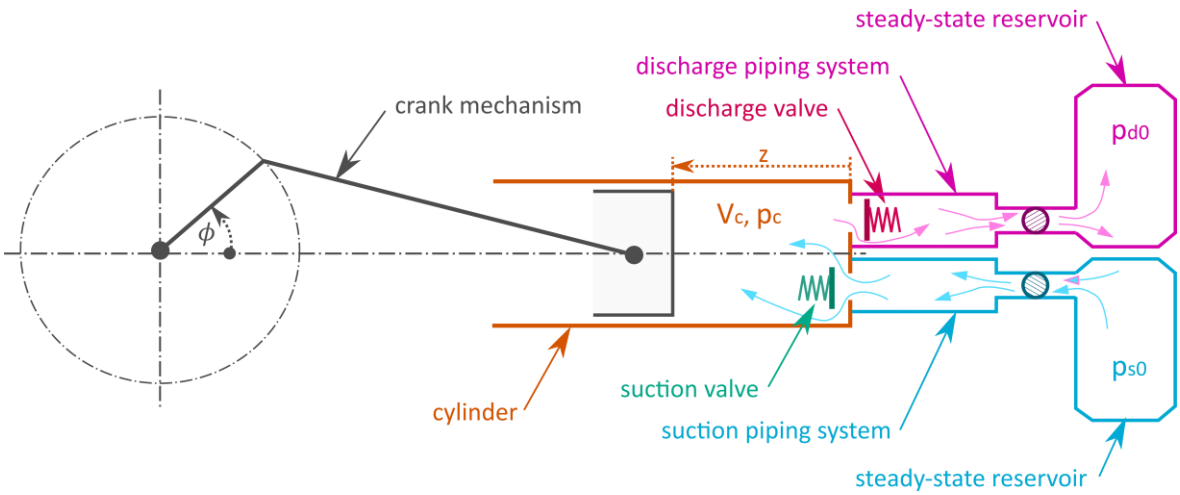

Figure 13 Compressor model

According to the part of the compressor that is neglected in the model, one can distinguish three other compressor models; the pipeless model, the valveless model and the pipe-and-valveless model. The former model, as its name suggests, assumes that the influence of the suction and discharge piping systems on valve behavior is insignificant and thus they can be omitted. This model is extensively utilized in literature concerning the valve dynamics. However, it was found from the experiments carried out by Maclaren [20] that such a simplification can be considered as invalid since the influence of the piping system on the valve dynamics can be considerable.

It is evident that the latter two models cannot be used for examining the valve dynamics since the valves are completely omitted in these models. The valveless model is used primarily for the investigation of pressure pulsations in the piping system connected to the piston compressor. Although the pipe-and-valveless model is significantly simplified since it does not take either the valves or the piping system into account, it finds its use in the prediction of forces acting on the piston and thus the load of the whole crank mechanism.

The approach to the modular structure of the proposed model and its subsequent implementation, also allows us to fulfill one of the goals stated in the Purpose of Research, particularly the one that stated to build a versatile model that can be further adjusted and easily broadened by others, for instance when the heat transfer through the cylinder wall is not to be omitted (heat transfer will be neglected in this thesis) etc. This can be simply done by modifying the mathematical description of one or more of the modules, of which the compressor model is composed of.

3.1.3 Simplifying Assumptions

In the previous section, the workings of the valve dynamics were explained, the general requirements of the compressor model were discussed and its overall structure was drafted. In the upcoming subchapters, the processes and effects will be described mathematically and it would be prudent to introduce some simplifying assumptions for this purpose. Based on these assumptions, a mathematical model can be derived from the physical one. Although according to literature pertaining to this topic these two models are commonly divided into two separate chapters, due to the drafted modular structure of the compressor model, we believe that this approach would be antithetical to the clarity and readability of this thesis. Instead, we will discuss each part of the model individually with its physical processes and subsequent simplifications. In this subchapter, we will elucidate the most significant simplifying assumptions as well as, wherever possible, their influence on the accuracy of the results, namely in cases where we have:

- A compressor with one single-acting cylinder
- Rigid bodies
- An ideal gas as the working fluid
- Spring-loaded valves with one degree of freedom
- 1D, quasi-steady subsonic flow
- No reverse flow

The compressor model drafted above, is based on a single stage reciprocating compressor with one single-acting cylinder. Each part of the compressor, i.e. the cylinder, the piston, the connecting rod etc. is assumed to be a rigid body and thus the deformations of compressor elements are not considered. This simplification is made strictly for completeness; however, its influence on the results can be reckoned as truly negligible.

The working fluid is assumed to be an ideal gas with a constant specific heat capacity. This simplification was made because it allows us to eliminate in an analytical way several time-dependent variables, e.g. enthalpy, internal energy etc., which would have required, had we had a case of a real gas as the working fluid, the use of numerical (iterative) methods. It follows that this assumption gives us the possibility to substantially simplify the relevant thermodynamic equations; however, for high pressures real gases do not strictly follow the ideal gas law and thus this simplification can affect the accuracy of the results. To illustrate how high the deviation from ideal behavior can be, we make use of a compressibility factor, which is defined in literature [21]. Assuming piston compressor parameters, the discharge pressure being up to $150\ bar$ and the temperature between $250 - 500\ K$, the corresponding compressibility factor ranges from 0.94 to 1.065 [22] and thus the systematic error produced by this simplifying assumption lies within the range of ± 6.5 %. Even though, this error is not negligible, it mainly influences the periodic results, namely the indicated work. Regarding strictly the valve dynamics, Costagliola [9] suggests

that there could be some influence in particular to the points of the valve opening or closing, however, these effects are subtle.

The valves in the compressor model are assumed to be spring-loaded with one degree of freedom. Although this assumption is not directly linked to the error in the results, it does not allow us to study the marginal but still somewhat interesting behavior of the valve plate, e.g. nonparallel collisions etc., which can occur under specific operating conditions [5].

The penultimate simplification is related to the fluid flow through the valve ports, which is, in the real compressor, unsteady at least with respect to time. One should bear in mind that in this thesis, the flow is treated as quasi-steady, i.e. being steady at a given time step and changing without delay to a new value in the following time-step. This approach is justified for valves with short channels since in this case delays in valve dynamics, due to the inertia of the gas resident in the valve channel, will presumably be insignificant [5]. For the sake of completeness, it is expected that the flow will remain subsonic, i.e. the Mach number will remain below 1.

Last but not least, if a valve closes late, there can be (for a certain small period of time) a situation, when the fluid flows in the opposite direction to its regular state, e.g. it is common that gas flows from the suction chamber into the cylinder; however, there can be a situation, where the pressure in the cylinder would have to surpass the pressure in the suction chamber so that the suction valve plate can seal up the valve port - and this is the moment, when reverse flow can occur. In this thesis, this problem is not discussed since there is evidence (see [12]) suggesting that it affects the periodical quantities rather than the valve dynamics.

3.2 Crank Mechanism

The crank mechanism, which is schematically depicted in Figure 14, comprises of a piston, which is connected via a connecting rod to the crankshaft. Since the piston forms the movable wall of the cylinder, it is necessary to know its position in calculating the cylinder volume and thus to determine the thermodynamic process inside. The derivation of this equation is later presented in this chapter.

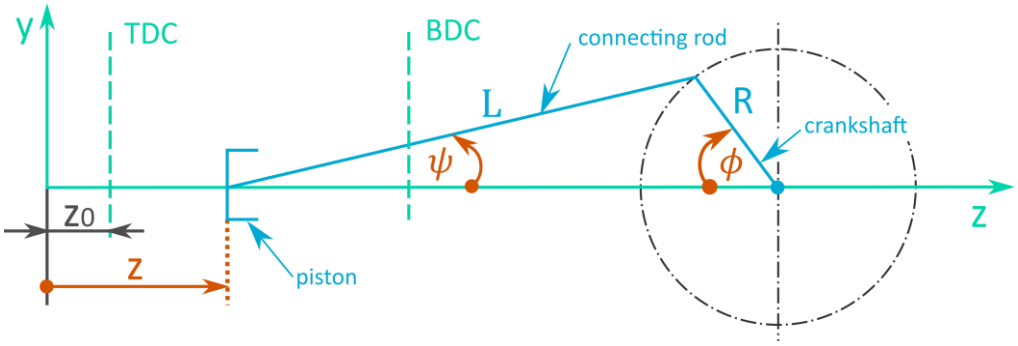

Figure 14 Schematic drawing of the crank mechanism

To formulate the equation of the instantaneous piston position, assume a set of generalized coordinates, as follows:

$$\vec{q} = [z, \psi, \phi]^T \tag{3.2.1}$$

These coordinates define the position of each moving body with respect to a nonmoving Cartesian coordinate system, in which the y-axis is identified with the steady front wall of the cylinder. The positive senses of these coordinates are defined by Figure 14.

Since the crank mechanism has one degree of freedom, only one of these coordinates can be independent. Let the ϕ coordinate be the independent one and then the remaining two coordinates can be expressed as a function of ϕ. For this purpose, two loop equations relating the three coordinates can be written as:

$$z = z_0 + L + R - L\cos\psi - R\cos\phi \tag{3.2.2}$$

$$L\sin\psi = R\sin\phi \tag{3.2.3}$$

where L stands for the connecting rod length, R denotes the crank radius and z_0 identifies the smallest distance between the cylinder and the piston, which is derived from the clearance volume.

Making use of the Pythagorean identity for the angle ψ, it follows that Eq. 3.2.3 can be rewritten as:

$$\cos\psi = \frac{1}{L}\sqrt{L^2 - R^2\sin^2\phi} \tag{3.2.4}$$

Substituting Eq. 3.2.4 into 3.2.2, we get the piston displacement z as a function of the crank angle ϕ:

$$z = z_0 + L + R - \sqrt{L^2 - R^2\sin^2\phi} - R\cos\phi \tag{3.2.5}$$

By substituting the crank angle ϕ with the following equation

$$\phi = \omega t \tag{3.2.6}$$

where ω is the angular velocity of the crankshaft, into the Eq. 3.2.5, we obtain the piston displacement as only a function of time, since ω is assumed to be constant:

$$z = z_0 + L + R - \sqrt{L^2 - R^2\sin^2(\omega t)} - R\cos(\omega t) \tag{3.2.7}$$

By the differentiation in time of Eq. 3.2.7, one can get the piston velocity w_z as follows:

$$w_z = R\,\omega\sin(\omega t)\left(1 + \frac{R\cos(\omega t)}{\sqrt{L^2 - R^2\sin^2(\omega t)}}\right) \tag{3.2.8}$$

3.3 Cylinder

The physical idea of the process, which takes place inside the cylinder, is rather straightforward. During the suction phase, when the suction valve is opened, the gas flows into the cylinder, where it is trapped after both valves are closed and thus the compression phase takes place. During this process, the pressure of the gas inside the cylinder, as well as its temperature, rises due to the reduction of the cylinder volume. Moreover, heat transfer through the cylinder walls and the piston is also present. Initially, when the temperature of the gas is lower than the temperature of the walls, the temperature of the gas will rise; however, should its temperature increase such, so that it is higher than that of the wall's, the heat transfer will take place the other way around and thus the gas will start to be cooled. If the pressure in the cylinder reaches sufficiently high values, the discharge valve plate will be pushed away and the compressed gas will be forced out of cylinder. Finally, when both of the valves are closed again, the pressure inside the cylinder decreases due to the expansion of the remaining compressed gas in the clearance volume.

3.3.1 Simplifying assumptions

To arrive at a mathematical description of the process outlined above, lets discuss the assumptions which are taken into consideration here:

- No gas leakage
- The kinetic and potential energy of the gas is neglected
- Homogenous system
- Adiabatic control volume

If either the valve plates or piston rod packings, are subject to a certain degree of wear, the gas inside the cylinder can leak. Nevertheless, in the derivations of the mathematical equations in the following sections, these leaks are not considered and thus it is assumed that the change of mass inside the cylinder is only caused by the gas flow through the valves during either the suction or the discharge phase.

The second simplification, i.e. neglecting both the kinetic and potential energy, is valid for the gas inside the cylinder and the suction/discharge chambers as well as for the gas entering or leaving it. Although the reason to neglect the potential energy is obvious since there are not any appreciable height differences, neglecting the kinetic energy requires careful deliberation. Regarding the gas flowing through the valves, it can be freely stated that despite the rather high velocity of the gas in a valve port, the kinetic energy is irrelevant if the control volume is chosen in such a way that its boundaries are out of the valve port. To vindicate the neglecting of kinetic energy of the gas in the cylinder or suction/discharge chamber, assume an adiabatic compression (pressure ratio equal to three) of air (20 °C). The compression work would be approximately 75000 J/kg. This is far more than the kinetic energy, because even in cases where the air would be accelerated from at rest to a velocity of 20 m/s, the kinetic energy would be only about 200 J/kg.

The cylinder volume is considered as a homogenous thermodynamic system, in which the physical properties are the same in all parts of the system. Despite there being evidence of changes in properties from one point to another [23], this assumption is requisite so that the energy distribution in the system is known and thus it is feasible to theoretically calculate it.

Despite the fact that the last simplification, i.e. not taking into account the heat transfer through both the cylinder walls and the piston, does influence the predicted compressor performance, e.g. its efficiency and indicated work, it does not significantly influence the valve dynamics [12] and thus it will be assumed.

3.3.2 General Governing Equations

In this subchapter, we present the derivation of the equation, which describes the change of the state of the gas inside the cylinder. For this purpose, we utilize the conservation of energy principle, which in its most general form states that the time rate change of energy inside the control volume is equal to the rate of net energy transfer. According to literature [24], this can be expressed as:

$$\frac{dE_{CV}}{dt} = \lim_{dt\to 0}\left(\frac{\delta E_{in}}{dt}\right) - \lim_{dt\to 0}\left(\frac{\delta E_{out}}{dt}\right) = \dot{E}_{in} - \dot{E}_{out} \tag{3.3.1}$$

where E_{CV} identifies the energy of gas inside the control volume, $\dot{E}_{in,out}$ is the rate of energy flowing into or out of the control volume.

According to Gramoll [25], the energy can be transferred by heat, work and mass only, and thus the energy balance can then be rewritten as:

$$\frac{dE_{CV}}{dt} = \dot{Q} - \dot{W} + \sum \dot{m}_{in} e_{in} - \sum \dot{m}_{out} e_{out} \tag{3.3.2}$$

where $\dot{Q}$ stands for the rate of total heat transfer to the system, $\dot{W}$ is the rate of total work done by the system and $e_{in,out}$ represents the total energy carried by a unit of mass as it enters or leaves the control volume (see Eq. 3.3.3).

$$e = \frac{w^2}{2} + gy + u + pv = \frac{w^2}{2} + gy + h \tag{3.3.3}$$

where $\frac{w^2}{2}$ is the kinetic energy, gy represents the potential energy, u stands for the internal energy and pv denotes the flow work. It is important to note that all of the terms are specific (i.e. per mass unit). Together the latter two terms form the specific enthalpy h. It shall be emphasized that the specific energy of gas inside the control volume can also be calculated as per Eq. 3.3.3, however, omitting the additional energy in the form of flow work.

3.3.3 Suction Phase

To apply the law of conservation of energy as stated above onto the cylinder, assume a control volume, as depicted in Figure 15. This control volume is valid for the suction phase and hence it has one inlet and no outlet. The assumption to treat the cylinder volume as a homogenous system leads to a discontinuity there, where the gas crosses the control surface since the gas approaching the volume is generally in a different thermodynamic state than the one inside. Hence, at this intersection the upstream gas conditions are assumed instead of the homogenous ones.

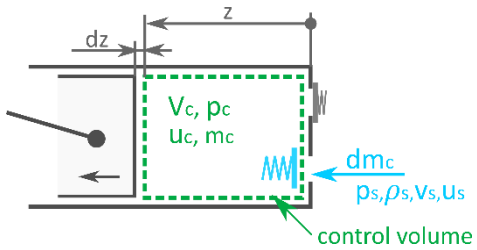

Figure 15 Control volume for compressor cylinder – suction phase

With respect to the simplifications established above, the combination of Eq. 3.3.2 and 3.3.3 yields:

$$d(m_c u_c) = dm_c h_s - dW = dm_c(u_s + p_s v_s) - dW \tag{3.3.4}$$

where dm_c is the change of mass caused by the gas entering the control volume.

There is no external work other than by the change of volume:

$$dW = p_c dV_c = p_c A_c dz \tag{3.3.5}$$

where p_c denotes the pressure inside the cylinder, A_c stands for the cross-sectional area of the cylinder and dz is an infinitesimal change of piston displacement.

The following derivation is based on utilizing the well-known ideal gas laws and principles, i.e. the equation of state (Eq. 3.3.6), internal energy (Eq. 3.3.7) and the relation between the specific heats (Eq. 3.3.8).

$$pv = rT \tag{3.3.6}$$

$$du = c_v dT \tag{3.3.7}$$

$$c_p = c_v + r = c_v \kappa \tag{3.3.8}$$

Combination of Eq. (3.3.4), (3.3.5) and (3.3.7) yields:

$$c_v T_c dm_c + c_v m_c dT_c = c_v T_s dm_c + p_s v_s dm_c - p_c A_c dz \tag{3.3.9}$$

The temperature of either the gas inside the control volume T_c or the one flowing inside T_s, can be expressed from Eq. 3.3.6. Moreover, the mass of the gas inside the control volume m_c is given by

$$m_c = \frac{A_c z}{v_c} \tag{3.3.10}$$

Hence, the Eq. 3.3.9 becomes

$$\frac{c_v}{r}p_c v_c dm_c + c_v \frac{A_c z}{v_c} dT_c = \frac{c_v}{r}p_s v_s dm_c + p_s v_s dm_c - p_c A_c dz \tag{3.3.11}$$

Since the z coordinate cannot be equal to zero, as is concluded from its definition in Figure 14, Eq. 3.3.11 can be freely multiplied by $\frac{r}{c_v A_c z}$. Along with the substitution of Eq. 3.3.8, we can write:

$$\frac{p_c r}{c_v z} dz = \kappa \frac{p_s v_s}{A_c z} dm_c - \frac{r}{v_c} dT_c - \frac{p_c v_c}{A_c z} dm_c \tag{3.3.12}$$

Let us closely look at the last element of the equation above. The infinitesimal change of mass dm_c can be attained by differentiation of the Eq. 3.3.10, i.e.:

$$dm_c = \frac{A_c}{v_c} dz + z A_c d\left(\frac{1}{v_c}\right) \tag{3.3.13}$$

Hence, this element can be rewritten as:

$$\frac{p_c v_c}{A_c z} dm_c = \frac{p_c}{z} dz + p_c v_c d\left(\frac{1}{v_c}\right) \tag{3.3.14}$$

Combination of Eq. 3.3.12 and 3.3.14 yields:

$$\frac{p_c r}{c_v z} dz = \kappa \frac{p_s v_s}{A_c z} dm_c - \frac{p_c}{z} dz - \left[p_c v_c d\left(\frac{1}{v_c}\right) + \frac{r}{v_c} dT_c\right] \tag{3.3.15}$$

wherein the elements in the square brackets denotes time change in pressure inside the cylinder, as is true that:

$$dp_c = d\left(\frac{r T_c}{v_c}\right) = r T_c d\left(\frac{1}{v_c}\right) + \frac{r}{v_c} dT_c = p_c v_c d\left(\frac{1}{v_c}\right) + \frac{r}{v_c} dT_c \tag{3.3.16}$$

Finally, by dividing the equation by a differential of time and substituting the specific volume for density, we can write:

$$\frac{dp_c}{dt} = \kappa \left(\frac{p_s}{\rho_s A_c z} \Theta_{cs} - \frac{p_c w_z}{z}\right) \tag{3.3.17}$$

where $w_z = \frac{dz}{dt}$ stands for the piston velocity and $\Theta_{cs} = \left.\frac{dm_c}{dt}\right|_{suction}$.

The Eq. 3.3.17 describes the change in pressure in the compressor cylinder during the suction phase. Equations for calculating the piston position z and its velocity v_z have already been derived in chapter 3.2. Nevertheless, additional equations are needed for determining the thermodynamic state of the gas in the suction chamber, i.e. p_s and v_s, and the change of mass inside the cylinder due to the gas flowing inside, i.e. $\left.\frac{dm_c}{dt}\right|_{suction}$. The former can be found in chapter 3.5, the latter then in chapter 3.4.2.

3.3.4 Discharge Phase

In the case of discharge phase, assume an adiabatic control volume as depicted in Figure 16, which has one outlet and no inlet.

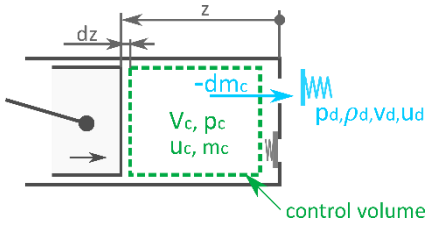

Figure 16 Control volume for compressor cylinder - discharge phase

The derivation of the equation to describe the change in pressure inside the cylinder, when the gas is being discharged, is done entirely analogously to the suction phase. Hence, the resulting equation yields:

$$\frac{dp_c}{dt} = -\kappa\left(\frac{p_c}{\rho_c A_c z}\Theta_{cd} + \frac{p_c w_z}{z}\right) \tag{3.3.18}$$

wherein $\Theta_{cd} = -\frac{dm_c}{dt}\Big|_{discharge}$ and ρ_c stands for the density of gas inside the cylinder, which can be simply expressed as:

$$\rho_c = \frac{m_c}{A_c z} \tag{3.3.19}$$

Note that the additional equation for calculating the change of mass inside the cylinder due to the gas flowing out of the control volume is given in chapter 3.4.2.

3.3.5 Expansion and Compression

Whether during the suction or discharge phase, the mass transfer and its influence on the thermodynamic state of the gas inside the cylinder were required to have been considered. However, both the expansion and compression phases are characterized by both the suction and discharge valve being closed and thus no mass transfer occurs. It follows that

$$\frac{dm_c}{dt}\Big|_{\substack{suction\\discharge}} = 0 \tag{3.3.20}$$

and so in both cases Eq. 3.3.17 and 3.3.18 reduce to:

$$\frac{dp_c}{dt} = -\kappa\frac{p_c w_z}{z} \tag{3.3.21}$$

3.4 Suction and Discharge Valve

In this chapter, we intend to present the mathematical description of the valve behavior. First, we present the equation describing the gas flow through the valve as a function of time or rather of the valve plate lift, which is truly the sine qua non-of linking the thermodynamic state of gas in the cylinder to the one present in suction or discharge chamber. Second, the force balance on valve plate lift is drawn up in order to predict the valve plate motion.

One should bear in mind that since the mathematical description is fundamentally the same for both the suction and discharge valve, this section refers to both simultaneously. Hence, some changes in the pressure notation are made:

- Pressure p_u denotes the pressure in front of the valve (in respect to the normal gas flow), i.e. for the suction valve it corresponds to the pressure in the suction chamber p_s , whereas for the discharge valve it refers to the pressure in the cylinder p_c
- Pressure p_d stands for the pressure behind the valve, i.e. for the suction valve it refers to the pressure in the cylinder p_c, for the discharge valve it corresponds to the pressure in the discharge chamber p_d

3.4.1 Simplifying assumptions

Regarding the simplifying assumptions that take place in terms of valve modeling, most of them has already been discussed, namely:

- Spring-loaded rigid body with one degree of freedom (valve plate can only move in the direction perpendicular to the plane of the seat)
- Quasi-steady flow
- Ideal gas
- No reverse flow

Moreover, another remark is needed particularly in relation to the transition of the real compressor valve to the model one. Up to now, it has been tacitly assumed that the reciprocating compressor or rather the model of it, in which the valve dynamics is examined, has solely one suction and one discharge valve; a design that there is only one valve port in each valve through which the gas flows. However, in real-life compressor valves (discussed in chapter 2.2) there are usually many ports. Moreover, the compressor can be equipped with more than one suction and discharge valve. Customarily in these cases [12], the valve model may be based either on the concept of one larger replacement valve or many small valves, however with the same properties. In this thesis, it is assumed that the former approach is utilized.

3.4.2 Valve Flow Modeling

The complexity of fluid flow through the valve, i.e. its turbulent character (see Figure 17) does not permit a straightforward analytical solution of mass flow. One can achieve the desired results either with an experiment or a CFD simulation (with proper validation and verification of the results). Nonetheless, both methods are unsuitable for our purpose and thus a different approach must be invoked.

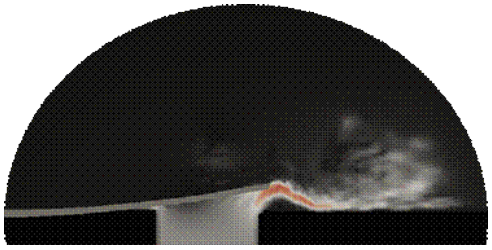

Figure 17 LES simulation of gas flow through the compressor reed valve [43]

Figure 18 depicts a valve, in which the plate is assumed to be at rest at an arbitrary distance from the valve seat.

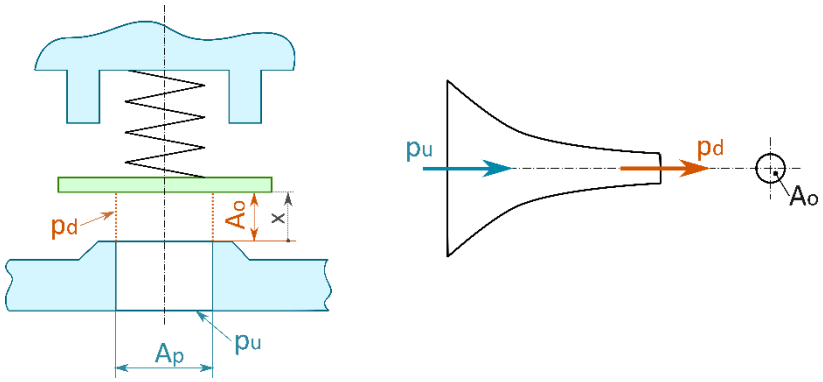

Figure 18 Diagram of a generic valve and its replacement by a nozzle

In the compressor models found in literature, the mass flow of the gas through the valve is oftentimes calculated as an incompressible flow through a converging channel as per the following equation:

$$\dot{\theta} = \alpha\epsilon A_o\sqrt{2\rho_u(p_u - p_d)} \tag{3.4.1}$$

where A_o is the flow area ($A_o = \pi D_p x$), i.e. the area between the valve plate and the valve seat [3], ρ_u signifies the inlet density, p_u stands for the total inlet pressure, whereas p_d denotes the static pressure in the space downstream of the valve port. The coefficients α, ϵ are determined experimentally and they harmonize the calculated (incompressible) mass flow with a real value.

[3] Strictly speaking, the flow area shall be the smaller of the areas of A_o, A_p, where A_p stands for the cross-sectional area of the valve port, because if it were the other way around than it was tacitly assumed in the text (i.e. $A_p < A_o$), then A_p would become the limiting factor in terms of the mass flow rate.

According to corresponding literature [5] it is stated that the former, so-called *flow coefficient* α, accounts for the influence of viscosity, the vena contracta after flow separation and the non-uniform state of gas in the cross-sections perpendicular to the flow direction. Since from completed experiments [12] it can be seen that the values of the flow coefficient are below 1, i.e. the predicted mass flow rate is higher than the real one, we feel that it could be questionable if the lower mass flow rate was purely due to the above stated reasons or rather due to the irreversibility in throttling flow (i.e. generating entropy). Moreover, the experiments showed that the value of the coefficient almost entirely depends on the geometrical shape of the flow passage (and thus of the valve plate lift) instead of either operating conditions or the size of the valve.

The second coefficient, i.e. the so-called *expansion coefficient* ϵ, allows for the compressibility of the gas. However, in this case, experiments [12] proved that its value is not a function of purely pressure ratio across the valve, but also of the valve geometry, its size as well as the properties of the gas.

In this thesis, we will avoid utilizing the expansion coefficient due to the variety of factors influencing it, by modeling the fluid flow as the outflow of gas from a pressurized vessel through a convergent nozzle by assuming isentropic expansion between the upstream and downstream conditions. In cases with ideal gas, it can be calculated by invoking the well-known *Saint-Venant-Wantzel* equation:

$$\dot{\theta} = \alpha A_o \sqrt{\frac{2\kappa}{\kappa - 1} p_u \rho_u \left(\left(\frac{p_d}{p_u} \right)^{\frac{2}{\kappa}} - \left(\frac{p_d}{p_u} \right)^{\frac{\kappa+1}{\kappa}} \right)} \tag{3.4.2}$$

wherein the flow coefficient is used to account for the irreversibility of the process. One should bear in mind that if the pressure ratio in Eq. 3.4.2 is equal to the critical pressure ratio

$$\frac{p_d}{p_u} = \left(\frac{2}{\kappa + 1} \right)^{\frac{\kappa}{\kappa - 1}} = 0.528|_{\kappa=1.4} \tag{3.4.3}$$

the valve will become choked and thus Eq. 3.4.2 cannot be used as a mass flow rate model. However, Ninković [2], based on Böswirth's findings, states that compressor valves do not become choked in accordance to Eq. 3.4.3, yet they do at much higher-pressure ratios; hence, beyond the critical pressure ratio, the necessitation of undergoing an experiment or a CFD simulation is inevitable in order to arrive at a mass flow rate.

By substituting the flow area into Eq. 3.4.2, we get:

$$\dot{\Theta} = \alpha \pi D_p x \sqrt{\frac{2\kappa}{\kappa - 1} p_u \rho_u \left(\left(\frac{p_d}{p_u} \right)^{\frac{2}{\kappa}} - \left(\frac{p_d}{p_u} \right)^{\frac{\kappa+1}{\kappa}} \right)} \tag{3.4.4}$$

By noticing that by comparing Eqs. 3.4.1 and 3.4.2, one can arrive at a means, by which the expansion coefficient can be theoretically determined as follows:

$$\epsilon = \sqrt{\frac{\kappa}{\kappa - 1}\frac{p_u}{p_u - p_d}\left(\left(\frac{p_d}{p_u}\right)^{\frac{2}{\kappa}} - \left(\frac{p_d}{p_u}\right)^{\frac{\kappa+1}{\kappa}}\right)} \tag{3.4.5}$$

This can be considered a basic approach to determine the expansion coefficient, since one can find other more sophisticated ways to theoretically determine ϵ in literature [26], which found its use, for instance, in those cases where strong contractions take place etc.

3.4.3 Valve Dynamics

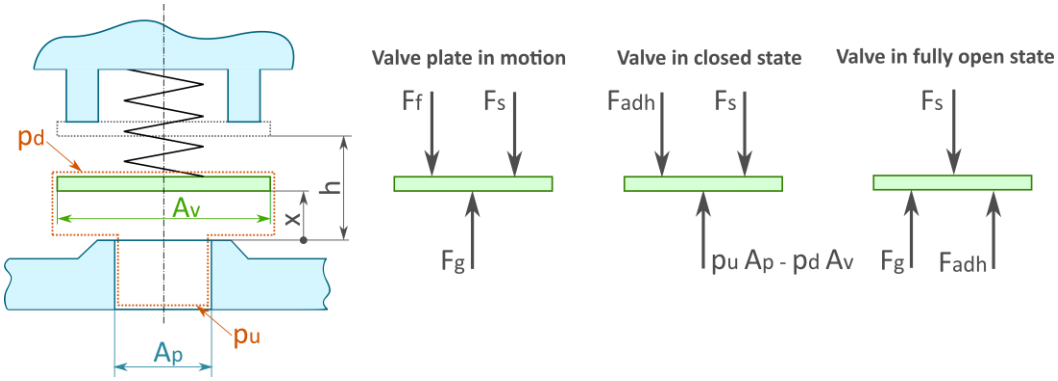

Figure 19 Force balance on valve plate

As already stated, the movable valve plate is considered to be a mass-spring system with a single degree of freedom (Figure 19). Hence, the equation of motion is based on Newton's second law:

$$m\frac{d^2x}{dt^2} + F_f + F_s = F_g \tag{3.4.6}$$

where m is the mass in motion, x stands for the distance of the valve plate from the seat, F_g stands for the gas force, F_f denotes the fluid friction force and F_s indicates the spring force. If the valve plate reaches an obstacle (a seat or limiter), a rebound can occur. Afterwards, the plate comes into direct contact with the obstacle, accompanied with the appearance of an adhesion force F_{adh}.

Before proceeding to the analysis of these quantities individually, let us look at the force balances for the valve plate, when it is at rest, i.e. when it is in contact with the limiter or the seat, and what conditions must be fulfilled so that its movement is enforced again.

Valve in Closed State

If the valve is closed, then the following inequation is fulfilled:

$$p_u A_p - p_d A_v \leq F_s + F_{adh} \tag{3.4.7}$$

When this inequality condition reverses, the valve plate will lift, i.e.:

$$p_u A_p - p_d A_v > F_s + F_{adh} \tag{3.4.8}$$

Valve in Fully Open State

If the sum of the forces pushing the valve plate towards the limiter is higher than the spring force acting in the opposite direction, then the valve plate will remain in a fully open state, i.e.:

$$F_s \leq F_g + F_{adh} \tag{3.4.9}$$

Analogously to the previous event, when the inequality is not fulfilled anymore, i.e. the following is true:

$$F_s > F_g + F_{adh} \tag{3.4.10}$$

the valve plate will then start to move back towards the valve seat.

3.4.3.1 The Mass of the System

The mass m in Eq. 3.4.6 does not refer solely to the mass of the valve plate, but since the spring generally has a non-negligible mass, it needs to also be included in the term of m. Moreover, as the valve plate moves through the fluid, some of the volume of the surrounding fluid needs to be deflected. This effect can be covered by the so-called *added mass*, which can be determined by means of potential flow theory. However, since the working fluid in the compressor is assumed to be air, its density is much lower in comparison with the material of the plate and thus the added mass would be considerably lower than the mass of the plate. It follows that this effect can be neglected.

Regarding the mass of the spring, it cannot be simply added to the mass of the plate, since the velocity, with which the spring elements move, is proportional to the length of the spring, i.e. $\frac{\zeta}{l}\frac{dx}{dt}$. Instead, an *effective mass* needs to be determined. This can be done theoretically based on the kinetic energy of the spring.

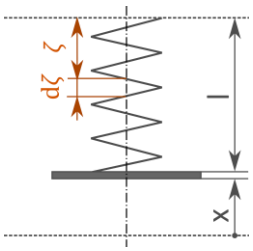

Figure 20 Effective spring mass

If the kinetic energy $dE_{k,spring}$ of a spring element (with mass $\frac{d\zeta}{l}m_{spring}$) is equal to $\frac{1}{2}\frac{d\zeta}{l}m_{spring}\left(\frac{\zeta}{l}\frac{dx}{dt}\right)^2$, the kinetic energy of the whole spring is then:

$$E_{k,spring} = \int_{\zeta=0}^{\zeta=l} dE_{k,spring} = \frac{1}{2}\frac{m_{spring}}{3}\left(\frac{dx}{dt}\right)^2 \tag{3.4.11}$$

It follows that the inertial effect of the spring can be accounted for by adding one third of the spring mass to the mass of the valve plate, i.e.:

$$m = m_{plate} + \frac{1}{3}m_{spring} \tag{3.4.12}$$

3.4.3.2 Spring Force

The majority of compressor valve springs can be modeled as springs with linear characteristics (see Figure 21) [9].

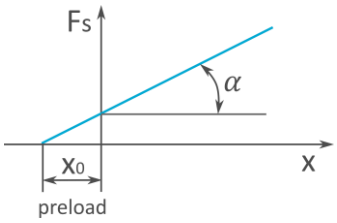

Figure 21 Linear spring characteristic

In this case, the spring force is given simply by:

$$F_s = k(x_0 + x) \tag{3.4.13}$$

where k is the spring stiffness ($k = \tan\alpha$) and x_0 stands for the preload deflection.

3.4.3.3 Valve Plate Impacts

As already mentioned, the valve plate is limited in its motion by the valve limiter and the valve seat. The former limits the motion when the valve plate is lifting, whereas the latter comes into action when the valve is about to close. When the moving plate strikes against these fixed obstacles, it will rebound with a velocity that is fundamentally lower than the one at the moment of impact. In order to avoid the rebound of the valve plate, the kinetic energy would have to be entirely dissipated (absorbed).

The valve plate impacts are modeled based on Newton's experimental law, which presents us with the following equation [27]:

$$\left.\frac{dx}{dt}\right|_{t^+} = -c_r \left.\frac{dx}{dt}\right|_{t^-} \tag{3.4.14}$$

Where c_r is the restitution coefficient, $\left.\frac{dx}{dt}\right|_{t^-}$ denotes the (relative) velocity just before the impact, whereas $\left.\frac{dx}{dt}\right|_{t^+}$ stands for the (relative) velocity immediately after the impact. Obviously, if the restitution coefficient equals zero, no rebound occurs and thus the impact is referred to as *inelastic*. On the other hand, should the coefficient be equal to 1, then the valve plate rebounds with the same velocity as it had at the moment of impact. This kind of impact is called *fully elastic*. These are essentially extreme cases, since in reality the restitution coefficient will typically range from zero to one and thus the impact will be *semi-elastic*. Since the impacts give rise to stress concentration, which leads to impact fatigue, it is evident that a value of zero is desired for the restitution coefficient.

The drawback here is that the knowledge of valve parts' materials and their elastic properties is insufficient for a theoretical prediction of the restitution coefficient [5], because of many more factors involved in. For instance, the classical impact between two solid bodies is not likely to occur here, since as the valve approaches an obstacle, it has to displace the gas and the oil in the space between the obstacle and the plate.

Lastly it should be remarked that the influence of valve plate impacts in the mathematical model is accounted for by the initial conditions needed to solve the system of ODEs. In other words, the system of ODEs is being solved until the valve plate strikes against a seat or guard when the system of ODEs will be solved anew; however, the initial velocity of the valve plate there will be in conformity with Eq. 3.4.14.

3.4.3.4 Friction Force

Assuming the valve plate is in an arbitrary position between the valve seat and the limiter, but is not touching either of them, then the motion of the valve plate is damped by the fluid friction opposing the motion of the valve plate. As Ninković [2] points out, this friction force acting on the moving plate can be assumed to be proportional to the velocity of the plate, i.e.:

$$F_f = c_f \frac{dx}{dt} \tag{3.4.15}$$

where c_f denotes the friction coefficient.

From the experiments done by Touber [12] one can see that the friction coefficient is basically independent of gas density and thus the same value can be used for both the suction and discharge valves, if they are of the same design and dimensions. Moreover, but somewhat surprisingly, his experiments showed a weak dependence of the friction coefficient on the oil droplets in the gas stream. However, we feel that more experiments might be desirable to further verify this statement, since the author only states the percentage of oil in the gas stream, but does not discuss for instance the size of the oil droplets etc., which could likely influence the results.

3.4.3.5 Adhesion

When the valve is in contact with the limiter or the seat, an adhesion (or sometimes referred to as *stiction*) appears. It negatively influences the valve behavior, since the valve will not start moving immediately after the upstream pressure p_u exceeds the downstream pressure p_d. Nevertheless, a sufficient pressure difference is needed to overcome the stiction effect. Hence the valve plate starts moving much later than in absence of adhesion.

Strictly speaking, adhesion is present in both lubricated and non-lubricated machines. However, in the former, the effect is far more noticeable and the situation is much more complicated, since it is mainly caused by the deformation of a lubricating oil film in the gap between the valve plate and the obstacle [2]. It follows that the amount of oil, its viscosity varying with its temperature etc., influences this effect. Many of the compressor models presented in literature (for example [5] [28]) tacitly assume the latter case and as a consequence of which they completely omit the stiction effect. In this thesis, the former case is modeled, i.e. the stiction in the case of a lubricated machine.

The complex nature of the physical background of adhesion in a lubricated machine, which is beyond the scope of this thesis, gives rise to many models trying to simulate this effect. However, most of them are semi-empirical. Recently, a study by Pizarro-Recabarren,

Barbosa and Deschamps [29] was published, regarding the stiction effect in automatic compressor valves. They proposed a very extensive model for the prediction of stiction, departing from the Reynolds equation for hydrodynamic lubrication, in which they consider effects like oil film rupture etc. However, as they state, experimental work is needed to validate their model.

In this thesis, we will utilize a different theoretical model proposed by Khalifa and Liu [30], in which it is assumed that the entire space between the plate and the obstacle (delimited by D_p and D_v) is always occupied by oil. Moreover, the change in cross-section of the oil film preceding its rupture is not considered here. The outcome of this model encompasses the fact that the rupture of the oil film cannot be predicted and that the effect of stiction can only be considered when the valve plate is stationary, even though in real-life the adhesion force ceases to exist at the moment the oil film starts to disrupt, not the moment in which the valve plate is set in motion.

The oil film stiction force can be expressed as a sum of the force component due to the viscous effects F_{visc}, the capillary force F_{cap} and the interfacial tension force F_{ten} [29], i.e.:

$$F_{adh} = F_{visc} + F_{cap} + F_{ten} \tag{3.4.16}$$

In the Khalifa and Liu model [30], no account is made for the liquid-gas interfacial tension, i.e. $F_{ten} = 0$. Since the valve plate is stationary, the viscous force (which is proportional to the velocity of the plate) also vanishes and thus one can get:

$$F_{adh} \equiv F_{cap} = \frac{\pi \gamma_{LG} D_p^2 \cos\beta}{2h_{film}} \left(\left(\frac{D_v}{D_p} \right)^2 - 1 \right) \tag{3.4.17}$$

wherein γ_{LG} stands for surface tension, β denotes a meniscus contact angle and h_{film} refers to oil film thickness (see Figure 22).

Strictly speaking, Eq. 3.4.17 applies to the contact area between the valve plate and the seat and thus different areas should be used to arrive at the equation for the adhesion force between the valve plate and the guard. However, in this thesis Eq. 3.4.17 will be used for the latter case as well, since we are not in possession of the dimensions of the valve limiter. Moreover, the stiction effect is accounted for only in cases where the valve plate is pressed against the obstacle for a finite time. This is in compliance with the fact, that short moments

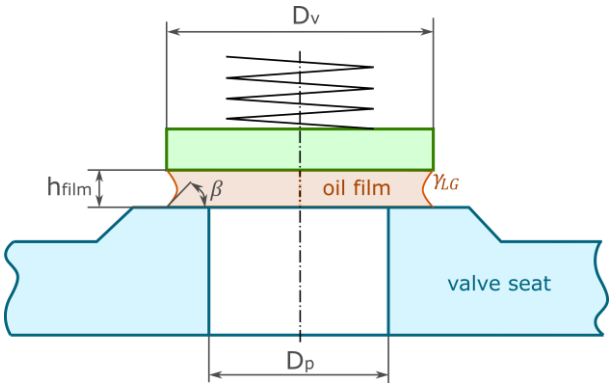

Figure 22 Stiction

of contact, such when the valve plate strikes against the obstacle and rebounds immediately, do not give rise to a noticeable adhesion effect [30].

3.4.3.6 Fluid-Structure Interaction

In view of the fact that our interest in this thesis is focused on automatic compressor valves; the essence of predicting the motion of the valve plate lies in the interaction of the fluid flow with the plate. However, the physical complexity of this interaction, caused by both the flow and the plate, incurs difficulties if one wants to predict it instead of purely foreseeing it.

It is reasonable to expect the flow (in a real-life valve) to be turbulent, three-dimensional, compressible, unsteady, and likely to be a multi-phase flow containing oil particles. The valve plate can generally be classified as a *sharp-edged bluff body* immersed in a fluid flow field, which it resists. Hence, the fluid flow exerts the force acting on the body, which originates from the uneven pressure distribution around the valve plate. If the pressure distribution was known, this force could be easily calculated as a surface integral of the pressure around the valve plate. Unfortunately, this is not happening here.

As Habing [5] states, even in cases with incompressible flow, the force acting on the body immersed in a fluid flow field could generally be expressed in only two exceptional cases; either for a steady viscous creeping flow ($R_e \ll 1$) or for an irrotational inviscid unsteady flow. However, the same author also concludes that neither of these two approaches is applicable for compressor valves.

Hence, the gas force exerted on the valve plate will be modeled as the force acting on the plate in quasi-steady flow, i.e.:

$$F_g = c_g A_v (p_u - p_d) \tag{3.4.18}$$

whereby A_v denotes the valve plate area and c_g stands for the gas force coefficient[4], which is a function of the valve plate lift, i.e. $c_g(x)$. This method of calculating gas force is customarily employed in corresponding literature (for instance see [5] [12] [2] [31]), since it is widely recognized as a workable definition.

The values of the gas coefficient are subject to the experiment, which requires the use of a dynamometer attached to the valve plate. Experimental data for various valve designs can be found in a book by Touber [12]. He obtained the coefficients under steady conditions, i.e. during the measurement the valve plate was retained in a definite position between the seat and the limiter. Due to the rather complicated measurement, he demonstrated a method on how to obtain this coefficient without explicitly measuring it.

[4] In the literature, the gas coefficient is also referred to as a drag coefficient and then the gas force is called the drag force.

By applying the momentum equation to a control volume enclosing the valve plate, Tauber [12] obtained the following equation[5]:

$$c_g = \left(1 + \left(\alpha\epsilon\frac{\pi D_v x}{A_p}\right)^2\right)\frac{A_p}{A_v} - \frac{\left(\alpha\epsilon\left(A_v - A_p\right)\right)^2}{A_v A_p} \tag{3.4.19}$$

whereby α, ϵ are the flow and expansion coefficients respectively. These have already been discussed in chapter 3.4.2. Although this equation does not entirely relinquish the dependence on experimental coefficients, it helps to reduce the need for further measurements. Moreover, it can provide us with a valuable insight into the parameters, on which the value of the gas coefficient mostly depends, as will be demonstrated later on in chapter 5.2.1.

3.5 Piping System

Consider the situation in Figure 23, where the gas flows through the discharge valve into a plenum chamber, subsequently entering a pipeline and then encountering a valve before exiting into the steady-state reservoir. The same, however, applies in reverse order for the suction piping system and so both are covered in this chapter.

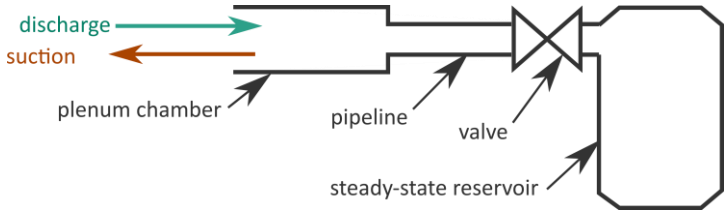

Figure 23 Generic piping system

If the volume of the plenum chambers were infinite, there would be no pressure pulsations in the piping systems. Since in a real-life compressor, the volume of these chambers is finite, the presence of pressure pulsations is inevitable. These were studied by various authors (for example see Bráblík [32], Maclaren [20]) and from their research one can conclude that the study of phenomena in the whole piping system is not indispensable for the study of valve dynamics. It is enough to know the time-dependent pressure in the plenum chambers, while other parts of the piping system can be considered to be irrelevant.

[5] We would like to point out to the reader the difference in the borrowed equation. Based on the momentum equation for the control volume, Touber [12] derived an equation for the gas force as $F_g = \left(1 + \left(\alpha\epsilon\frac{\pi D_v x}{A_p}\right)^2\right)\frac{A_p}{A_v}(p_u - p_d)A_v - \frac{\left(\alpha\epsilon\left(A_v - A_p\right)\right)^2}{A_v A_p}(p_u - p_d)A_v$. The gas coefficient is then obtained by comparing this equation with Eq. 3.4.18. However, the resulting c_g in his book is that $c_g = \left(1 + \left(\alpha\epsilon\frac{\pi D_v x}{A_p}\right)^2\right)\frac{A_p}{A_v} - \frac{\left(\alpha\epsilon\left(A_v - A_p\right)\right)^2}{A_v - A_p}$. It is obvious that there is an inaccuracy in the denominator of the second element of the equation, since there should instead be the product of the areas A_v, A_p instead of their subtraction.

Hence, it is justifiable to replace the entire piping system with a much simpler, but still satisfactory, replacement - the single degree of freedom oscillator, in which the gas in the plenum chamber acts as a spring, whereupon it is considered to be compressible, and the fluid in the pipeline acts as a mass, after which it is assumed to be incompressible, see Figure 24.

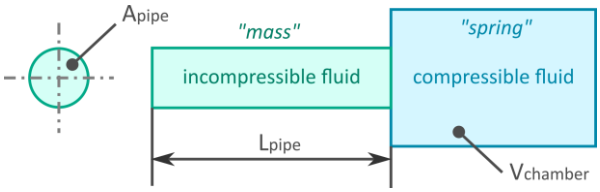

Figure 24 Helmholtz resonator concept

This method of accounting for the influence of pressure pulsations is extensively discussed, including an experimental comparison, in a book by Touber [12] and thus only the main idea of the model and the equations involved in it are summarized here.

Pipeline

The pipe is modelled as a straight one of length L_{pipe} with a constant cross-sectional area A_{pipe}. It is assumed to be one-dimensional incompressible flow inside, the motion of which (as a gas column) is governed by Newton's second law:

$$m\frac{du}{dt} = \sum F \tag{3.5.1}$$

where m stands for the mass of the gas, u means its velocity and $\sum F$ denotes the sum of forces acting on the gas column. Since A_{pipe} is constant, one can divide with it Eq. 3.5.1 and so the following can be obtained:

$$\frac{m}{A_{pipe}^2}\frac{d(uA_{pipe})}{dt} = \sum p = p_1 - p_2 - \Delta p_{drop} \tag{3.5.2}$$

wherein $\frac{m}{A_{pipe}^2} = m_a$ is referred to as *acoustical mass*, pressures p_1, p_2 are stagnation pressures in the spaces connected by the pipeline, Δp_{drop} stands for the pressure drop in the pipe (see Eq. 3.5.3).

$$\Delta p_{drop} = \xi\frac{1}{2}\rho u^2 = \left(\lambda\frac{L_{pipe}}{D_{pipe}} + \sum K\right)\frac{1}{2}\rho u^2 \tag{3.5.3}$$

where the first element in the parenthesis stands for major losses due to friction, the other one in the parenthesis for minor losses resulting from a local resistance.

By combining Eq. 3.5.2 with Eq. 3.5.3, one can obtain the flow equation in its general form:

$$\frac{d\Theta}{dt} = \frac{A_{pipe}}{L_{pipe}}(p_1 - p_2) - \frac{\xi}{2\rho L_{pipe}A_{pipe}}\Theta^2 \tag{3.5.4}$$

The drawback resulting from the simplification is that, since the value of ρ is constant throughout the length of the pipe, this generally leads to discontinuities at both ends of the pipe. This can be solved with a further assumption that ρ equals to an upstream value of

ρ_1, a downstream value of ρ_2 or to an average of ρ_1 and ρ_2. Based on experiments, the cited author suggests utilizing the former approach.

Plenum Chambers

Fundamentally, the thermodynamic process inside the plenum chambers is entirely analogous (even with the simplifications) to the one inside the compressor cylinder discussed in chapter 3.3. Moreover, the volume of the plenum chambers is constant in time.

Figure 25 Suction plenum chamber

Figure 26 Discharge plenum chamber

Regarding the *suction plenum chamber* and suction phase (Figure 25), the following equations can be derived:

$$\frac{dp_s}{dt} = \frac{\kappa}{V_s}\left(\frac{p_{s0}}{\rho_{s0}}\Theta_s - \frac{p_s}{\rho_s}\Theta_{cs}\right) \tag{3.5.5}$$

wherein V_s is the volume of the suction plenum chamber, $\Theta_s = \frac{dm_{in}}{dt}$ and $\Theta_{cs} = \left.\frac{dm_c}{dt}\right|_{suction}$.

The mass flow going in and out of the plenum chamber is linked to the mass of the gas inside the plenum chamber, which is governed by the law of conservation of mass, i.e.:

$$\frac{d\rho_s}{dt} = \frac{1}{V_s}(\Theta_s - \Theta_{cs}) \tag{3.5.6}$$

It shall be pointed out, that Eqs. 3.5.5 and 3.5.6, which are explicitly intended for suction phase, reduce for other phases since if the suction valve is closed, then Θ_{cs} equals zero.

Analogously to the preceding suction chamber, in case of the *discharge plenum chamber* and discharge phase (Figure 26), the following equations can be written as:

$$\frac{dp_d}{dt} = -\frac{\kappa}{V_d}\left(\frac{p_d}{\rho_d}\Theta_d - \frac{p_c}{\rho_c}\Theta_{cd}\right) \tag{3.5.7}$$

$$\frac{d\rho_d}{dt} = -\frac{1}{V_d}(\Theta_d - \Theta_{cd}) \tag{3.5.8}$$

where V_d is the volume of the discharge plenum chamber, $\Theta_d = \frac{dm_{out}}{dt}$ and $\Theta_{cd} = -\left.\frac{dm_c}{dt}\right|_{discharge}$. Moreover, if the discharge valve is closed the Eqs. 3.5.7 and 3.5.8 reduce since Θ_{cd} equals zero.

Correction of the Model

It is necessary to say that this means of replacing the suction and discharge piping system with a one-degree of freedom oscillator, will not agree in every detail with the real-life case. However, one should bear in mind that this is not required either. It is quite enough if the

deviation from the real case is low enough so as to permit the prediction of influencing the valve plate behavior. To mitigate this deviation, the cited author proposes (on a theoretical basis) a means of converting the dimensions of the real piping system to the ones used in the equations above, i.e. L_{pipe}, A_{pipe} and thus the interested reader is referred to the source [12].

3.6 Periodical Quantities

In light of what was written in chapter 3.1.1 above anent not granting attention to the periodical quantities (i.e. the quantities, the value of which is related to the entire compressor cycle), we may perhaps be forgiven for calling attention here to some of them since they will later on help us to follow the trends of the concepts and models discussed previously. Specifically, a brief overview of three periodical quantities is presented here – indicated work, indicated valve work and volumetric efficiency.

3.6.1 Indicated Work

The work, which is transmitted by the piston to the gas in the cylinder over the entire compressor cycle, is given by the commonly-known equation:

$$W_i = \oint p_c dV_c = A_c \oint p_c dz \tag{3.6.1}$$

Considering the form, in which other equations were derived, it will be more convenient to use the differential form of Eq. 3.6.1, i.e.:

$$\frac{dW_i}{dt} = A_c p_c \frac{dz}{dt} = A_c p_c w_z \tag{3.6.2}$$

3.6.2 Indicated Valve Work

The indicated valve work, i.e. the part of the indicated work connected with the pressure drop across the valves, can be expressed analogously to the previous; however, it is necessary to differentiate between the suction and discharge phases. Hence, the resulting equations in differential form are respectively:

$$\left.\frac{dW_{iv}}{dt}\right|_{suction} = (p_s - p_c) A_c |w_z| \tag{3.6.3}$$

$$\left.\frac{dW_{iv}}{dt}\right|_{discharge} = (p_c - p_d) A_c |w_z| \tag{3.6.4}$$

wherein the absolute value of the piston velocity w_z is used so that the late valve closing is not reflected in the indicated valve work. These equations will be integrated solely during the suction (Eq. 3.6.3) or discharge (Eq. 3.6.4) phases of the compressor cycle.

3.6.3 Volumetric Efficiency

The volumetric efficiency, i.e. the ratio of the truly sucked-in air V_{real} and the geometrically-swept volume of the compressor V_{swept}, is defined as [12]:

$$\eta_v = \frac{V_{real}}{V_{swept}} = \frac{\theta_{cs}}{\rho_{s0}} \frac{1}{2RA_c} \tag{3.6.5}$$

wherein $\theta_{cs} = \frac{dm_c}{dt}\Big|_{suction}$. As a side note, V_{real} could be also determined per mass flow through the discharge valve, or as a difference of mass of air inside the compressor cylinder between the compression and expansion phases.

3.7 Summary of the Mathematical Model

In the previous chapters, a detailed description of the equations that are utilized to simulate the processes, which take place in the reciprocating compressor and which are necessary to predict the dynamics of the valve, was presented. Here, we will summarize these equations in a structured tabular form, which, as we believe, will give the reader a comprehensive idea of the entire mathematical model and will hereinafter be referred to in chapter 4, where we describe the implementation of this mathematical model.

In order to arrive at the coveted solution, i.e. the behavior of the compressor and its valves, it is inevitable to solve the non-linear system of first-order ODEs. Moreover, this system of equations varies according to the current phase of the compressor cycle. That is, as a matter of fact, the reason why we feel it is desirable to present the system of ODEs for each phase in the subsequent subchapters. The switching between these systems is made on the level of the developed tool according to the conditions for transition, which are also stated later. Lastly, the input parameters of the mathematical model will be summarized.

3.7.1 Suction Phase

cylinder	*mass equation*	$\frac{dm_c(t)}{dt} = \theta_{cs}(t)$	(3.7.1)
	energy equation	$\frac{dp_c(t)}{dt} = \kappa\left(\frac{p_s(t)}{\rho_s(t)A_c z(t)}\theta_{cs}(t) - \frac{p_c(t)\,w_z(t)}{z(t)}\right)$	(3.7.2)
suction valve	*valve dynamics equations*	$w_{x,s}(t) = \frac{dx_s(t)}{dt}$	(3.7.3)
		$m_s \frac{dw_{x,s}(t)}{dt} + F_{f,s}(t) + F_{s,s}(t) = F_{g,s}(t)$	(3.7.4)
suction piping system	*suction chamber energy equation*	$\frac{dp_s(t)}{dt} = \frac{\kappa}{V_s}\left(\frac{p_{s0}}{\rho_{s0}}\theta_s(t) - \frac{p_s(t)}{\rho_s(t)}\theta_{cs}(t)\right)$	(3.7.5)
	suction chamber mass equation	$\frac{d\rho_s(t)}{dt} = \frac{1}{V_s}\left(\Theta_s(t) - \theta_{cs}(t)\right)$	(3.7.6)
	suction line dynamics equation	$\frac{d\Theta_s(t)}{dt} = \frac{A_s}{L_s}\left(p_{s0} - p_s(t)\right) - \frac{\xi_s}{2L_s A_s \rho_{s0}}\Theta_s^2(t)$	(3.7.7)

discharge piping system	*discharge chamber energy equation*	$\frac{dp_d(t)}{dt} = -\frac{\kappa}{V_d}\frac{p_d(t)}{\rho_d(t)}\Theta_d(t)$	(3.7.8)
	discharge chamber mass equation	$\frac{d\rho_d(t)}{dt} = -\frac{1}{V_d}\Theta_d(t)$	(3.7.9)
	discharge line dynamics equation	$\frac{d\Theta_d(t)}{dt} = \frac{A_d}{L_d}(p_d(t) - p_{d0}) - \frac{\xi_d}{2L_dA_d\rho_d(t)}\Theta_d^2(t)$	(3.7.10)

Table 2 System of ODEs - suction phase

This system of ten non-linear differential equations for ten unknown variables $(m_c, p_c, p_s, p_d, \rho_s, \rho_d, x_s, w_{xs}, \Theta_s, \Theta_d)$, which is, however, solved only in cases, where the suction valve plate is moving in an arbitrary position between the seat and the plate. If it comes into direct contact with the guard, i.e. when the suction valve is fully opened, then Eqs. 3.7.3 and 3.7.4 are excluded, since variables x_s, w_{xs} are not unknown anymore.

In the differential equations for the suction phase, the time-dependent variables are calculated as follows:

mass flow	$\theta_{cs}(t) = \alpha_s\pi D_{p,s}x_s(t)\sqrt{\frac{2\kappa}{\kappa-1}p_s(t)\rho_s(t)\left(\left(\frac{p_c(t)}{p_s(t)}\right)^{\frac{2}{\kappa}} - \left(\frac{p_c(t)}{p_s(t)}\right)^{\frac{\kappa+1}{\kappa}}\right)}$		(3.7.11)
friction force	$F_{f,s}(t) = c_{f,s}\frac{dx_s(t)}{dt}$		(3.7.12)
spring force	$F_{s,s}(t) = k_s\left(x_{0,s} + x_s(t)\right)$		(3.7.13)
gas force	$F_{g,s}(t) = c_{g,s}(t)\,A_{v,s}\left(p_s(t) - p_c(t)\right)$		(3.7.14)
	gas flow coefficient	$c_{g,s}(t) = \left(1 + \left(\alpha_s\epsilon_s(t)\frac{\pi D_{v,s}x_s(t)}{A_{p,s}}\right)^2\right)\frac{A_{p,s}}{A_{v,s}} - \frac{\left(\alpha_s\epsilon_s(t)(A_{v,s}-A_{p,s})\right)^2}{A_{v,s}A_{p,s}}$	(3.7.15)
	expansion coefficient	$\epsilon_s(t) = \sqrt{\frac{\kappa}{\kappa-1}\frac{p_s(t)}{p_s(t)-p_c(t)}\left(\left(\frac{p_c(t)}{p_s(t)}\right)^{\frac{2}{\kappa}} - \left(\frac{p_c(t)}{p_s(t)}\right)^{\frac{\kappa+1}{\kappa}}\right)}$	(3.7.16)
piston position	$z = z_0 + L + R - \sqrt{L^2 - R^2\sin^2(\omega t)} - R\cos(\omega t)$		(3.7.17)
piston velocity	$w_z = R\,\omega\sin(\omega t)\left(1 + \frac{R\cos(\omega t)}{\sqrt{L^2 - R^2\sin^2(\omega t)}}\right)$		(3.7.18)

Table 3 Time-dependent variables - suction phase

The last two equations, regarding the piston position and its velocity, are the same for the whole compression cycle and thus they will not be stated anymore.

Last remarks shall be made here concerning the equations for calculating the time-independent variables, which appeared in the equations above, i.e. the valve plate area A_{vs}, valve port area A_{ps} and the cylindrical cross-sectional area A_c. These are generally known and thus it is not needed to explicitly state them here.

3.7.2 Discharge Phase

cylinder	*mass equation*	$\frac{dm_c(t)}{dt} = -\theta_{cd}(t)$	(3.7.19)
	energy equation	$\frac{dp_c(t)}{dt} = -\kappa\left(\frac{p_c(t)}{\rho_c(t)A_c z(t)}\theta_{cd} + \frac{p_c(t)\,w_z(t)}{z(t)}\right)$	(3.7.20)
discharge valve	*valve dynamics equations*	$w_{x,d}(t) = \frac{dx_d(t)}{dt}$	(3.7.21)
		$m_d\frac{dw_{x,d}(t)}{dt} + F_{f,d}(t) + F_{s,d}(t) = F_{g,d}(t)$	(3.7.22)
suction piping system	*suction chamber energy equation*	$\frac{dp_s(t)}{dt} = \frac{\kappa}{V_s}\frac{p_{s0}}{\rho_{s0}}\,\theta_s(t)$	(3.7.23)
	suction chamber mass equation	$\frac{d\rho_s(t)}{dt} = \frac{1}{V_s}\Theta_s(t)$	(3.7.24)
	suction line dynamics equation	$\frac{d\Theta_s(t)}{dt} = \frac{A_s}{L_s}\left(p_{s0} - p_s(t)\right) - \frac{\xi_s}{2L_s A_s \rho_{s0}}\Theta_s^2(t)$	(3.7.25)
discharge piping system	*discharge chamber energy equation*	$\frac{dp_d(t)}{dt} = -\frac{\kappa}{V_d}\left(\frac{p_d(t)}{\rho_d(t)}\Theta_d(t) - \frac{p_c(t)}{\rho_c(t)}\Theta_{cd}(t)\right)$	(3.7.26)
	discharge chamber mass equation	$\frac{d\rho_d(t)}{dt} = -\frac{1}{V_d}\left(\Theta_d(t) - \Theta_{cd}(t)\right)$	(3.7.27)
	discharge line dynamics equation	$\frac{d\Theta_d(t)}{dt} = \frac{A_d}{L_d}\left(p_d(t) - p_{d0}\right) - \frac{\xi_d}{2L_d A_d \rho_d(t)}\Theta_d^2(t)$	(3.7.28)

Table 4 System of ODEs - discharge phase

Similarly to the preceding phase, these ten ODEs form a non-linear system with ten unknown variables, which are, however, in cases where the discharge phase takes place, slightly different; namely $m_c, p_c, p_s, p_d, \rho_s, \rho_d, x_d, w_{xd}, \Theta_s, \Theta_d$.

The time-dependent variables in these differential equations are calculated as follows:

mass flow		$\theta_{cd}(t) = \alpha_d \pi D_{p,d} x_d(t)\sqrt{\frac{2\kappa}{\kappa-1}p_c(t)\rho_c(t)\left(\left(\frac{p_d(t)}{p_c(t)}\right)^{\frac{2}{\kappa}} - \left(\frac{p_d(t)}{p_c(t)}\right)^{\frac{\kappa+1}{\kappa}}\right)}$	(3.7.29)
friction force		$F_{f,d}(t) = c_{f,d}\frac{dx_d(t)}{dt}$	(3.7.30)
spring force		$F_{s,d}(t) = k_d\left(x_{0,d} + x_d(t)\right)$	(3.7.31)
gas force		$F_{g,d}(t) = c_{g,d}(t)\,A_{v,d}\left(p_c(t) - p_d(t)\right)$	(3.7.32)
	gas flow coefficient	$c_{g,d}(t) = \left(1 + \left(\alpha_d \epsilon_d(t)\frac{\pi D_{v,d} x_d(t)}{A_{p,d}}\right)^2\right)\frac{A_{p,d}}{A_{v,d}} - \frac{\left(\alpha_d \epsilon_d(t)\left(A_{v,d} - A_{p,d}\right)\right)^2}{A_{v,d}A_{p,d}}$	(3.7.33)
	expansion coefficient	$\epsilon_d(t) = \sqrt{\frac{\kappa}{\kappa-1}\frac{p_c(t)}{p_c(t)-p_d(t)}\left(\left(\frac{p_d(t)}{p_c(t)}\right)^{\frac{2}{\kappa}} - \left(\frac{p_d(t)}{p_c(t)}\right)^{\frac{\kappa+1}{\kappa}}\right)}$	(3.7.34)

Table 5 Time-dependent variables - discharge phase

3.7.3 Valves Closed

In cases where both valves are closed, i.e. with no mass transfer in the cylinder, the following system of ODEs comes into action:

cylinder	*mass equation*	$\frac{dm_c(t)}{dt} = 0$	(3.7.35)
	energy equation	$\frac{dp_c(t)}{dt} = -\kappa \frac{p_c(t)\, w_z(t)}{z(t)}$	(3.7.36)
suction piping system	*suction chamber energy equation*	$\frac{dp_s(t)}{dt} = \frac{\kappa}{V_s} \frac{p_{s0}}{\rho_{s0}}\, \theta_s(t)$	(3.7.37)
	suction chamber mass equation	$\frac{d\rho_s(t)}{dt} = \frac{1}{V_s} \Theta_s(t)$	(3.7.38)
	suction line dynamics equation	$\frac{d\Theta_s(t)}{dt} = \frac{A_s}{L_s}\left(p_{s0} - p_s(t)\right) - \frac{\xi_s}{2L_s A_s \rho_{s0}} \Theta_s^2(t)$	(3.7.39)
discharge piping system	*discharge chamber energy equation*	$\frac{dp_d(t)}{dt} = -\frac{\kappa}{V_d} \frac{p_d(t)}{\rho_d(t)}\, \Theta_d(t)$	(3.7.40)
	discharge chamber mass equation	$\frac{d\rho_d(t)}{dt} = -\frac{1}{V_d} \Theta_d(t)$	(3.7.41)
	discharge line dynamics equation	$\frac{d\Theta_d(t)}{dt} = \frac{A_d}{L_d}(p_d(t) - p_{d0}) - \frac{\xi_d}{2L_d A_d \rho_d(t)} \Theta_d^2(t)$	(3.7.42)

Table 6 System of ODEs – closed valves

It is obvious that only seven unknown variables are solved in this case, namely $p_c, p_s, p_d, \rho_s, \rho_d, \Theta_s, \Theta_d$.

3.7.4 Conditions for Transition

In the table below we summarize the conditions, which will be implemented inside the tool in order to switch between the phases of a compression cycle and thus to solve the corresponding system of differential equations.

valves closed	→	*suction phase with valve plate moving*	$p_s A_{p,s} - p_c A_{v,s} > F_{s,s} + F_{adh,s}$	(3.7.43)
	←		$x_s = 0$	(3.7.44)
suction phase with valve plate moving	→	*suction phase with fully open valve*	$x_s = h_s$	(3.7.45)
	←		$F_{s,s} > F_{g,s} + F_{adh,s}$	(3.7.46)
valves closed	→	*discharge phase with valve plate moving*	$p_c A_{p,d} - p_d A_{v,d} > F_{s,d} + F_{adh,d}$	(3.7.47)
	←		$x_d = 0$	(3.7.48)
discharge phase with valve plate moving	→	*discharge phase with fully open valve*	$x_d = h_d$	(3.7.49)
	←		$F_{s,d} > F_{g,d} + F_{adh,d}$	(3.7.50)

Table 7 Conditions for transition

When the phase changes and a new system of ODEs is about to be solved, a new vector of initial conditions for it is, quite naturally, needed. Usually the initial conditions agree with the last values of the variables at the designated time-step, after which the solving of the previous system was terminated.

An exception lies in the case where a phase transition will be made based on Eqs. 3.7.44, 3.7.45, 3.7.48 or 3.7.49, where one must deal with a rebound before the transition can proceed. This means that when a valve plate touches an obstacle (seat or guard), the phase will not change immediately and instead the same system of differential equations will be solved anew, however, with the initial conditions, in which the initial velocity of the plate will be calculated as $-c_r w_{last}$, wherein c_r stands for the coefficient of restitution and w_{last} denotes the velocity in the moment of impact. This is repeated until the initial velocity is very low, then the phase transition will proceed. For the actual implementation, see chapter 4.3.1.

3.7.5 Input Parameters

Finally, lets summarize the variables, which are considered to be input parameters in the mathematical model, i.e. the value of all these forty parameters has to be given. Bear in mind that all of them are required to be in basic SI units in the developed simulation tool.

Ideal gas	
heat capacity ratio	κ
ideal gas constant	r
Crank mechanism	
connecting rod length	L
cylinder diameter	D_c
clearance length	z_0
angular velocity of the crankshaft	ω
radius of the crankshaft	R
Suction valve	
spring preload deflection	$x_{0,s}$
maximum valve plate lift	h_s
spring stiffness	k_s
mass (plate with equivalent of spring)	m_s
valve plate diameter	$D_{v,s}$
valve port diameter	$D_{p,s}$
coefficient of restitution	$c_{r,s}$
friction coefficient	$c_{f,s}$
flow coefficient	α_s
Adhesion	
surface tension	γ_{LG}
meniscus contact angle	β
oil film thickness	h_{film}

Discharge valve	
spring preload deflection	$x_{0,d}$
maximum valve plate lift	h_d
spring stiffness	k_d
mass (plate with equivalent of spring)	m_d
valve plate diameter	$D_{v,d}$
valve port diameter	$D_{p,d}$
coefficient of restitution	$c_{r,d}$
friction coefficient	$c_{f,d}$
flow coefficient	α_d
Suction piping system	
static pressure in steady-state reservoir	p_{s0}
static temperature in the reservoir	T_{s0}
volume of the suction chamber	V_s
effective length of the suction pipe	L_s
effective cross-sectional area of the pipe	A_s
loss coefficient in the suction pipe	ξ_s
Discharge piping system	
static pressure in steady-state reservoir	p_{d0}
static temperature in the reservoir	T_{d0}
volume of the discharge chamber	V_d
effective length of the discharge pipe	L_d
effective cross-sectional area of the pipe	A_d
loss coefficient in the discharge pipe	ξ_d

Table 8 Input parameters

4 Developing the Simulation Tool

This chapter is devoted to the process of building the tool, in which the valve behavior is predicted based on the given parameters of the compressor, the undertaking of which is the third task of this thesis. Moreover, one can consider this section to be an elaboration of the mathematical model, since in this chapter we bring the model to life.

Firstly, we discuss the structure of the program as well as the reasons why object-oriented programming (OOP) is used; we then look at the way how the equations are handled and the system into which it is integrated. Finally, the methods one can utilize to run the simulator are presented.

One should bear in mind however, that the whole simulation tool is composed of more than three thousand lines of code in total and thus it is impractical to describe the meaning of every line in this text. However, this is not required anyway, because the code itself is thoroughly and conscientiously annotated, so that one can easily figure out its functions. Hence, only the main principles and ideas are discussed in the following subchapters, so that the reader can grasp the concept of the tool and can not only use it properly but is also able to further modify it, if the need arises.

Last but not least, the tool is built in the commercially available software MATLAB in version 2016b, for which we own the student license. Be aware that the faultless functioning of the tool in older versions of MATLAB cannot be guaranteed.

4.1 General Remarks

4.1.1 Simulation Tool Requirements

In the section regarding the Purpose of Research, it was stated that the mathematical model should be implemented, while keeping its properties, i.e. its versatility and customizability. The essential question is however, what do we mean by this? Regarding the latter, consider the mathematical model as it was first proposed, i.e. that it includes various phenomena (e.g. rebound, pressure pulsations in the piping etc.) while omitting others (e.g. heat transfer through the cylinder etc.). If all of the equations describing these processes were to be merged together - providing us with a system of ODEs to solve without other additional ancillary equations - the model could very easily be implemented. But such an attitude would result in a complete waste of customizability, since additional changes in the equations would be, simply put, impractical. One could ask however, what about its versatility? Recall the types of compressor models (chapter 3.1.2), in which the valve dynamics can be studied. The model proposed in this thesis is a complete one, i.e. besides other things it includes the influence of the piping system on valve dynamics. On the other hand, the fly in the ointment here lies in the fact that in order to evaluate the influence rate,

it is also indispensable to simulate the valve dynamics without the pressure pulsations. It goes without saying that this holds true for other phenomena as well.

Among the phenomena, which influence valve behavior and are implemented in such a way, that they can be excluded from the simulation, are the following:

- rebound
- friction
- adhesion
- pressure pulsations in piping systems

4.1.2 Object-Oriented Programming

To fulfill the requirements, it is basically essential to keep the equations separated and to figure out a way how to combine them with ease in order to arrive at a system of equations that can be eventually solved. Basically, two approaches seem to make sense; either utilizing symbolic variables and expressions, or the use of function handles.

In the former method, the equations and variables would be defined as symbolic ones, then they could automatically be merged together and thus a system of symbolic equations would arise. However, since the system of ODEs, which is striven to be solved, is non-linear, the solution generally cannot be found explicitly and one must rely on numerical methods. Hence, the symbolic system must be converted to a non-symbolic one, which can be solved numerically later on. This is actually the pitfall of this approach, since according to our tests, the elapsed time needed to arrive at a solution is unsuitable, i.e. more than 25x higher in comparison with the latter approach.[6]

The latter approach, which is applied in this thesis, works on the presumption that the equations could be merged through function handles and thus evading the need for symbolic expressions. Simply put, instead of using substitution from one equation to another, function handles are used as input arguments for other functions; a detailed example is given in section 4.2.2.2. The merit of this method lies in the fact that one can avoid the conversion between symbolic and non-symbolic notation and thus rapidly reduce the computational time, but the drawback is that the code could very easily become unreadable and tangled, if not implemented properly.

The decision to utilize the programming paradigm based on the concept of objects seems now rather straightforward since it provides us with an elegant way to maintain the desired characteristics of the tool while keeping the code well-structured and thus easily readable. As a matter of fact, the OOP could help us achieve much more (such as data protection, general pattern creation and so on.), if we pursued things like encapsulation, inheritance,

[6] Bear in mind that the elapsed time for solving the equations (for one compressor cycle) in the last version of the tool is about three minutes (measured on a PC with 8 GB of RAM, Intel Core i7-3720QM) and thus with the symbolic approach, the elapsed time could easily exceed one hour.

or polymorphism. However, it would be, on the one hand, far beyond the scope of this thesis, and on the other hand, there would be no benefit for the purpose of study of valve behavior.

4.1.3 Structure of the Tool

The file structure of the tool comprises four files, namely

- *ReciprocatingCompressor_app.mlapp*
- *runTool.m*
- *ReciprocatingCompressor_class.m*
- *defaultParameters.m*

Either one of the former two files can be used to run the tool; these are discussed later in corresponding chapter 4.4. In the meantime, we will go through the penultimate file, i.e. *ReciprocatingCompressor_class.m*, which contains all the crucial parts of the simulation tool, i.e. from the assignment of equations, going through their solution and then on to the post-processing. The lastly-named file represents an auxiliary function solely for defining numerical values of input parameters and thus no special chapter is needed there.

4.2 Class Structure

The entire compressor model is implemented into a class (*ReciprocatingCompressor_class.m*), which is derived from the generic *handle* class. The compressor class encapsulates the properties and methods, i.e. the operations performed on the properties. The general structure of this class is outlined in Figure 27.

4.2.1 Class Properties

Regarding the class properties, they are divided, mainly for the purpose of clarity, into two categories and those in turn into subcategories. The first category, called the *Mathematical model* stores data regarding the mathematical model. For example, in the first subcategory called *Constants*, there are defined variables which are used later on to store the values of the input data, i.e. the quantities already defined in Table 8. The constant quantities, which are calculated from these input parameters, i.e. they do not change with time, are defined in the second subcategory *Constant Calculated Parameters*. Then, there is a subcategory labeled *Type of Compressor*, in which the variables, through which one can turn the effects influencing valve dynamics on or off, are defined. These groups of properties discussed up to now, are non-dependent properties, i.e. they store data. However, the last subcategory marked as *Time-dependent parameters & Equations* unites dependent properties, i.e. their value depends on some other value, such as time or the value of a non-dependent property.

```
classdef ReciprocatingCompressor_class < handle

  %% MATHEMATICAL MODEL
     properties (Access = public)     % Constants (Input data)
     properties (Access = public)     % Constant Calculated Parameters
     properties (Access = public)     % Type of Compressor
     properties (Dependent = true)    % Time-dependent parameters & Equations

  %% TOOL PARAMETERS
     properties (Access = public)     % Constant Tool Parameters
     properties (Dependent = true)    % Time-dependent Tool Parameters

  %% METHODS
     methods
        %% CLASS CONSTRUCTOR
           function obj = ReciprocatingCompressor_developer(varargin)

        %% GET-ACCESS METHODS FOR DEPENDENT PROPERTIES
           %% Time-dependent Properties
           %% Differential Equations
           %% Conditions For Transition

        %% SOLVING CYCLE & VALVE DYNAMICS

        %% POST-PROCESSING
     end
end
```

Figure 27 Structure of the compressor class

The second category, i.e. *Tool Parameters* is used to store data necessary for the flawless function of the tool. It consists of two subcategories, where the first one unites the non-dependent properties, e.g. the current phase of the compressor cycle etc., whereas the second one stores the dependent properties, e.g. the number of completed compressor cycles etc.

Bear in mind that our class properties merely define the name of variables, not their value. Values are assigned later on either in a class constructor (for non-dependent properties) or by *get-access* methods (for dependent properties).

4.2.2 Class Methods

The methods in the class are divided into four categories according to their purpose. Firstly, there is a *class constructer* method needed to create instances of the class. Then, there is a group of *get-access* methods, which are necessary to retrieve the value of the dependent properties. The insight into these two types of methods is given later in this subchapter.

The third group unites the functions, which are requisite for handling either the transition between the phases of the compression cycle (and thus the system of ODEs), or from the perspective of the integration of the ODEs as such. Since the essence of the entire simulation

tool lies in this part of the code, the detailed description of the process going on there is given in a separate chapter 4.3.

Finally, there is a group in which are joined together methods for the post-processing of the results, e.g. plotting the $p - V$ diagram of the cycle, plotting the lift of valves as a function of time, etc. Since these methods are very comprehensible, they are not described further in-depth in the text of this thesis.

4.2.2.1 Class Constructor

In simple terms, a class provides a definition for objects of its type, i.e. it specifies certain characteristics that all *instances* of that class share. To create an instance of a class with initialized values of all the non-dependent properties, a special function, generally known as the *class constructor,* is implicitly required. The name of this method must correspond to the name of the class; hence, in our case its name is *ReciprocatingCompressor_class*.

The constructor accepts one input argument (Figure 28), thereby a structure array of values of given input data. This structure array is created simultaneously with a function, which can be found inside the file called *defaultParameters.m*. This way helps us to evade the necessity to fill all the forty parameters into a class constructor syntax, which would be, at least in our opinion, inconvenient.

```
newCompressor = ReciprocatingCompressor_class(parameters);
```

Figure 28 Class constructor (function syntax)

Barring the direct assignment of property values from the structure array, all the equations for the calculation of values of the non-dependent quantities, such as valve port area, valve plate area, etc., which are to be calculated only once during the initialization of the class instance, are all found further inside this method.

4.2.2.2 Get-access Methods

Since dependent properties do not store data, for each one of them a *get-access* method needs to be defined. Its function is to determine a value for the property when the property is queried. However, by this value we do not strictly mean a numerical value, but rather the equation according to which the numerical value of that property will be calculated later on, during the moment when the system of ODEs is being solved. For this purpose, the *get-access* methods in our class returns a function handle in most cases.

Get-access Methods for Equations

For a deeper understanding of linking the equations between each other, let us look at, for example, a value for the dependent V_c property (i.e. the cylinder volume), which depends on the value of another dependent property z (i.e. the piston displacement). The *get-access* methods for both dependent properties are to be found below respectively.

```
function value = get.V_c(obj)   % Cylinder volume
     value = @(vars) obj.A_c * obj.z(vars);
end
```

Figure 29 Get-access method for cylinder volume

```
function value = get.z(obj)      % Piston dispacement
     value = @(vars) obj.z_0 + obj.L + obj.R - ...
                     sqrt(obj.L^2-obj.R^2*(sin(obj.omega*vars.t)).^2) - ...
                     obj.R*cos(obj.omega*vars.t);
end
```

Figure 30 Get-access method for piston displacement

When the V_c property is queried, the *get.V_c* method queries the z property before retrieving the V_c property, i.e. result would eventually be following:

```
value = @(vars) obj.A_c * (obj.z_0 + obj.L + obj.R - ...
                sqrt(obj.L^2-obj.R^2*(sin(obj.omega*vars.t)).^2) - ...
                obj.R*cos(obj.omega*vars.t));
```

Figure 31 Resulting equation for cylinder volume

This example nicely shows the reader, how by calling the class properties representing the equations between themselves, one can in a polished way link the equations together without losing any of their potential customizability. For instance, if one wanted to simulate the valve behavior in a compressor, in which the crank mechanism does not drive the piston movement, he would basically only modify the equation concerning the z property.

Furthermore, the *get-access* methods effortlessly allow us to handle the turning effects influencing the valve behavior on or off. The illustration of this can be demonstrated on a property, which stands for the friction force, see Figure 32.

```
function value = get.F_fs(obj)      % Friction force - suction valve
   if obj.dynamics_friction
      value = @(vars) obj.c_fs*vars.v_xs;
   else
      value = @(vars) 0;
   end
end
```

Figure 32 Get-access method for friction force (suction valve)

In this example the value, which the *get-access* method returns, depends on the logical value of the property called *dynamics_friction*. If this value is *false*, then the *get-access* method returns a zero value of the friction force, and thus this kind of force is not taken into account at all.

Get-access Methods for Conditions for Transition

The *get-access* methods for dependent properties, in which the conditions for transition are defined, differ from the *get-access* methods for equations by not returning the function handle. Instead, a logical value (*true/false*) is returned. The result of a logical 1 (*true*) is always returned in cases, where a condition is fulfilled, i.e. the according to the condition a transition between the phases of the compression cycle is required. Otherwise, a logical 0 (*false*) will be returned. The example of the code is given in Figure 33. In this code sample one might also observe how the stiction effect is left out if the value of the property *dynamics_stiction* is set to false.

```
function value = get.cond_startSuction(obj)      % Condition for suction phase beginning
   if obj.dynamics_stiction
      value = @(p_s,p_c) ((p_s*obj.A_ps - p_c*obj.A_vs) >= ...
                          (obj.F_ss0 + obj.F_sadhseat));
   else
      value = @(p_s,p_c) ((p_s*obj.A_ps - p_c*obj.A_vs) >= (obj.F_ss0));
   end
end
```

Figure 33 Get-access method for condition to move onto the suction phase

4.3 Solving the Compressor Cycle and Valve Dynamics

In the preceding paragraphs, the reader has been introduced into the means of development of our tool for predicting compressor valve behavior. Among other things, it was discussed how the equations are linked between each other and thus how the system of ODEs to integrate can be put together. Nonetheless, there has yet to have shed light on two key elements so far; the handling of the integration of the system of equations and the workings of switching between them.

The general structure of these processes follows from the simplified functional diagram, which is given in Figure 34. By following the arrows one can find the consequences of the main actions taken by the simulation tool. Any ancillary details such as the actual procedures to integrate the ODEs, the procedures taking place when the results are saved in a tabular form etc. have been omitted.

Every **rectangle** in the diagram contains an action, e.g. assigning a value, breaking a *for-cycle*, etc. Each **polygon** refers to a condition that needs to be tested. Last but not least, **rounded rectangles** denote the beginning of a repetitive process, typically the beginning of a *for-cycle*.

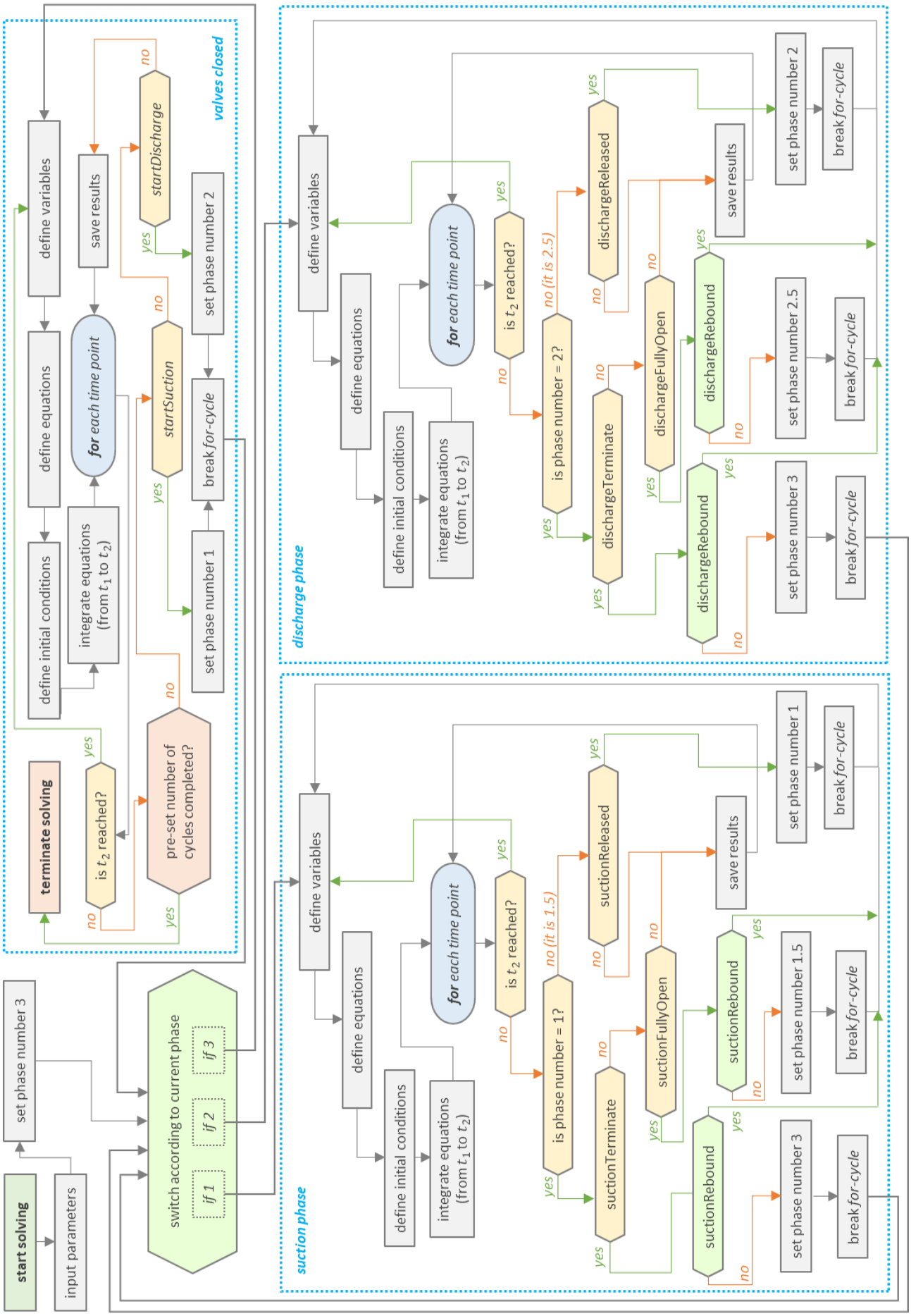

Figure 34 Functional diagram of solving cycle & valve dynamics

4.3.1 Switching Between Compressor Phases

From the mathematical model one can see that in order to obtain the valve behavior of the entire compressor cycle, it is necessary to distinguish between the processes, from which the cycle is composed of, i.e. suction, discharge, expansion and compression. Moreover, in cases where either a suction or discharge phase takes place, one must also distinguish whether the valve plate is in direct contact with the limiter or not. Furthermore, the transition to the former cannot be done immediately, because initially a rebound must be considered.

A certain simplification can be made regarding the expansion and compression, since the mathematical description for these is the same. Hence, they can be generalized into a single phase, which is henceforth labeled as *valves closed*. Furthermore, if we embrace a prerequisite that the compressor cycle starts and ends at a point, when both valves are being closed, then the suction/discharge phase with a fully open valve can be included as a limiting case in the suction/discharge phase with the valve plate in motion. Hence, the entire compressor cycle can be composed of three main phases; *suction*, *discharge* and *valves closed* - as can be seen from the functional diagram. In the simulation tool, a property called *phase* is defined, in which the ongoing phase of the compressor cycle is stored as a numerical value. The relation between the compressor phase and to its corresponding numerical value is listed in the following table.

suction phase with valve plate in motion	*1*
suction phase with fully open valve	*1.5*
discharge phase with valve plate in motion	*2*
discharge phase with fully open valve	*2.5*
valves closed	*3*

Table 9 Numerical representation of compressor phase

Naturally, several logic operations need to be carried out in order to determine the phase transitions and so as to compose the corresponding system of ODEs that can be eventually integrated. In the functional diagram, the conditions for transition are depicted in yellow polygons within a *for-cycle*. Table 10 links their string representation (i.e. class property name) to the actual equation from chapter 3.7.4. It is felt that it might be beneficial to not include solely the reference number, but also the equation as such in that table, since it will be needed shortly.

	Name of Condition	*Phase Transition*			*Equation*	
suction	*suctionTerminate*	*1*	→	*3*	(3.7.44)	$x_s = 0$
	suctionFullyOpen	*1*	→	*1.5*	(3.7.45)	$x_s = h_s$
	suctionReleased	*1.5*	→	*1*	(3.7.46)	$F_{s,s} > F_{g,s} + F_{adh,s}$
discharge	*dischargeTerminate*	*2*	→	*3*	(3.7.48)	$x_d = 0$
	dischargeFullyOpen	*2*	→	*2.5*	(3.7.49)	$x_d = h_d$
	dischargeeReleased	*2.5*	→	*2*	(3.7.50)	$F_{s,d} > F_{g,d} + F_{adh,d}$
valves closed	*startSuction*	*3*	→	*1*	(3.7.43)	$p_s A_{p,s} - p_c A_{v,s} > F_{s,s} + F_{adh,s}$
	startDischarge	*3*	→	*2*	(3.7.47)	$p_c A_{p,d} - p_d A_{v,d} > F_{s,d} + F_{adh,d}$

Table 10 Condition for transitions - property names & equations

As mentioned before, in order to solve a non-linear system of differential equations, one must typically rely on a numerical scheme to accurately approximate the solution. Regardless of the numerical method, a solution will be obtained as a set of discrete points instead of being continuous. This brings about a severe difficulty in the implementation of the conditions for the transition, specifically the ones with the equal sign.

Consider the suction valve plate to be moving towards the seat, leaving aside a rebound for a while. According to the conditions for the transition, in order to proceed from the suction phase to the phase with closed valves, the valve plate lift must equal zero. However, the resulting lift is in a form of discrete points (Figure 35) and thus, it would be irrational to expect that the solution will be received at such a time point, when the valve plate lift equals exactly zero. An analogous situation comes when the valve plate moves towards the limiter.

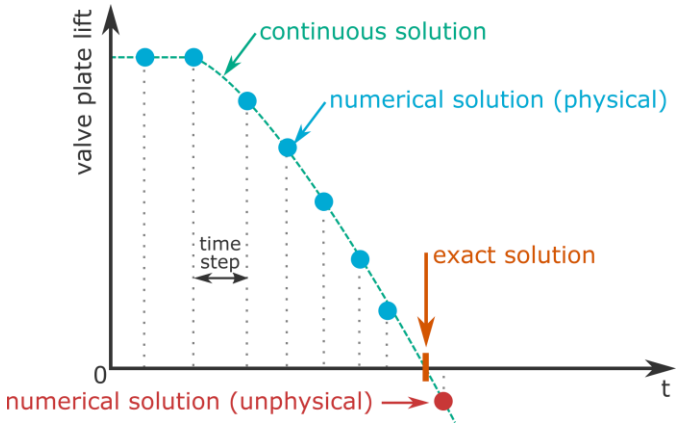

Figure 35 Continuous & numerical solution

It follows that the conditions for the transition with the equal sign need to be modified, but with regard to their meaning as well as to their physical admissibility. The altered conditions for the transition are to be found in Table 11 and the explanation of the implementation comes promptly afterwards.

	Name of Condition	*Phase Transition*			*Modified Equation*
suction	*suctionTerminate*	*1*	→	*3*	$x_s \leq 0$
	suctionFullyOpen	*1*	→	*1.5*	$x_s \geq h_s$
discharge	*dischargeTerminate*	*2*	→	*3*	$x_d \leq 0$
	dischargeFullyOpen	*2*	→	*2.5*	$x_d \geq h_d$

Table 11 Modified conditions for transition

It goes without saying that such a modification allows us to implement with ease the conditions for the transition; however, should no further action be carried out, the physical admissibility will be lost, since the conditions will be, by a large majority, fulfilled thanks to the inequality sign. It would mean, for example, that a condition is fulfilled when the valve plate lift is negative, which is not possible from the physical point of view. To avoid such dubious situations, an ingenious trick is used that one can figure out from the functional diagram (Figure 34).

Basically, in every time-step it is tested whether the solution fulfills a condition for transition related to the current compressor phase; if it does not then this solution is saved into the results. However, should it fulfill a condition for transition, then the phase transition proceeds but without saving the solution, since it is in all likelihood an unphysical solution. The last-saved solution will be used for the composition of initial conditions for the successive compressor phase; however, quantities such as valve plate lift or its velocity will be adjusted so that they correspond to the exact value it was aimed at. Apropos of this manual adjustment, there is virtually no influence over the results since this is rather a cosmetic alteration of the results. For example, it was observed that in the default compressor setup the difference between the last physical numerical solution of the valve plate lift and its aimed value is less than one-ten-thousandth of the lift.

Rebound

In the subsequent paragraphs, we will shed light on the way how the rebound effect is handled by the conditions for the transition. It is needless to say that in cases, where no rebound applies, the phase transitions based on conditions *suctionFullyOpen, suctionTerminate, dischargeFullyOpen* or *dischargeTerminate* will proceed instantly. However, should rebound be considered, these aforesaid phase transitions need to be postponed until the effect of rebound is over.

The rebound is to be taken into account through initial conditions indispensable for the time-dependent system of ODEs, specifically the initial velocity, which is calculated per Eq. 3.4.14 stated in chapter 3.4.3.3. This equation can be worded as follows: the initial valve plate velocity for the succeeding phase is equal to its velocity prior to the impact multiplied by the coefficient of restitution.

Technically speaking, the valve plate will bounce unless the impact velocity equals zero. It stands to reason that in real-life the bouncing effect is influenced and attenuated by other factors such as oil film etc. and thus, should the rebound velocity be sufficiently small, one can consider the bouncing effect to be overcome. In the same manner, the handling of the rebound effect is implemented in the simulation tool. Hence, the meaning of the conditions depicted in the functional diagram (Figure 34) in the light green polygons within a *for-cycle* are stated in the following table:

Name of Condition	*Condition*	*Allows phase transition*		
suctionRebound	$\left\|\frac{dx_s}{dt}\right\|_{t^+}\| < \epsilon_s$	*1*	→	*1.5*
		1	→	*3*
dischargeRebound	$\left\|\frac{dx_d}{dt}\right\|_{t^+}\| < \epsilon_d$	*2*	→	*2.5*
		2	→	*3*

Table 12 Conditions for rebound

Naturally, the magnitude of the tolerances ϵ_s and ϵ_d is the backbone of the decision whether the phase transition can be carried out or not. The potential failure of the transition towards a phase with a *fully open valve* does not bring about any issues, whereas the failure of the transition towards the *valves closed* phase does. If this phase transition fails to carry out, the simulator tool cannot terminate the solving of compressor cycle due to the presumption that the compressor cycle starts and ends at a point, when both valves are being closed. Based on our tests with the simulator, it was found out that unless the value of ϵ is lower than one thousandth of maximum valve plate lift[7], no failure occurs. Since the valve plate lift is customarily in units of millimeters, the tolerance can be considered to be sufficiently small to influence the results.

Additional Remarks

The implementation of the mathematical model presented in this thesis represents an innovative alternative to the implementation of similar mathematical models pertaining to valve dynamics, since in our model the proceeding of phase transitions from one phase to another solely depends on the immediate position of the valve plate, which is solely driven by the instantaneous thermodynamic states of gas in the cylinder and the plenum chambers. This is first and foremost in capturing the proper and arbitrary automatic valve behavior and it has been accomplished by the proposed logic operations in the functional diagram, the implementation of which was facilitated by utilizing the OOP.

For instance, in the model by Touber [12], the simulation of valve behavior is dependent on reference pressures and checkpoints. The former controls when the discharge or suction phase should occur, whereas the latter controls the sequence of events (e.g. bouncing valve

[7] Evidently, the smaller the time step is, the smaller the magnitude of the tolerance that can be chosen. The stated one-thousandth is valid for the default settings of the ODE solver, discussed later on in chapter 4.3.2.1.

plate, touching limiter etc.) The shortcomings of such an approach lie in the fact that the success of the simulation is dependent on the right choice of reference pressures, and moreover, the predefined (expected) sequence of events does not permit the simulation of arbitrary cases (such as the one, where the valve plate does not reach the limiter due to the chosen high maximum lift).

4.3.2 Integration of ODEs

In the preceding paragraphs, it was stated that in order to solve a non-linear system of differential equations, one must typically rely on a numerical scheme to accurately approximate the solution. The reader can also grasp the idea of the kind of difficulties that are brought about by this in terms of conditions for transition.

Further on inside this chapter, let us give an insight into the process of the integration as such, which begins with the definition of unknown variables, continues with defining the system of ODEs and its initial conditions to finish with the process of integration itself.

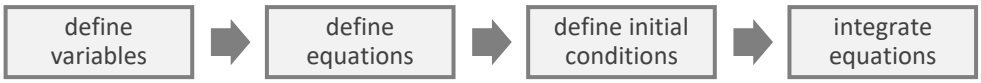

Figure 36 Process of integration of ODEs

4.3.2.1 Numerical Method of Integration

For solving the initial value problem, it was decided to utilize, presumably by far the most popular and powerful general-purpose numerical method, the *Runge-Kutta Method*. The mathematical description of this method exceeds the scope of this thesis and thus the interested reader is referred to corresponding literature [33].

The *six-stage, fifth-order accurate Runge-Kutta* method based on an algorithm of Dormand and Prince is integrated into MATLAB as a function called *ode45* [34] [35]; its syntax is the following:

```
[T,Y] = ode45(@(t,y)eqns,timeSpan,init,options);
```

Figure 37 Function syntax of ode45

This function integrates the system of ODEs - *eqns* - with the initial conditions *init* over a given time range *timeSpan*, i.e. from t_1 to t_2, returning results Y at time-points T within this time range. It shall be pointed out that the time-points are not equally distributed, i.e. with an equal time-step, but a variable one is used instead.

The magnitude of the time-step can be considered to be a crucial parameter in view of the computational time consumption. The larger it is, the lower the computational time. However, it might be at the expense of the accuracy of the results. Generally speaking, larger time-steps are permissible, when the rate of change of the unknown variable is small; but should it be high, a smaller time-step is required.

It follows that utilizing a variable time-step is rather economical; however, it can also introduce some difficulties. Here we are about to get to the crux of the matter regarding the incorporation of the *for-cycle* into the functional diagram (Figure 34). If the time-step were fixed, its magnitude could be set (through the *options* parameter in the function syntax of *ode45*) to match the magnitude of the time range. In other words, the integration of ODEs could be carried out step-by-step and in each the conditions for the transition could be tested and thus to eliminate the unknowing of the moment when the integration process should be halted, i.e. time t_2, which defines the end of the time range.

However, the time-step in *ode45* is variable, meaning that its magnitude is not firmly preset and thus the solution is returned in a beforehand unknown number of time-steps within the time range, which needs to be defined in advance. But how can one provide time t_2 if it is not known? The explanation is to be found in Figure 38.

Assume a fixed predefined magnitude of the time range interval, in which the ODEs are integrated. Since the beginning of the time range t_1 is known, then t_2 is known as well. The solution is returned in several points within this time range. Using the *for-cycle* it is checked time-point by time-point whether the phase transition should occur. If so, then the for-cycle is halted and the rest of the time-points are dropped. Obviously, in cases, where a phase transition does not occur in any of the time-points, then the same system of ODEs is to be solved anew.

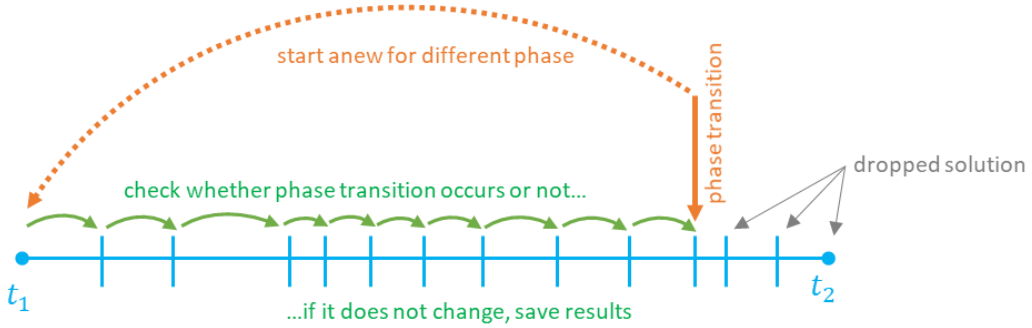

Figure 38 Schematic process of integration

During the development of the simulator, we modified the *ode45* function such that the variable time-step was removed and instead used the fixed one as described above, i.e. omitting the need of a *for-cycle*. Although it did work, it was a rather intense modification of a crucial function, which is neither officially documented nor recommended by *MathWorks* and thus we have rather decided for the approach with a *for-cycle* instead. However, it allowed us to compare the computational time of these two approaches. It was found out that, should the predefined magnitude of the time range be reasonably small (in our simulator it is used 1/100000 of the angular velocity of the crankshaft), then the influence of the computational time, which is caused by the fact that some solution might be unused, is truly negligible since it is being counterbalanced by the economical aspect of the variable-time step.

4.3.2.2 Defining Unknown Variables and Equations

As one of the hardest parts, one can consider the actual definition of the system of ODEs so that MATLAB understands it. There is a very specific way to define differential equations in MATLAB, as a function that takes one vector of variables (i.e. y in function syntax in Figure 37) in the differential equations, plus a time vector (i.e. t in Figure 37) as an argument. The *ode-solver* calls these vectors by default.

Here it comes to the *vars* input parameter in the function syntax of the dependent properties, such as with the z property in Figure 30, which was not purposely heeded thus far. This parameter refers to a structure array, in which the field names denote the unknown variables in the system of ODEs. Although this might seem marginal at first, in this, basically, resides the gimmick of omitting the need for either a symbolic approach or putting the equations together by hand, since the *vars* structure array will eventually be replaced by a vector, which is required from an ODE solver.

The reason why we do not evade this somewhat complicated procedure by working with that vector from the very beginning lies, for the sake of brevity, in maintaining the versatility of the tool. For a deeper understanding, assume once again that the influence of the piping systems is neglected. Then the number of ODEs will reduce, since the thermodynamic state of the gas in the plenum chambers will be considered to be independent of time and thus will be assumed to be known. As the number of ODEs is reduced, the number of unknown variables reduces. Owing to the fact, that the unknown variables are defined as fields in a structure array - which can be modified - it is very simple to replace them with a constant value instead of a reference to the vector field in y. For a graphic illustration, see Figure 39.

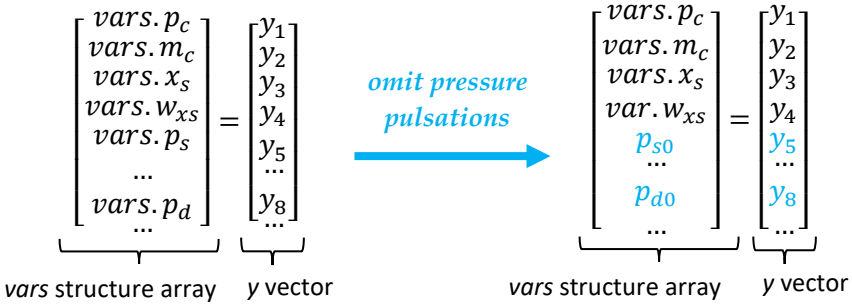

Figure 39 Variable structure array replacement by a vector

If the unknown variables were, from the very beginning, defined as vector elements of y instead of a field in a structure array *vars*, then it would not be possible to replace those unknown variables with a constant value, since this vector is called by the ODE solver and cannot be modified from outside.

4.3.2.3 Initial Conditions

To start with the integration process, it is prudent to assume values for each of the unknown variables at a time-point in the cycle. Between phase transitions, this does not introduce any difficulties, since the values at the end of the current integration process are used (with

modifications in cases of rebound) as the initial conditions for the subsequent one. However, in the very beginning, i.e. typically the zero-time point, prior data is generally not known.

If one were to solve the compressor model without a piping system, this would not present a severe difficulty since a convenient time-point could be chosen, typically the one when the piston is in a dead center and one can assume the valves to be closed. This would give us a good estimate on the initial conditions; however, if the same approach is to be applied in cases with a complete cycle, in which the estimation of the initial conditions is not as straightforward, it is necessary to let the simulator pass through several cycles to obtain a convergent solution. According to our tests with the simulator, at least four cycles should be completed before the results converge sufficiently.

4.4 Running the Simulation Tool

There are two possibilities to run the developed tool, either with a command line or a GUI. The latter can work solely in a version of MATLAB 2016b and later, since it is built in the *App Designer* environment. The former approach does not require the *App Designer* environment so it can be possible to run the app through this method in an older version of MATLAB.

However, be aware that both methods were thoroughly tested in the 2016b version. Although the command line method will work in older versions of MATLAB, it cannot be guaranteed that the tool itself will not run into troubles in these older versions, since with each version of the software, *MathWorks* implements changes into built-in functions, adding new ones while dropping support for others, which can ultimately result in incompatibilities.

4.4.1 Command Line

The commands, through which the simulator can be started and controlled, are found in the figure below, or with more examples and details in file *runTool.m*.

```
% Define values for input parameters
  inputParameters = defaultParameters;
% Create a new instance of compressor
  Compressor = ReciprocatingCompressor_class(inputParameters);
% Solve compressor cycle & Valve dynamics
  Compressor.solve_cycleDynamics;
% Plot results (by calling methods on the class)
   Compressor.plotResults('time');
```

Figure 40 Example of starting the application through set of commands

Firstly, a structure containing the values of input parameters is created; afterwards it is passed to the class constructor as an input parameter. The constructor creates a new instance of the compressor class and thus the methods can be called on that instance. To

solve the entire compressor cycle including the valve dynamics, the method *solve_cycleDynamics* is called. Lastly, the results are plotted by method *plotResults*.

4.4.2 Graphical User Interface

To eliminate typing the commands in a command window and moreover, to help ensure a certain level of user-friendliness, a GUI was created. It provides point-and-click control of all the options built inside the tool.

The GUI consists of six tabs, between which the user can switch via the title (top) bar of the application. In the bottom part, there is a status bar, which shows the current state of the application and thus provides the user with feedback. For example, if the application is busy, i.e. it is solving the compressor cycle and the valve dynamics, the background of this bar will turn amber; otherwise, it is green.

The tab called *Compressor Parameters* (Figure 41) is intended to be the home page of the application. Here, the user can define the compressor parameters, e.g. its dimensions, suction and discharge pressure, the phenomena of valve dynamics, etc. Naturally it is possible to create multiple compressors with different parameters and then compare their results.

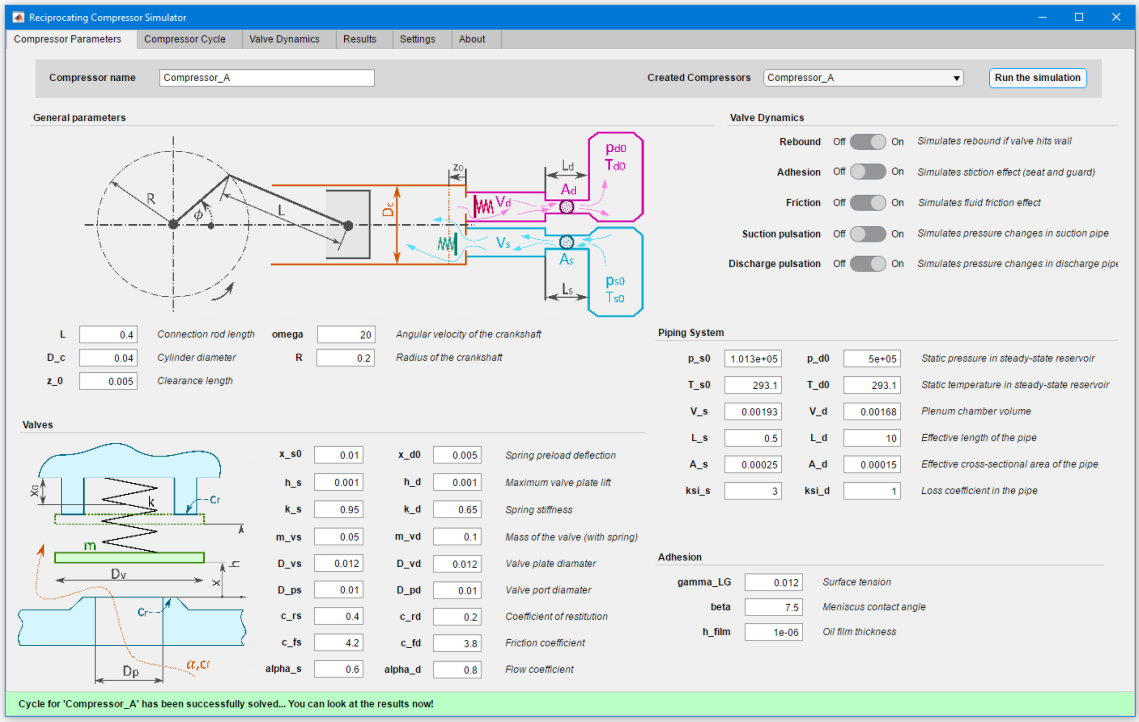

Figure 41 Home page of the application

The second tab - *Compressor Cycle* - depicts the *p-V* diagram of the entire compressor cycle, whereas in the third tab - *Valve Dynamics* (Figure 42) - one can find the significant quantities (valve plate lift, mass flow, pressure in the cylinder, etc.) as functions of time. A detailed summary of all the quantities recorded during the process of solving can be found in the

Results tab. Moreover, there is also an option to export results with the configuration and parameters of the compressor to a single *.xlsx* file.

The *Settings* tab (Figure 43) is a place where the user can define the magnitude of tolerances used for example in rebound conditions etc. In addition, a user can go through compressors he created to compare their results. The last tab - *About* - states the developer of the app, university, and title of this master thesis, of which it was a part of.

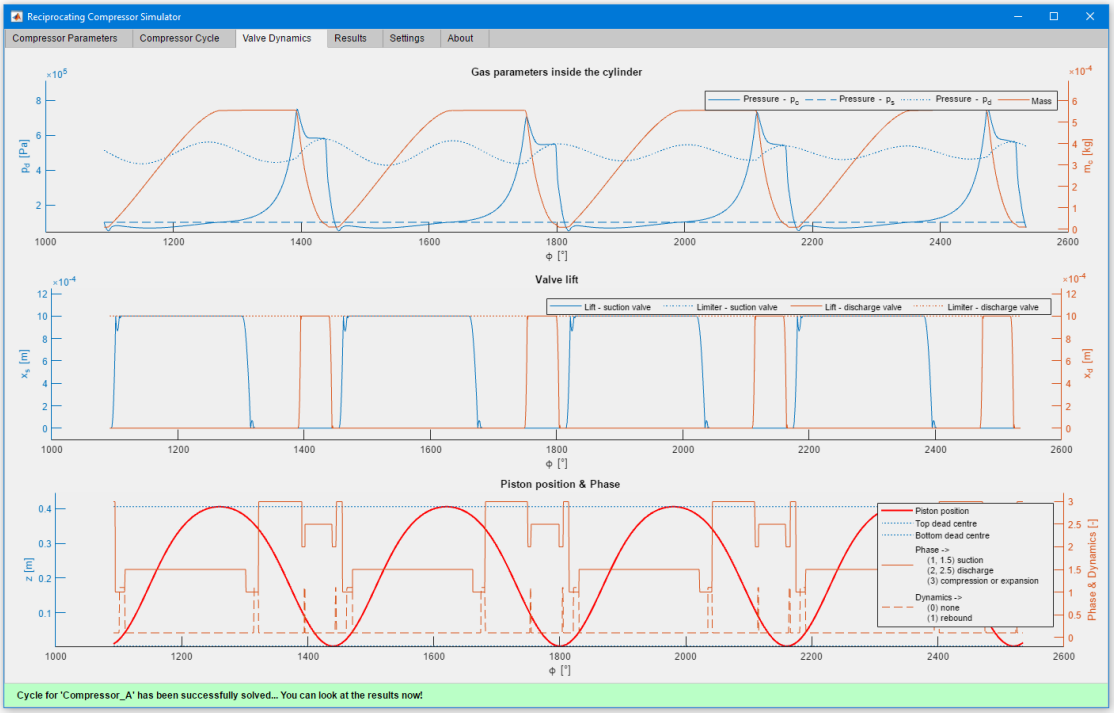

Figure 42 Valve dynamics page of the application

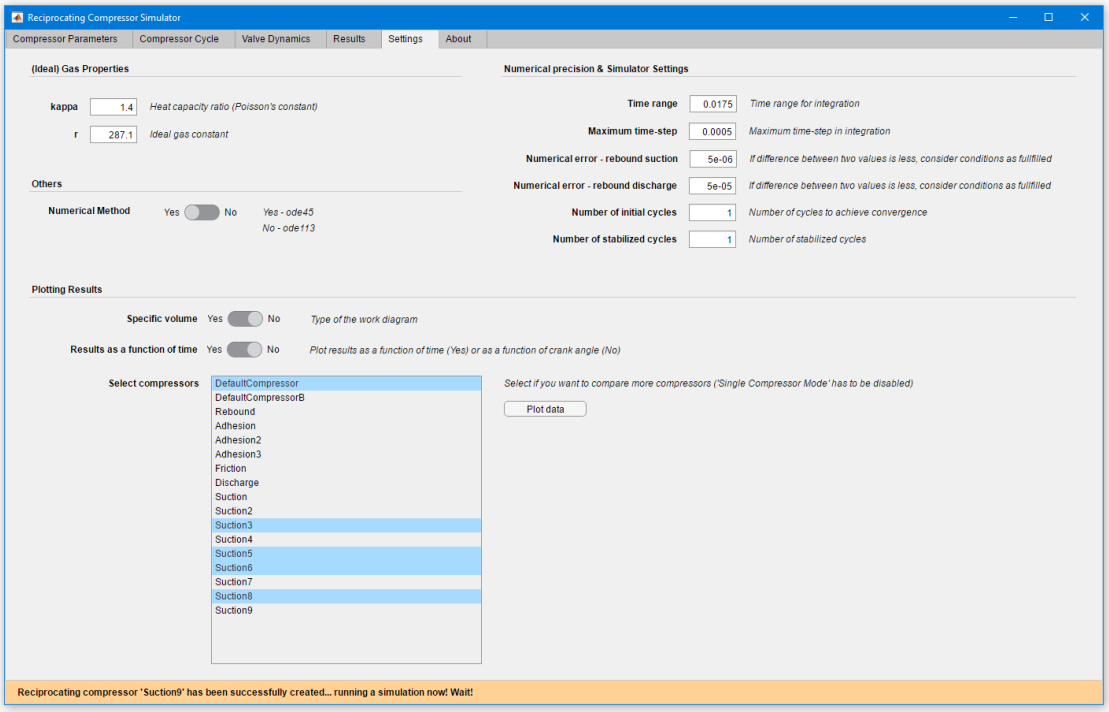

Figure 43 Settings tab of the application

5 Results of the Simulation

This chapter presents the results that were obtained with the developed simulation tool based on the proposed and extensively discussed mathematical model in the previous chapters of this thesis. At the outset, the results for the predefined valves and the compressor design will be pursued. Albeit it might segue from the current discourse it would not be altogether irrelevant to adduce here the deeper insight into the mathematical model and its dependencies on experimentally-obtained coefficients. Last but definitely not the least, the different valve parameters are taken into consideration in the final analysis to perform a study about their influence on valve behavior, while focusing on the individual valve dynamic effects and their mutual influence on the valve behavior as such.

5.1 Reference Compressor Configuration

The simulation tool offers an overview of compressor valve behavior by evaluating its dynamics under various working conditions or different valve geometries. In this section, the results obtained by the simulation tool for a default compressor setup are presented. This compressor comprises of a cylinder with a diameter of 120 mm with a stroke length of 90 mm. It compresses a gas from 1 bar to 3 bars, the suction valve plate diameter is 36 mm, whereas the discharge one is 38 mm. The valve port diameters are 34 and 36 mm respectively. The compressor speed is assumed to be modest with 300 rpm. For other parameters, see attachment A.

5.1.1 Variables as a Function of the Crank Angle

In the process of the simulation, there are thirty-four parameters, which are constantly being tracked and recorded. We do not aim to present each of them in the text of this thesis; however, the interested reader is referred to the enclosed DVD, where he can find the raw data extracted from the simulation. Among the parameters, which we have chosen to closely examine here and which are depicted in Figure 44 as a function of the crank angle, are:

- Valve plate lifts x_s, x_d
- Valve plate velocities w_{xs}, w_{xd}
- Cylinder pressure p_c
- Suction chamber pressure p_s
- Discharge chamber pressure p_d
- Piston displacement z

It should be pointed out, that in each of these plots, there is a crank angle on the x axis. The initial value is not zero due to the cycles passed prior to achieving a convergent solution (these are not depicted). Since in automatic valves, the beginning and the end of a compressor cycle is determined by the force balances on the valve plates, not the piston position itself, the cycle does not finish or start at the very moment, when the piston reaches a dead center.

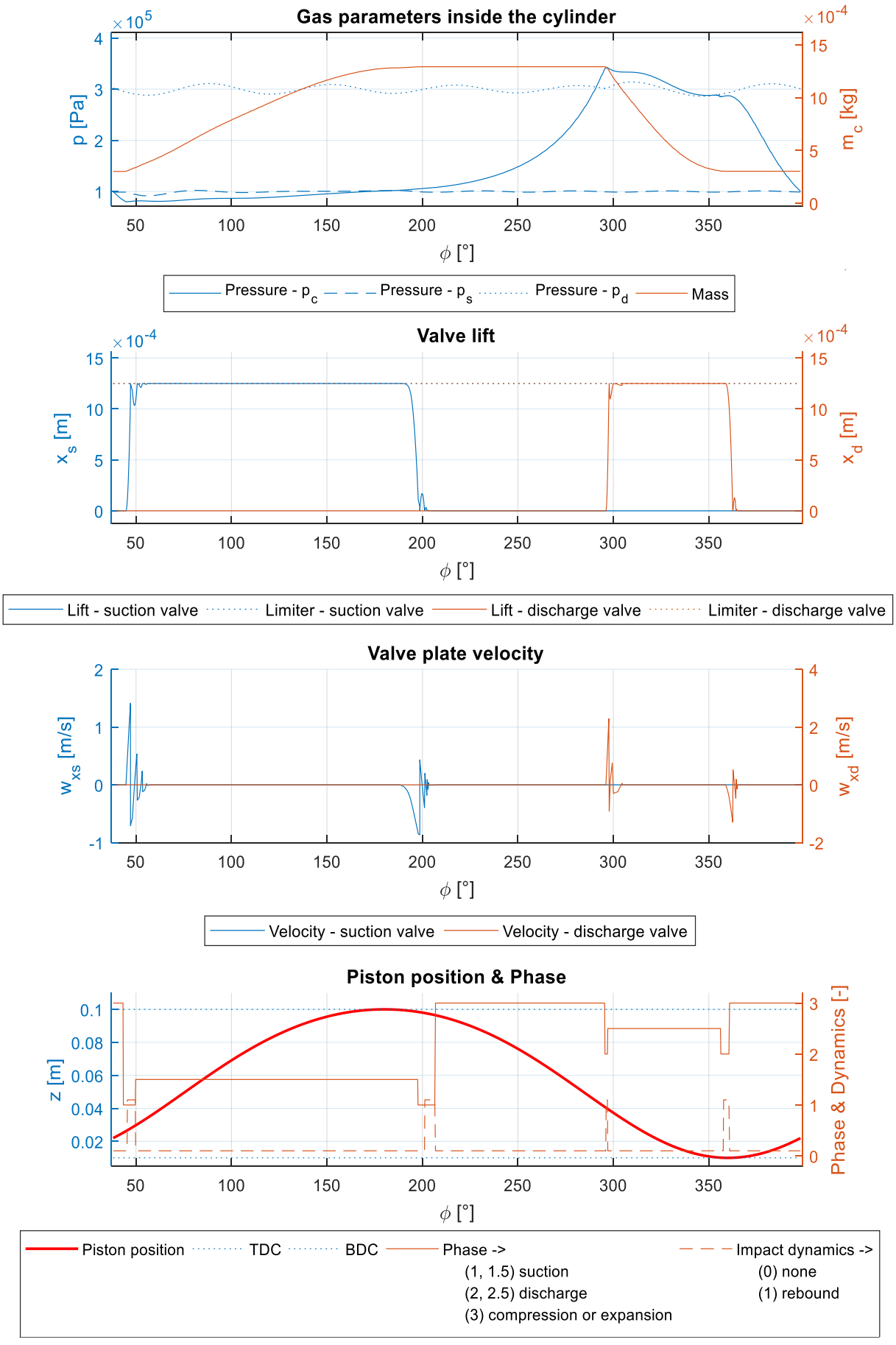

Figure 44 Results of the simulation for a default compressor setup

Turning our attention to the course of the pressure in the cylinder during the entire compressor cycle, it can be observed that, at first, as the piston moves towards the bottom dead center, thus increasing the volume of the cylinder, the pressure decreases until the pressure difference in front of and behind the valve plate balances the spring and the adhesion forces and thus allows for the suction valve plate to lift. The gas flowing into the cylinder causes the pressure inside to slowly, but steadily, rise. Once both the adhesion and the gas force are overbalanced by the spring force, the suction valve plate returns towards the seat, letting the compression phase progress. The course of the pressure inside of the cylinder during both the discharge and the expansion phases can be interpreted in a similar manner. However, it is worth noticing that due to different valve characteristics chosen in the simulation, the decrease in cylinder pressure (approx. 0.2 bar lower than p_{s0}) during the suction process is not as significant as the increase in cylinder pressure for the discharge phase (approx. 0.45 bar higher than p_{d0}). Moreover, during the discharge phase, there seems to be a relatively strong influence of pressure p_c by the pressure waves in the discharge plenum chamber, as one can observe that during this phase in question, the pressure p_c tends to slide over the p_d. This further supports the importance of a complete model, rather than a simplified pipe-less one.

Regarding the valves, one can find from the results that the duration of suction phase, i.e. the period, during which the suction valve plate is not in direct contact with a seat, is approx. twice as long as the duration of discharge phase. Moreover, one can see the rebound effect at the moment, when a valve plate strikes against an obstacle, i.e. a seat or a guard. In the velocity chart, one can observe the jump change of velocity in these moments, as was previously discussed in chapter 3.4.3.3 regarding valve plate impacts.

The last diagram depicts the piston displacement and its corresponding compressor cycle phase. Hence, one can observe that the closing of both the suction and the discharge valves, i.e. the transition to the expansion or compression phases, does not occur at the very moment of piston movement reversal (as would occur in mechanically operated valves). This delay is approx. 20° for the suction valve, whereas only 4° for the discharge one. Last but not least, this chart also provides the information about the beginning and the end of the bouncing effect (i.e. *Impact dynamics).*

5.1.2 Indicator Diagram

The indicator diagram of the compressor cycle, i.e. the variation of pressure and volume within the cylinder, is depicted in Figure 45. Moreover, here the fluctuating pressures in the adjacent plenum chambers are also shown. It should be emphasized that the areas below the suction pressure and above the discharge pressure refer to the contributions to the indicated work resulting from the pressure drops across each of the valves, i.e. these areas refer to the loss of energy (expressed in the form of indicated suction/discharge valve work) due to the deviation of real-life valve behavior from that of an idealistic one, as was

depicted earlier in Figure 12. Speaking in numbers, the indicated work is 139.5 J, the indicated suction/discharge valve work is 10.2 J and 14.4 J respectively. It implies that the work connected with the pressure drop across the suction valve accounts for 7.3% of the entire work done, whereas the contribution of pressure drops across the discharge valve is about 10.3%.

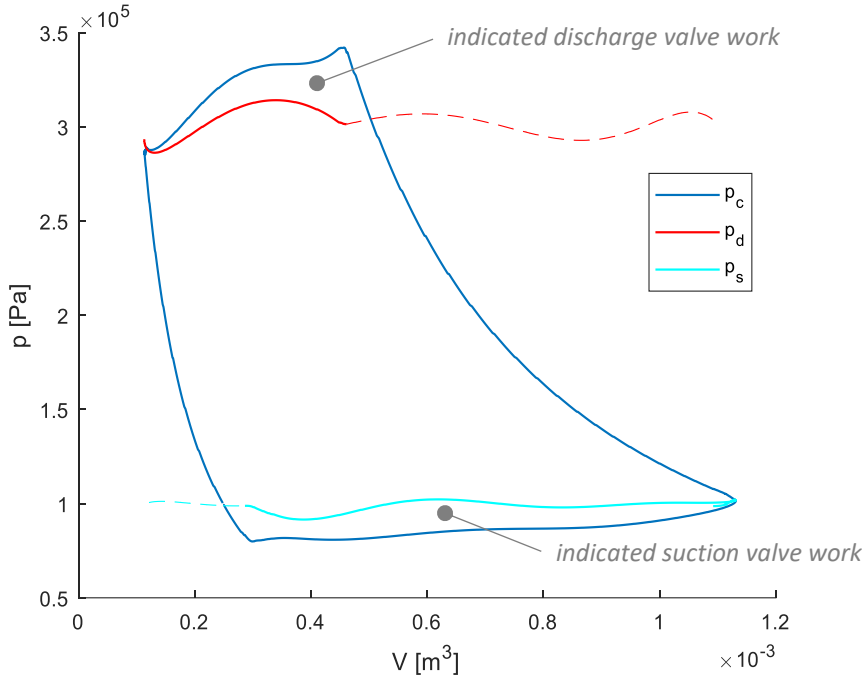

Figure 45 Indicator diagram for the default compressor setup

5.1.3 Comparison of the Results

In the very beginning of this thesis, it was stated that one of the drawbacks of this thesis involved the lack of an experiment to validate the proposed mathematical model and its implementation. To make the best of addressing this difficulty, the results will be compared with experimental data published in a book by Touber [12].

However, in order to properly validate the theoretically obtained results, they would have to be compared with experimental results obtained under the same operating conditions. As mentioned previously, not all of the dimensions of the compressor and its valves could be chosen to match the test compressor used in Tauber's experiments, since some of them were not clearly stated in the description of his test compressor, such as the clearance volume, the spring preload deflection, the equivalent mass of the valve plate with its spring or the coefficients of restitution. Among other things, our mathematical model assumes a lubricated machine (unlike the test compressor). It stands to reason that in view of the importance of the sameness of the operating conditions, we will instead focus on comparing trends rather than the exact numerical values.

In Figure 46a, one can see the experimental data of cylinder pressure p_c, the suction plenum chamber p_s, the discharge plenum chamber p_d, the suction valve plate lift x_s and the discharge valve plate lift x_d. In Figure 46b, one can observe the same quantities extracted from our simulator tool. As can be seen, there are no noticeable differences in terms of pressure waveform, however, one can clearly discern the moments when a valve plate strikes either the guard or seat, and when the valve plate is moving towards the seat. These inconsistencies presumably result from the differences in parameters regarding the valves as discussed in the paragraph above. Nonetheless, it can be concluded, based on this comparison, that the trends are correct.

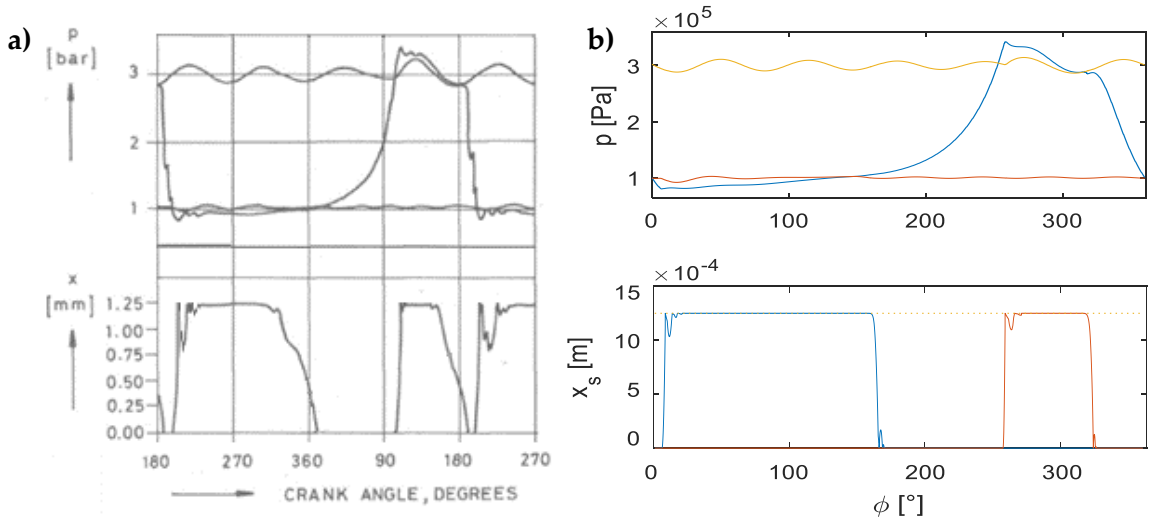

Figure 46 Comparison of the experimental and theoretical results

A related and interesting point to consider here would be the comparison of our results with other simulators, particularly commercial ones, since it was stated that such a simulation tool is necessary in the initial stages of valve development. For this purpose, we obtained an output from a proprietary software used by *Dott. Ing. Mario Cozzani Srl* (Figure 47), a company that has been designing and producing valves for reciprocating compressors since 1946.

In Figure 48, one can see, for comparison purposes, the output from the developed simulation tool. Bear in mind however, that the used input parameters are the same as with our previous results, however, in this case the influence of the piping system is omitted as was done with the output from the commercially developed simulator. Evidently, our open-source simulator gives very comparable results, at least in terms of trends.

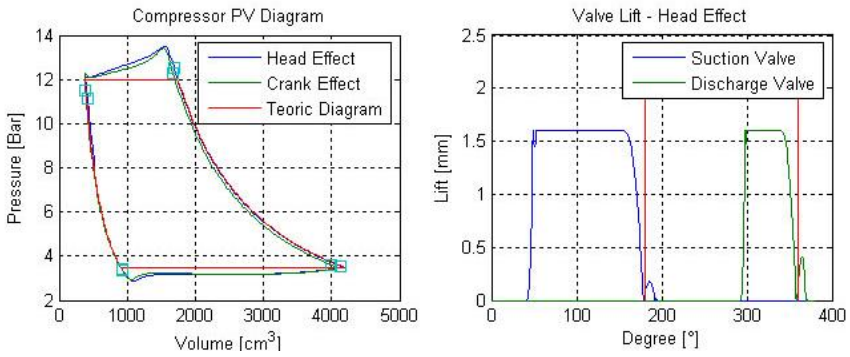

Figure 47 Output of valve behavior simulator - Dott. Ing. Mario Cozzani Srl [44]

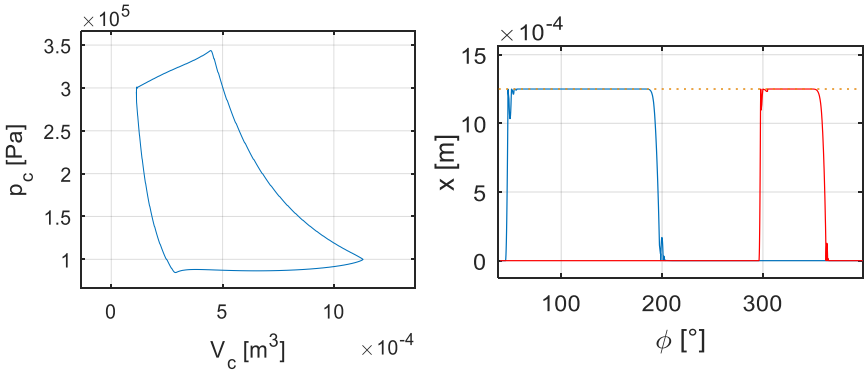

Figure 48 Output from the developed simulation tool

5.1.4 Accuracy of the Results

In the previous subchapter, it was concluded that the trends of the valve behavior predicted by the simulation tool are correct. Regardless of the fact that the only certainty is that the uncertainties are truly uncertain, let us summarize here the influences on the accuracy of the output from the simulator tool, which can be divided, based on their origin, as follows:

- Errors resulting from the simplifying assumptions
- Errors present in the input parameters
- Errors resulting from the numerical method used to solve ODEs

The former group, which contains errors resulting from the transition from the physical model to the mathematical one, was extensively discussed in chapter 3. The second group refers to errors that can be present in the input parameters, particularly the experimental coefficients. To examine the dependency of the proposed mathematical model on these parameters (and thus their accuracy), it is desirable to perform a sensitivity analysis (later in chapter 5.2.1). Without further discussion, it is reasonable to expect that these errors in question are the most serious ones, albeit their quantification without a proper experiment is intractable.

The latter group unites errors that relate to the method of solving the initial condition problem, i.e. both the numerical method and initial conditions. But how can one decide whether the method is giving inaccurate results, since the true solution is not known?

According to Olver [33], a useful and practically employed idea is to integrate the differential equations using two numerical schemes (of varying orders of accuracy) and then compare the results. Therefore, in addition to the *fourth-order Runge-Kutta method*, we tried the *Adams-Bashforth-Moulton predictor-correctors method* [36] (of order 1 to 13, implemented as *ode113* in MATLAB). In Figure 49, one can see the p-V diagrams, whereas in Table 13, there is a comparison of the periodical quantities.

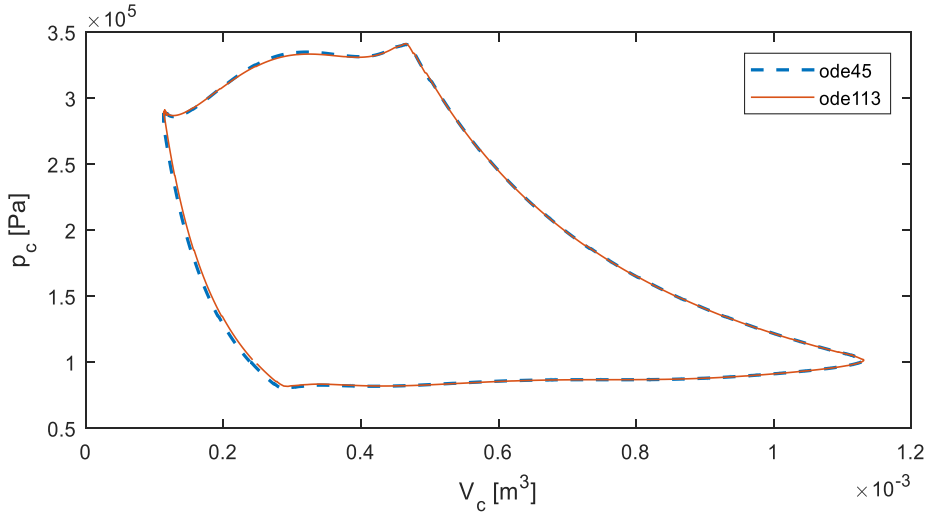

Figure 49 Comparison of the solution from different ode solvers

	$W_i[J]$	$W_{ivs}[J]$	$W_{ivd}[J]$	η_v [%]
Runge-Kutta *(ode45)*	139.5513	10.2400	14.3785	81.78
Adams-Bashforth-Moulton (*ode113*)	139.5505	10.2371	14.3651	81.71

Table 13 Comparison of periodical quantities - different ode solvers

It follows that the deviation of the periodical quantities is reasonably small, the variation being in the hundredths. Furthermore, there are no noticeable deviations in terms of the trends in *p-V diagram* and thus it can be concluded that the two solutions are reasonably close. Hence, it is safe to assume that both methods are giving accurate results.

A slightly different situation arises in terms of the choice of initial conditions at the very beginning of the integration process, as discussed in chapter 4.3.2.3. Figure 50 depicts the completed compressor cycles prior to the moment, when the solution is considered to be convergent. This decision is made on the basis of difference of two successive cycles; if the difference in pressure in the cylinder does not exceed one thousandth of the discharge pressure, it is assumed that convergence was achieved.

It can be observed, that more initial cycles are needed in cases, where the influence of the piping systems is considered (Figure 50a) relative to the second one (Figure 50b), where this influence is neglected. This concurs well with the statement made earlier that only a rough estimation of initial conditions is available in the former case.

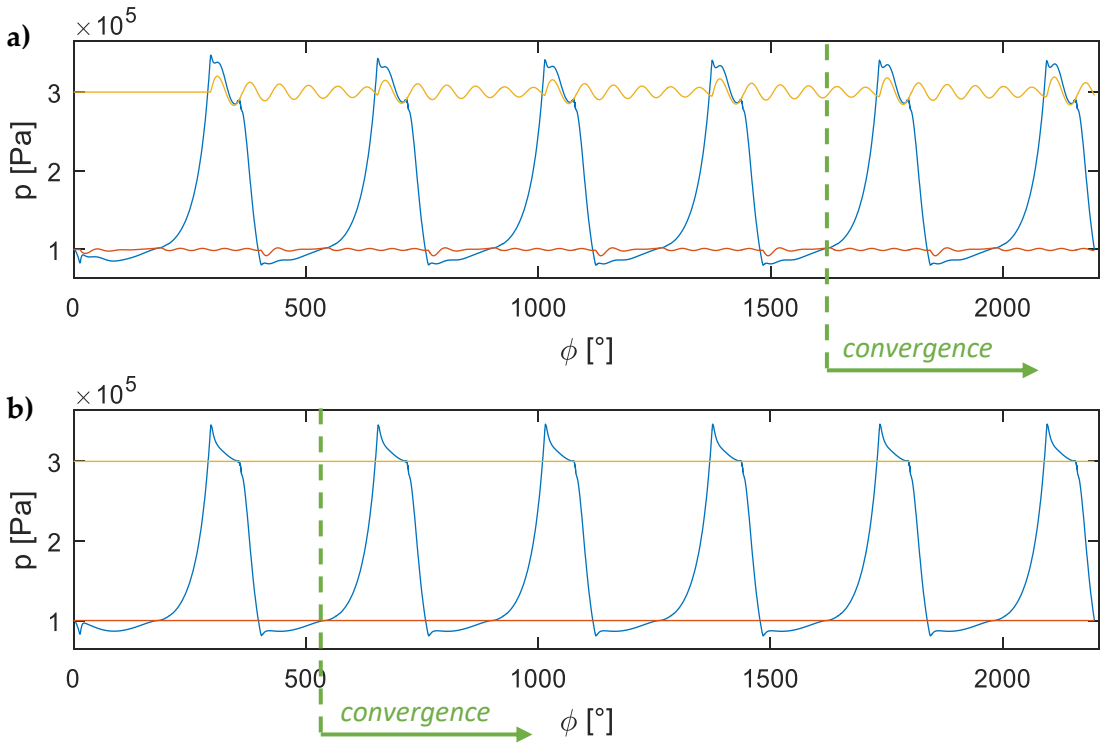

Figure 50 Compressor cycles prior to convergent solution

5.2 Modified Compressor Parameters

5.2.1 Sensitivity Analysis

As the mainstay of the mathematical model in terms of valve behavior, one can consider the fluid-structure interaction. Recall that the gas force acting on the valve plate is calculated per a gas coefficient. This coefficient can be obtained experimentally; however, since we strive for a theoretical approach, we calculate it via an expansion coefficient and a flow coefficient. The former can be determined theoretically; however, the latter must be obtained experimentally and so one might consider this substitution of the gas coefficient to be unbeneficial at first since the gas force does not entirely enough to relinquish the dependence on experimental coefficients. However, it should be emphasized that the flow coefficient is required anyway to calculate the mass flow through the valve and so this substitution helps to reduce the need for further measurements. Moreover, it can provide us with a valuable insight into the parameters, on which the value of the gas coefficient mostly depends. For this purpose, we will perform the sensitivity analysis of c_g, which, as we believe, can help to increase our understanding and intuition of the system.

$$c_g = \left(1 + \left(\alpha\epsilon\frac{\pi D_v x}{A_p}\right)^2\right)\frac{A_p}{A_v} - \frac{\left(\alpha\epsilon\left(A_v - A_p\right)\right)^2}{A_v A_p} \tag{5.2.1}$$

First lets adjust Eq. 5.2.1 by substituting for the areas $A_v = \frac{\pi D_v^4}{4}$ and $A_p = \frac{\pi D_p^2}{4}$, i.e.:

$$c_g = \left(1 + \left(\alpha\epsilon \frac{4D_v x}{D_p^2}\right)^2\right)\left(\frac{D_p}{D_v}\right)^2 - \frac{\left(\alpha\epsilon\left(D_v^2 - D_p^2\right)\right)^2}{D_v^2 D_p^2} \tag{5.2.2}$$

Suppose that the function above models the output of a process, where x (the valve plate lift) is the input and $D_p, D_v, \alpha, \epsilon$ are models of the system parameters. For the purposes of analysis, let the normal operating point (NOP) be:

$$x_0 = 1.5, D_{p0} = 10, D_{v0} = 12, \alpha_0 = 0.6, \epsilon_0 = 0.9, \tag{5.2.3}$$

which produces $c_g \cong 0.76$.

Now let us ask ourselves what is the easiest way to change the value of c_g, i.e. a slight variation in which parameter will have the biggest impact on the resulting value of c_g? This sounds a lot like a natural problem for a *relative-sensitivity* analysis of function c_g. The relative-sensitivity functions (the following equations) are formed by multiplying the partial derivative by the normal value of the parameter and dividing it by the normal value of the function [37].

$$\bar{S}_{D_p}^{c_g} = \left.\frac{\partial c_g}{\partial D_p}\right|_{NOP} \frac{D_{p0}}{c_{g0}} = \left(\frac{2D_{p0}}{D_{v0}^2} - \frac{32(x_0\alpha_0\epsilon_0)^2}{D_{p0}^3} - (\alpha_0\epsilon_0)^2\left(\frac{2D_{p0}}{D_{v0}^2} - \frac{2D_{v0}^2}{D_{p0}^3}\right)\right)\frac{D_{p0}}{c_{g0}} \cong 2.12 \tag{5.2.4}$$

$$\bar{S}_{D_v}^{c_g} = \left.\frac{\partial c_g}{\partial D_v}\right|_{NOP} \frac{D_{v0}}{c_{g0}} = \left(-\frac{2D_{p0}^2}{D_{v0}^3} - (\alpha_0\epsilon_0)^2\left(\frac{2D_{v0}}{D_{p0}^2} - \frac{2D_{p0}^2}{D_{v0}^3}\right)\right)\frac{D_{v0}}{c_{g0}} \cong -2.40 \tag{5.2.5}$$

$$\bar{S}_{\alpha}^{c_g} = \left.\frac{\partial c_g}{\partial \alpha}\right|_{NOP} \frac{\alpha_0}{c_{g0}} = \left(\frac{32\alpha_0\epsilon_0^2 x_0^2}{D_{p0}^2} - 2\alpha_0\epsilon_0^2\left(\frac{D_{v0}^2}{D_{p0}^2} + \frac{D_{p0}^2}{D_{v0}^2} - 2\right)\right)\frac{\alpha_0}{c_{g0}} \cong 0.17 \tag{5.2.6}$$

$$\bar{S}_{\epsilon}^{c_g} = \left.\frac{\partial c_g}{\partial \epsilon}\right|_{NOP} \frac{\epsilon_0}{c_{g0}} = \left(\frac{32\epsilon_0\alpha_0^2 x_0^2}{D_{p0}^2} - 2\epsilon_0\alpha_0^2\left(\frac{D_{v0}^2}{D_{p0}^2} + \frac{D_{p0}^2}{D_{v0}^2} - 2\right)\right)\frac{\epsilon_0}{c_{g0}} \cong 0.17 \tag{5.2.7}$$

$$\bar{S}_{x}^{c_g} = \left.\frac{\partial c_g}{\partial x}\right|_{NOP} \frac{x_0}{c_{g0}} = \left(\frac{32x_0\alpha_0^2\epsilon_0^2}{D_{p0}^2}\right)\frac{x_0}{c_{g0}} \cong 0.28 \tag{5.2.8}$$

These equations give us insight into the behavior of the system only in the case where one of the parameters is being changed. However, what about the interactions, i.e. how the system behaves when changing two parameters at the same time? These interaction terms are obtained by, for instance, the partial derivative of c_g with respect to x containing D_p. Below are only the non-zero relative-sensitivity functions.

$$\bar{S}_{x-D_p}^{c_g} = \left.\frac{\partial^2 c_g}{\partial x \partial D_p}\right|_{NOP} \frac{x_0 D_{p0}}{c_{g0}^2} = \left(-\frac{64x_0\alpha_0^2\epsilon_0^2}{D_{p0}^3}\right)\frac{x_0 D_{p0}}{c_{g0}^2} \cong -0.73 \tag{5.2.9}$$

$$\bar{S}_{x-\alpha}^{c_g} = \left.\frac{\partial^2 c_g}{\partial x \partial \alpha}\right|_{NOP} \frac{x_0\alpha_0}{c_{g0}^2} = \left(\frac{64x_0\alpha_0\epsilon_0^2}{D_{p0}^2}\right)\frac{x_0\alpha_0}{c_{g0}^2} \cong 0.73 \tag{5.2.10}$$

$$\bar{S}_{x-\epsilon}^{c_g} = \left.\frac{\partial^2 c_g}{\partial x \partial \epsilon}\right|_{NOP} \frac{x_0\epsilon_0}{c_{g0}^2} = \left(\frac{64x_0\epsilon_0\alpha_0^2}{D_{p0}^2}\right)\frac{x_0\epsilon_0}{c_{g0}^2} \cong 0.73 \tag{5.2.11}$$

$$\bar{S}_{x^2}^{c_g} = \frac{\partial^2 c_g}{\partial x^2}\Big|_{NOP} \frac{x_0^2}{c_{g0}^2} = \left(\frac{32\alpha_0^2\epsilon_0^2}{D_{p0}^2}\right)\frac{x_0^2}{c_{g0}^2} \cong 0.36 \tag{5.2.12}$$

$$\bar{S}_{D_p-D_v}^{c_g} = \frac{\partial^2 c_g}{\partial D_p \partial D_v}\Big|_{NOP} \frac{D_{p0}D_{v0}}{c_{g0}^2} = \left(-\frac{6D_{p0}}{D_{v0}^3} + \alpha_0^2\epsilon_0^2\left(\frac{6D_{p0}}{D_{v_0}^3} + \frac{4D_{v0}}{D_{p_0}^3}\right)\right)\frac{D_{p0}D_{v0}}{c_{g0}^2} \cong -0.50 \tag{5.2.13}$$

$$\bar{S}_{D_p-\alpha}^{c_g} = \frac{\partial^2 c_g}{\partial D_p \partial \alpha}\Big|_{NOP} \frac{D_{p0}\alpha_0}{c_{g0}^2} = -\left(\frac{64\alpha_0 x_0^2\epsilon_0^2}{D_{p_0}^3} + 2\alpha_0\epsilon_0^2\left(\frac{2D_{p_0}}{D_{v_0}^2} - \frac{2D_{v_0}^2}{D_{p_0}^3}\right)\right)\frac{D_{p0}\alpha_0}{c_{g0}^2} \cong 0.78 \tag{5.2.14}$$

$$\bar{S}_{D_p-\epsilon}^{c_g} = \frac{\partial^2 c_g}{\partial D_p \partial \epsilon}\Big|_{NOP} \frac{D_{p0}\epsilon_0}{c_{g0}^2} = \left(-\frac{64\epsilon_0 x_0^2\alpha_0^2}{D_{p_0}^3} - 2\epsilon_0\alpha_0^2\left(\frac{2D_{p_0}}{D_{v_0}^2} - \frac{2D_{v_0}^2}{D_{p_0}^3}\right)\right)\frac{D_{p0}\epsilon_0}{c_{g0}^2} \cong 0.78 \tag{5.2.15}$$

$$\bar{S}_{D_p^2}^{c_g} = \frac{\partial^2 c_g}{\partial D_p^2}\Big|_{NOP} \frac{D_{p0}^2}{c_{g0}^2} = \left(\frac{2}{D_{v0}^2} + \frac{96(x_0\alpha_0\epsilon_0)^2}{D_{p_0}^4} - (\alpha_0\epsilon_0)^2\left(\frac{2}{D_{v_0}^2} + \frac{6D_{v_0}^2}{D_{p_0}^4}\right)\right)\frac{D_{p0}^2}{c_{g0}^2} \cong 2.54 \tag{5.2.16}$$

$$\bar{S}_{D_v-\alpha}^{c_g} = \frac{\partial^2 c_g}{\partial D_v \partial \alpha}\Big|_{NOP} \frac{D_{v0}\alpha_0}{c_{g0}^2} = \left(-4\alpha_0\epsilon_0^2\left(\frac{D_{v0}}{D_{p0}^2} - \frac{D_{p0}^2}{D_{v0}^3}\right)\right)\frac{D_{v0}\alpha_0}{c_{g0}^2} \cong -1.50 \tag{5.2.17}$$

$$\bar{S}_{D_v-\epsilon}^{c_g} = \frac{\partial^2 c_g}{\partial D_v \partial \epsilon}\Big|_{NOP} \frac{D_{v0}\epsilon_0}{c_{g0}^2} = \left(-4\epsilon_0\alpha_0^2\left(\frac{D_{v0}}{D_{p0}^2} - \frac{D_{p0}^2}{D_{v0}^3}\right)\right)\frac{D_{v0}\epsilon_0}{c_{g0}^2} \cong -1.50 \tag{5.2.18}$$

$$\bar{S}_{D_v^2}^{c_g} = \frac{\partial^2 c_g}{\partial D_v^2}\Big|_{NOP} \frac{D_{v0}^2}{c_{g0}^2} = \left(\frac{6D_{p0}^2}{D_{v0}^4} - (\alpha_0\epsilon_0)^2\left(\frac{2}{D_{p_0}^2} + \frac{6D_{p0}^2}{D_{v_0}^4}\right)\right)\frac{D_{v0}^2}{c_{g0}^2} \cong 3.65 \tag{5.2.19}$$

$$\bar{S}_{\alpha-\epsilon}^{c_g} = \frac{\partial^2 c_g}{\partial \alpha \partial \epsilon}\Big|_{NOP} \frac{\alpha_0\epsilon_0}{c_{g0}^2} = \left(\frac{64\alpha_0\epsilon_0 x_0^2}{D_{p0}^2} - 4\alpha_0\epsilon_0\left(\frac{D_{v0}^2}{D_{p0}^2} + \frac{D_{p0}^2}{D_{v0}^2} - 2\right)\right)\frac{\alpha_0\epsilon_0}{c_{g0}^2} \cong 0.46 \tag{5.2.20}$$

$$\bar{S}_{\alpha^2}^{c_g} = \frac{\partial^2 c_g}{\partial \alpha^2}\Big|_{NOP} \frac{\alpha_0^2}{c_{g0}^2} = \left(\frac{32\epsilon_0^2 x_0^2}{D_{p0}^2} - 2\epsilon_0^2\left(\frac{D_{v0}^2}{D_{p0}^2} + \frac{D_{p0}^2}{D_{v0}^2} - 2\right)\right)\frac{\alpha_0^2}{c_{g0}^2} \cong 0.23 \tag{5.2.21}$$

$$\bar{S}_{\epsilon^2}^{c_g} = \frac{\partial^2 c_g}{\partial \epsilon^2}\Big|_{NOP} \frac{\epsilon_0^2}{c_{g0}^2} = \left(\frac{32\alpha_0^2 x_0^2}{D_{p0}^2} - 2\alpha_0^2\left(\frac{D_{v0}^2}{D_{p0}^2} + \frac{D_{p0}^2}{D_{v0}^2} - 2\right)\right)\frac{\epsilon_0^2}{c_{g0}^2} \cong 0.23 \tag{5.2.22}$$

Since it is well-known that if the partial derivatives are continuous, then $\frac{\partial^2 c_g}{\partial x \partial D_p} = \frac{\partial^2 c_g}{\partial D_p \partial x}$ etc.; no other second-order partial derivatives are needed. Likewise, we could investigate the third-order partial derivatives etc., however, the meaning of these high-order derivatives is too insignificant for our purposes.

From these relative-sensitivity functions one can see which parameters have the greatest effect on c_g for a certain percent change in the parameters. In Figure 51, the results following from the sensitivity analysis are distinctly depicted.

It follows that the highest impact on the value of the gas coefficient is in the change in valve port area A_p and valve plate area A_v. This is in line with expectations; however, more interestingly, the increase of the valve plate area, while not touching other parameters, will result in a decrease of c_g, whereas the increase of the valve port area will lead to an increase in c_g.

Nevertheless, the reason why we intended to utilize the sensitivity analysis, was mainly to investigate the reliance of c_g on the flow and the expansion coefficients, i.e. α, ϵ. From the results one can observe that there is a relatively weak dependence of the gas coefficient on

α, ϵ in comparison to other parameters. This is rather important because, as discussed in chapter 3.4.2, the expansion coefficient can be determined theoretically and thus the whole matter of mass flow and fluid-structure interaction as such can be built solely on the flow coefficient, which, however, is not the parameter influencing the valve behavior the most. Moreover, recall that this coefficient depends on the geometrical shape of the valve, while being almost entirely independent of its size. This suggests that regardless of the semi-empirical approach in modeling the gas force, it does not restrict the applicability of the model as such.

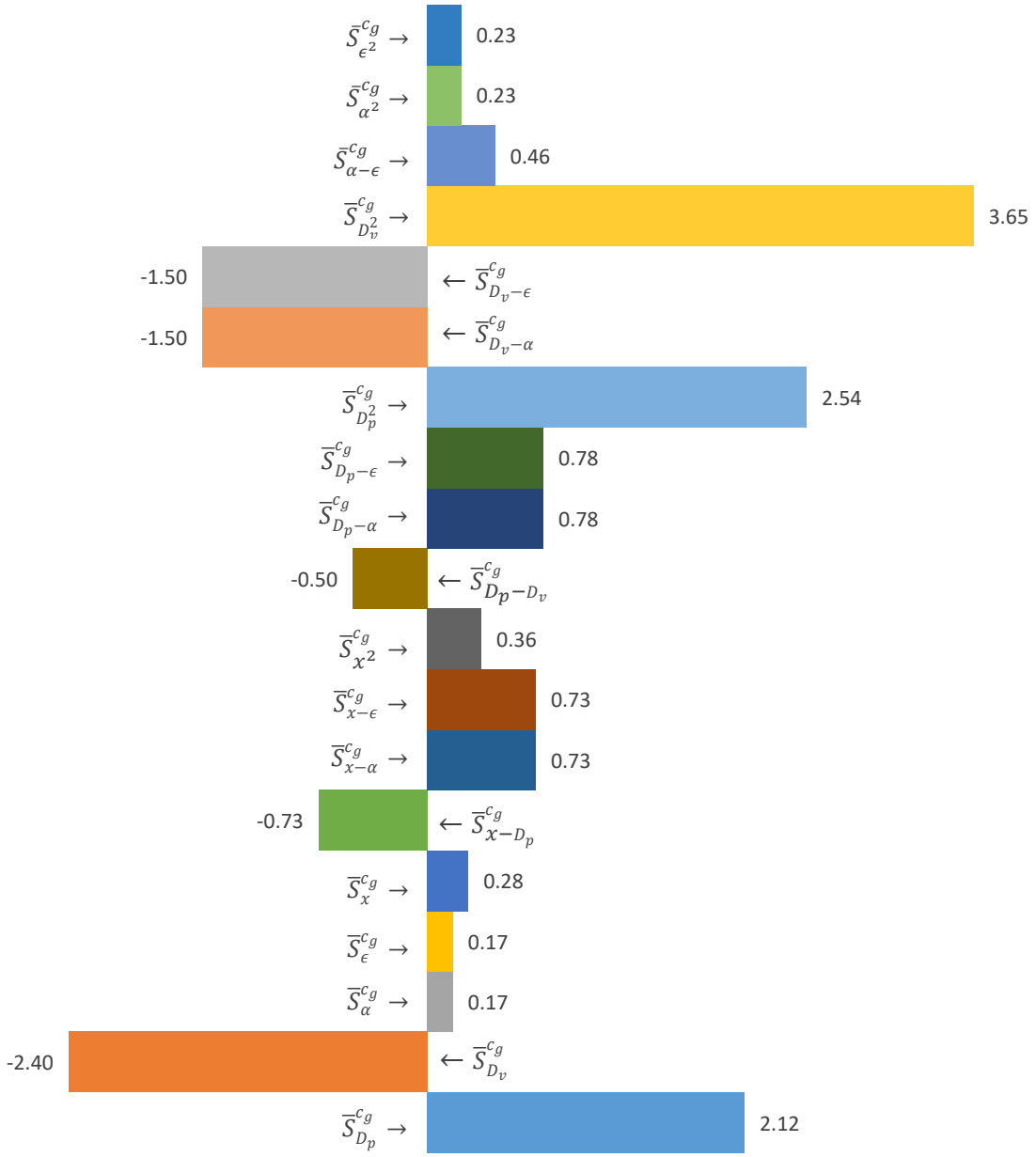

Figure 51 Sensitivity analysis for the gas coefficient c_g

5.2.2 Individual Phenomena Effect

Lets now examine, how the individual phenomena of valve dynamics influence *ideal*[8] behavior of the valve. For this purpose, each of the charts below depicts an *ideal* valve plate movement with its movement influenced by the phenomena in question. The compressor parameters, in other aspects, correspond to the default ones.

Adhesion

Starting with the adhesion effect (Figure 52), the results correspond to the statement made earlier, that adhesion delays the valve opening and closing. Speaking in numbers, suction valve opening is delayed by 2.8°, whereas its closing is delayed only by 0.8°. Regarding the discharge valve, it can be stated that the delay, due to the stiction, is not as significant in terms of crank angle, 1.2° or 0.6° for opening and closing respectively.

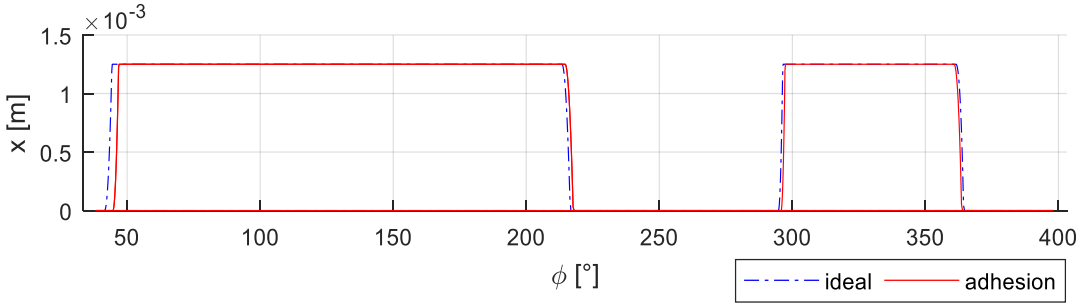

Figure 52 Influence of adhesion

Friction

As shown in Figure 53, the fluid friction influences the slope of the curve indicating the stroke of the plate lift during its motion towards either the seat or the limiter, not the moment, when the valve plate is set in motion as in the previous case. Due to this effect, the period of opening and closing is lengthened by 3.2° or 4.1° respectively for the suction valve and 1.4° or 2.1° respectively for the discharge valve.

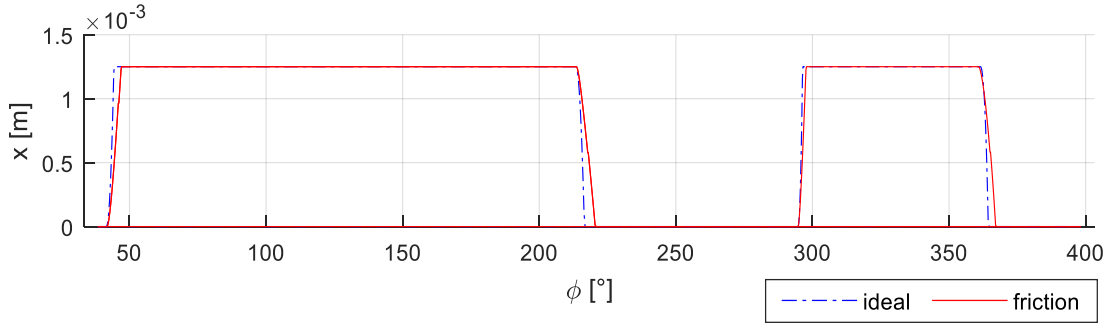

Figure 53 Influence of friction

[8] Bear in mind, that by *ideal* behavior (or movement) it is meant to neglect friction, adhesion, rebound and pressure pulsations, i.e. the valve plate still moves with a finite velocity, not infinite as it would in cases of truly idealistic behavior.

Rebound

In Figure 54, one can notice the bouncing effect in the moment when a valve plate strikes against a limiter or a guard. This collision is modeled as semi-elastic, i.e. it is assumed that there is some sort of kinetic energy recovery during the collision. The velocity charts show that the opening of both the suction and discharge valves passes off faster relatively to their closing, presumably due to the interaction between the valve and its environment ($\frac{d}{dt}\Delta p$).

It is plausible that the nature of the proposed mathematical model could have influenced the rebound effect, since flow separation at the edges of the valve plate result in turbulent free jets, in which the energy is dissipated, is not modeled; i.e. it is not postulated that the potential rebound could be stifled by the resulting low pressure in the air cushion when the valve tries to move away from the obstacle, especially the guard.

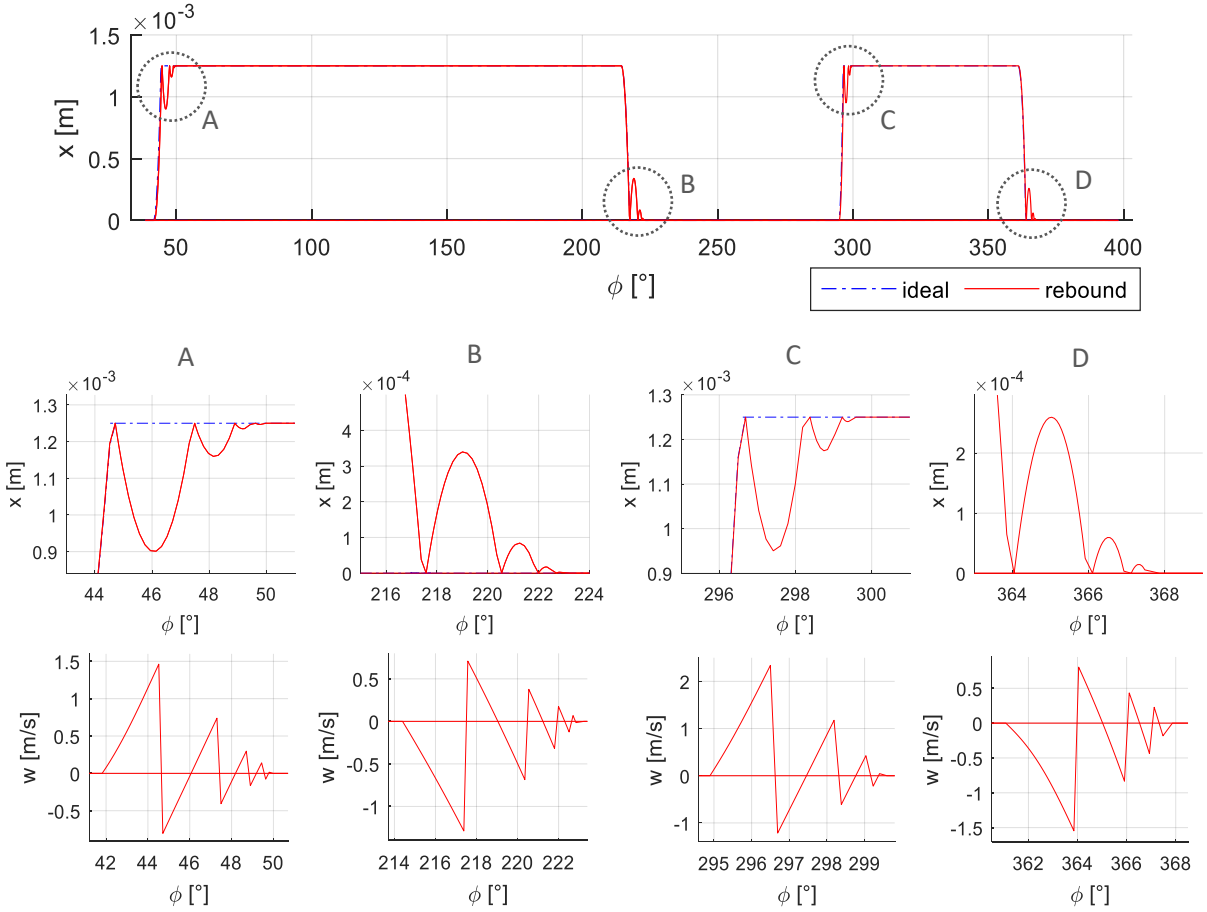

Figure 54 Influence of rebound

Plenum Chambers

It is beyond doubt that one of the reasons of good trend agreement of theoretical results with experimental ones (chapter 5.1.3) is the presence of pressure pulsations in both the suction and discharge plenum chambers, despite utilizing the relatively simple replacement model (i.e. the Helmholtz resonator concept). The comparison of results for when the pressure pulsations are modeled or not can be observed in Figure 55.

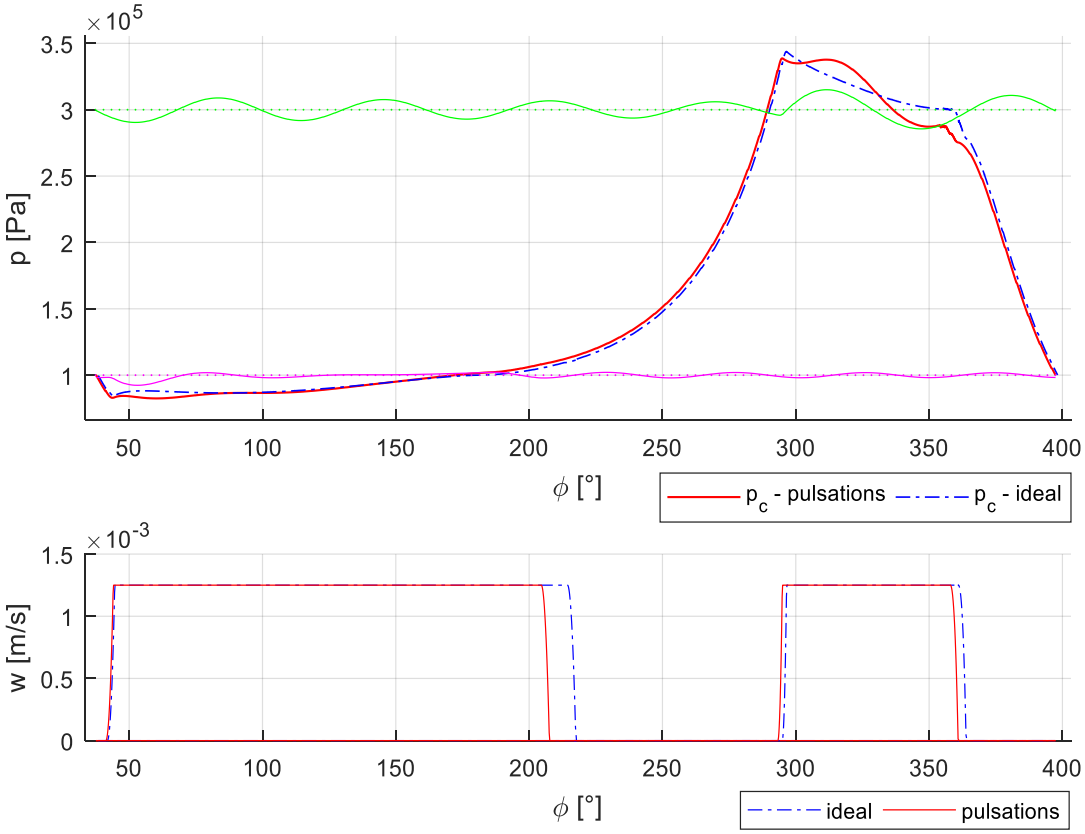

Figure 55 Influence of piping systems

Regarding a deeper breakdown of the concept used to account for pressure pulsations; the single degree of freedom oscillator consists of a purely inert (*mass-like*) and purely compliant (*spring-like*) element. Therefore, when a piping system is isolated, i.e. a compressor valve is closed, the gas inside performs free damped oscillations (with a frequency equal to the natural frequency of the system); however, should the valve be opened, the oscillations will become forced, since they will be excited by the flowing gas. The free oscillations are not harmonic, since the governing equations used to describe the piping systems are not linear. Moreover, from the governing equations one can also conclude that the frequency of pulsations can be considered to be inversely proportional to the volume of the plenum chamber; the lower the volume, the higher the frequency (see Figure 56, where the pressure pulsations in cases with half of the volume of both of the plenum chambers are depicted).

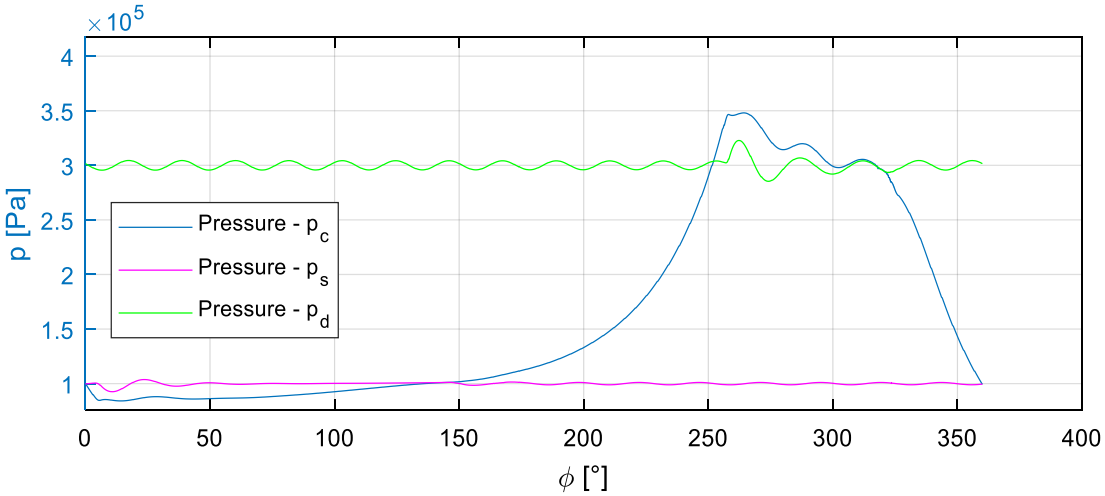

Figure 56 Pressure pulsations in case of half-volume plenum chambers

Outlining plausible restrictions of the utilized piping model, it stands to reason, that since in real-life systems either the inert or compliant properties are distributed over these systems (not concentrated into separate elements as is the case with the Helmholtz resonator concept), this real-life system will have an infinite number of degrees of freedom and thus will oscillate in different modes of vibration, each of them corresponding to a certain natural frequency. Jaspers [38], based on his experimental recordings, concludes that the first mode of vibration dominates, whereas the higher ones only distort the shape of the pressure initial wave (see Figure 57 and Figure 58). This effect is not modeled by the simplified model.

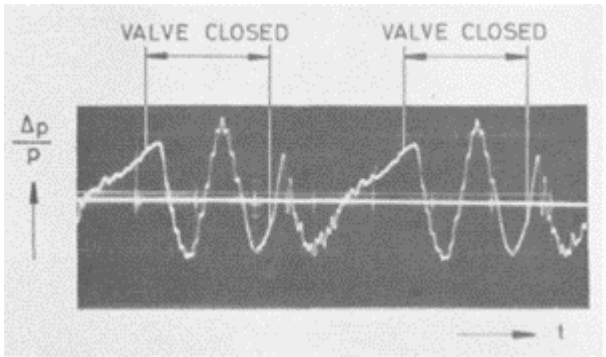

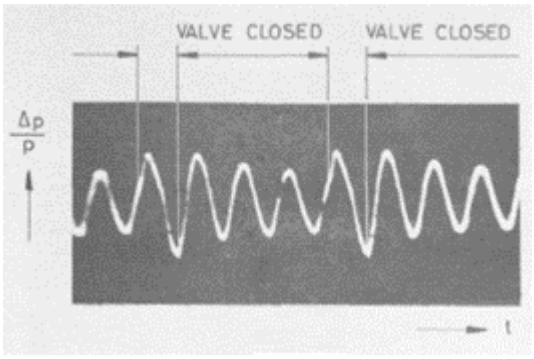

Figure 57 Recording of pressure pulsations by Jaspers [38] *Figure 58 Recordings of pressure pulsations by Bráblík [32]*

Influence on the Periodical Results

Concerning the influence of the phenomena discussed in the preceding paragraphs on the periodical quantities of the reciprocating compressor, see Figure 59, which depicts the percentage change from the *ideal* valve behavior. Bear in mind that the points are connected solely in order to provide a better visual guidance, i.e. there is no physical basis regarding the connecting lines.

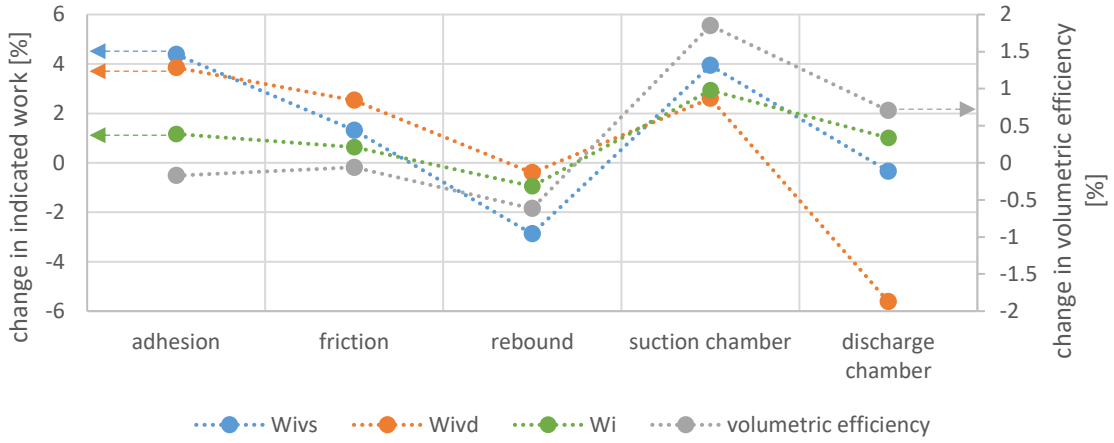

Figure 59 Influence on the periodical results

It can be concluded that the adhesion and friction slightly increase the compressor indicated work, but moreover they substantially increase both the suction and discharge indicated valve work (i.e. valve losses), which is not desirable. A slightly different situation can be observed in the case with the rebound effect, which decreases the indicated work as well as the indicated valve work for the suction and discharge valves; however, the rebound may induce undesirable valve plate oscillations.

Furthermore, it can be noticed that, although the individual phenomena of the valve dynamics tend to decrease the volumetric efficiency, the piping systems increase it nevertheless. This is in accordance with the experimental observations made by Touber [12], who also proposed the idea that the design of the suction piping system could be used as a method to increase the volumetric efficiency. However, it comes at the cost of a larger increase of the indicated work and moreover results in the appearance of eventual resonance phenomena in piping systems.

5.2.3 Varying Design Parameters

Further inspection of the factors influencing the valve dynamics can be done through variation of the design parameters. The tests to be found below were conducted under different pressure ratios, compressor speeds, and valve design parameters. The goal of the former two is to show how different operating conditions can affect the valve behavior and the losses of the valves, whereas some *unsteady* valve behaviors will be briefly shown in the latter case.

Central to all the tests, the valve behavior can be listed as follows: As the suction valve opens, the pressure inside the cylinder starts to rise slowly until the valve closes so that the compression of the gas can proceed. If the conditions are such that the discharge valve can be opened, it is blown up quickly, whilst the pressure inside the cylinder immediately decreases. The valve plate clings onto the limiter after a little rebound until the gas force becomes sufficiently depleted in holding it against the spring force and thus the valve plate

will return to the seat. Although the trends of the valve plate movement are basically the same for all the tests, some details can be noticed.

Valve Movement under Different Discharge Pressures

Suction pressure is kept constantly at 1 bar, while discharge pressure is adjusted from 3 bars up to 7 bars. Figure 60 depicts *p-V* diagrams, whereas Figure 61 shows the valve lift as a function of the crank angle.

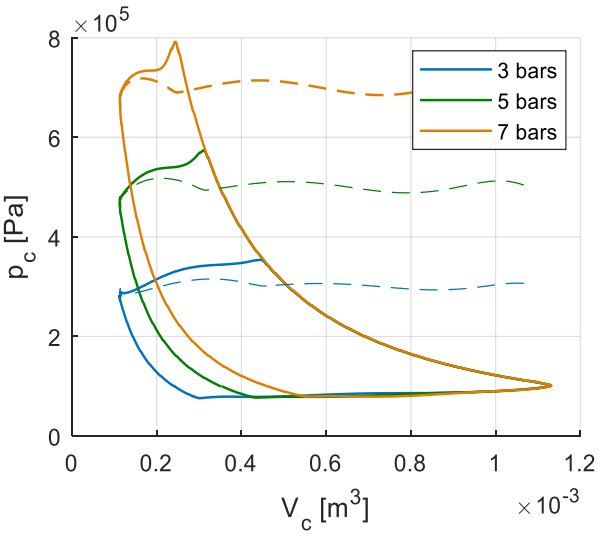

Figure 60 p-V diagrams - various discharge pressures

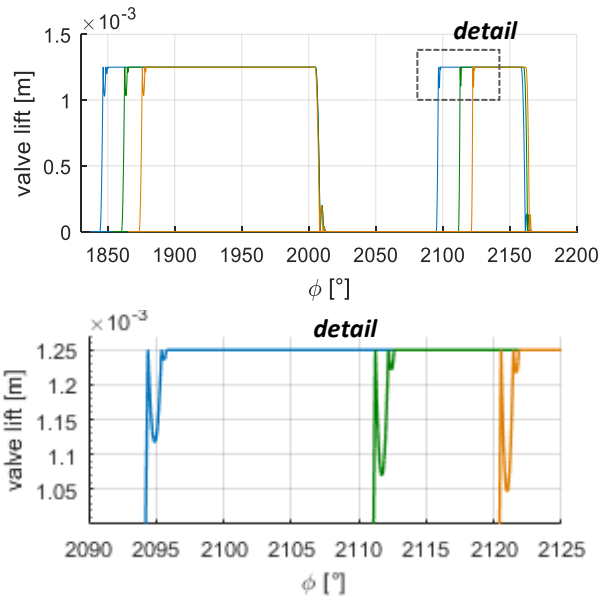

Figure 61 Valve lift - various discharge pressures

One can see from both of the above diagrams that the increasing discharge pressure shortens the magnitude of the suction and discharge phases, while at the same time it lengthens both the compression and expansion phases. Careful examination of the valve movement indicates the higher the discharge pressure is, the higher the impact velocities for the discharge valve are, whereas in the case of the suction valve the impact velocities are uninfluenced by the varying discharge pressure (see Figure 62). Moreover, the rebound process tells us that the discharge valve is blown higher by the higher discharge pressure

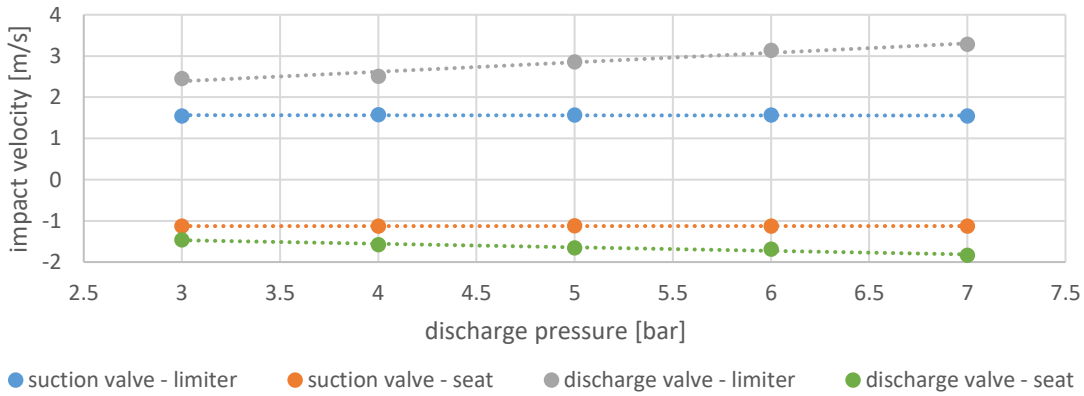

Figure 62 Impact velocities - various discharge pressures

(see Figure 61). In order to be thorough, the lines in the charts below are best-fit linear trendlines, i.e. they are obtained by utilizing the regression analysis method of *least squares*.

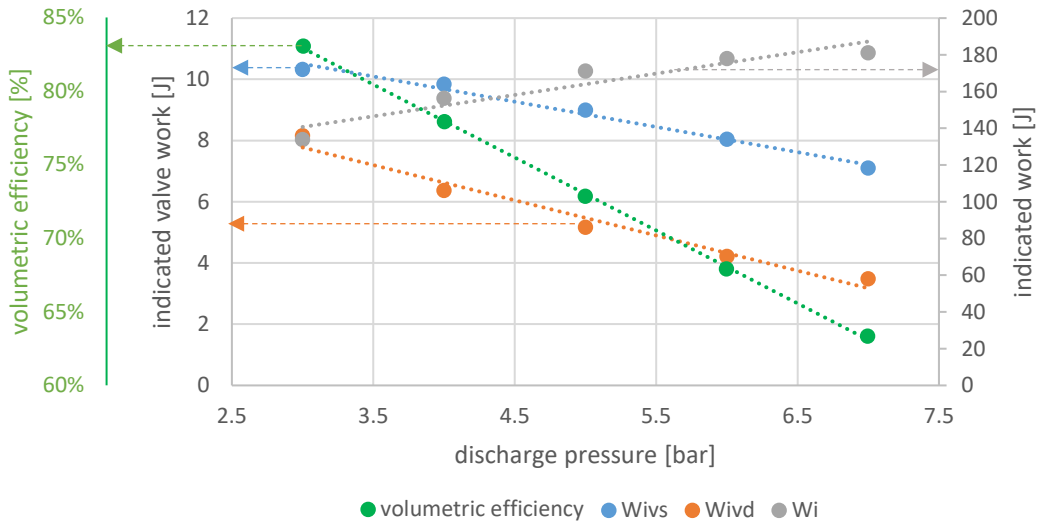

Figure 63 Periodical quantities - various discharge pressures

In Figure 63, the courses of periodical quantities for the various tested discharge pressures are depicted. It is needless to say that the indicated work rises as the compression ratio rises. Moreover, it can be observed that the indicated valve work for both the suction and the discharge valves becomes smaller as the corresponding phase proceeds faster, i.e. as the discharge pressure increases; however, it is at the cost of a substantial decrease in the volumetric efficiency.

Valve Movement under Different Compressor Speeds

Through adjusting the frequency of the current, the revolutions are gradually increased from 300 rpm up to 550 rpm. As shown in Figure 64, the discharging period decreases after increasing the compressor speed. Also, the impact velocities rise, as can be observed in Figure 65. Regarding the periodical quantities, see Figure 66.

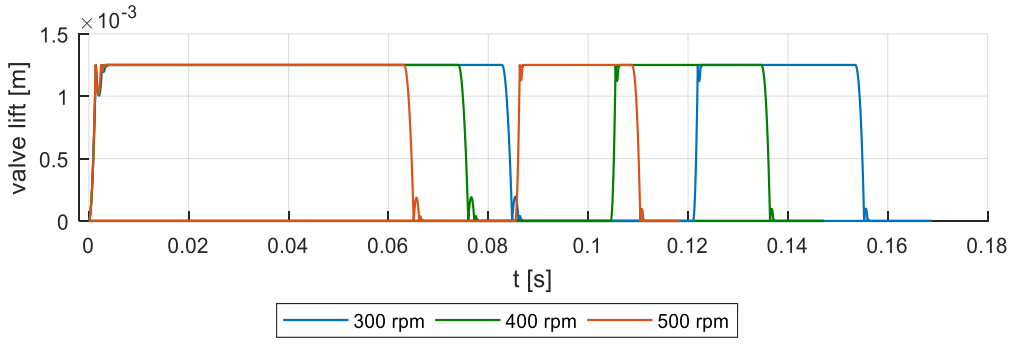

Figure 64 Valve movement under various compressor speeds

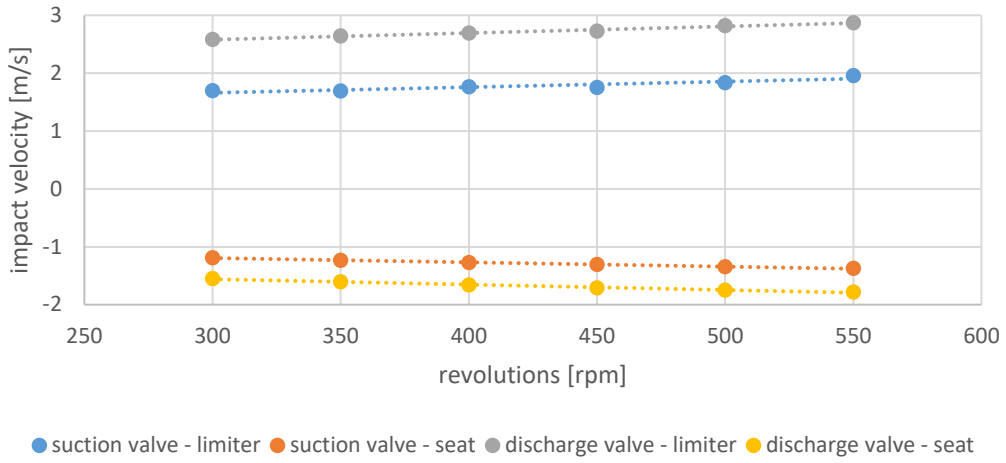

Figure 65 Impact velocities - various compressor speeds

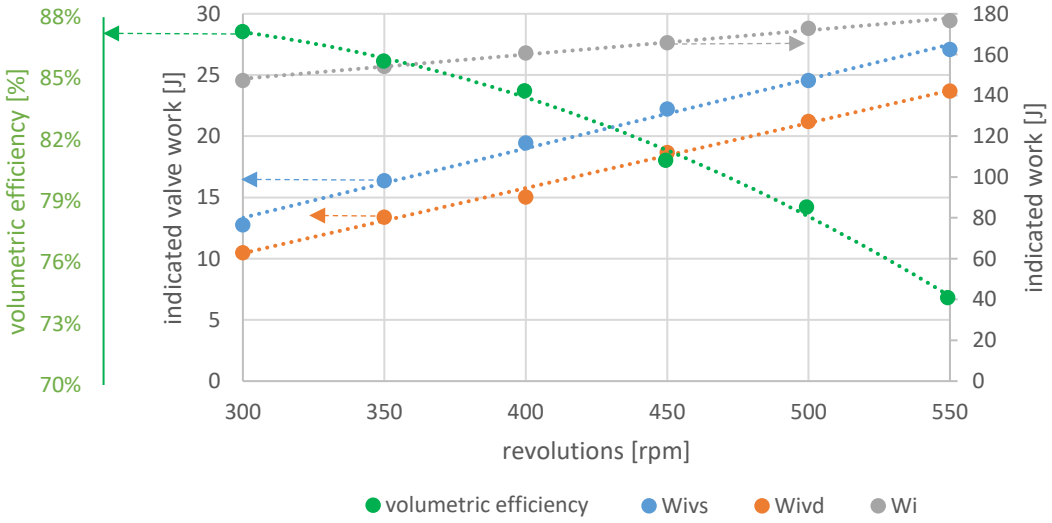

Figure 66 Periodical quantities - various compressor speeds

Valve Movement for Different Valve Parameters

Since the valve is modeled as a mass-spring system, it goes without saying that such a system is also potentially an oscillating system, in which the excitation necessary to give rise to the oscillating behavior of the sealing element is provided by the interaction of the system with the flow. This phenomenon, known in the corresponding literature as *flutter*, is truly undesired behavior since it is a widely-held view that it can result in premature valve failures [2].

Flutter has been investigated by several researchers, both theoretically and experimentally. Hence, the interested reader can be referred to the recent literature of Böswirth [13], where a theoretical model of valve flutter, verified experimentally, is formulated. Even though that our interest in this thesis is not concerned with an elaboration of unsteady valve behaviors, it is felt that it would be beneficial to show that the proposed mathematical

model (and its proper implementation in the simulation tool), can predict the presence of these behaviors, which can be considered, after all, to be an important aspect of utilizing the simplified approach (i.e. one-dimensional, quasi-steady flow, etc.) in modeling valve behavior in the initial stages of valve design development [17].

For this purpose, let us modify the discharge valve parameters in the default compressor setup by increasing the spring stiffness (to 750 N/m) and afterwards gradually increasing the distance between the limiter and the seat. The results of the simulation are shown in Figure 67.

It can be observed that by increasing the allowed valve plate lift, the gas force is not, due to the more intense decrease in pressure in the cylinder after the valve opening (see Figure 68), high enough to hold the valve plate pushing against the limiter. As the spring force overbalances the gas force (reduced by the friction force) and the valve starts to close, the pressure in the cylinder starts to rise (due to the fact that the piston has yet to reverse its motion and also due to the pressure pulsations in the discharge plenum chamber), leading to the oscillating behavior of the valve plate. It is also worth noting that from the results one can see that increasing the maximum valve plate lift leads to an increase in impact velocities on the limiter, and thus higher loads and wear.

It is needless to say that thanks to the identification of such undesirable behavior, the valve design can be appropriately modified in order to avoid them. To make the idea of which parameters should be modified and how they should be modified, see the following equation:

$$\omega\, p_u > \frac{k^{1.5}\, h_{max}}{3\, c_d A_v m_p^{0.5}} \tag{5.2.23}$$

wherein p_u is the upstream pressure, k stands for the spring stiffness, h_{max} denotes the maximum possible valve plate lift, A_v refers to the valve plate area, m_p is the equivalent mass of the plate and its spring and c_d stands for the drag (gas) coefficient. This criterion, derived by Upfold [39] for the inlet valve based on his experimental records of valve motion, should be fulfilled so that the oscillations or flutter of the valve plate do not occur.

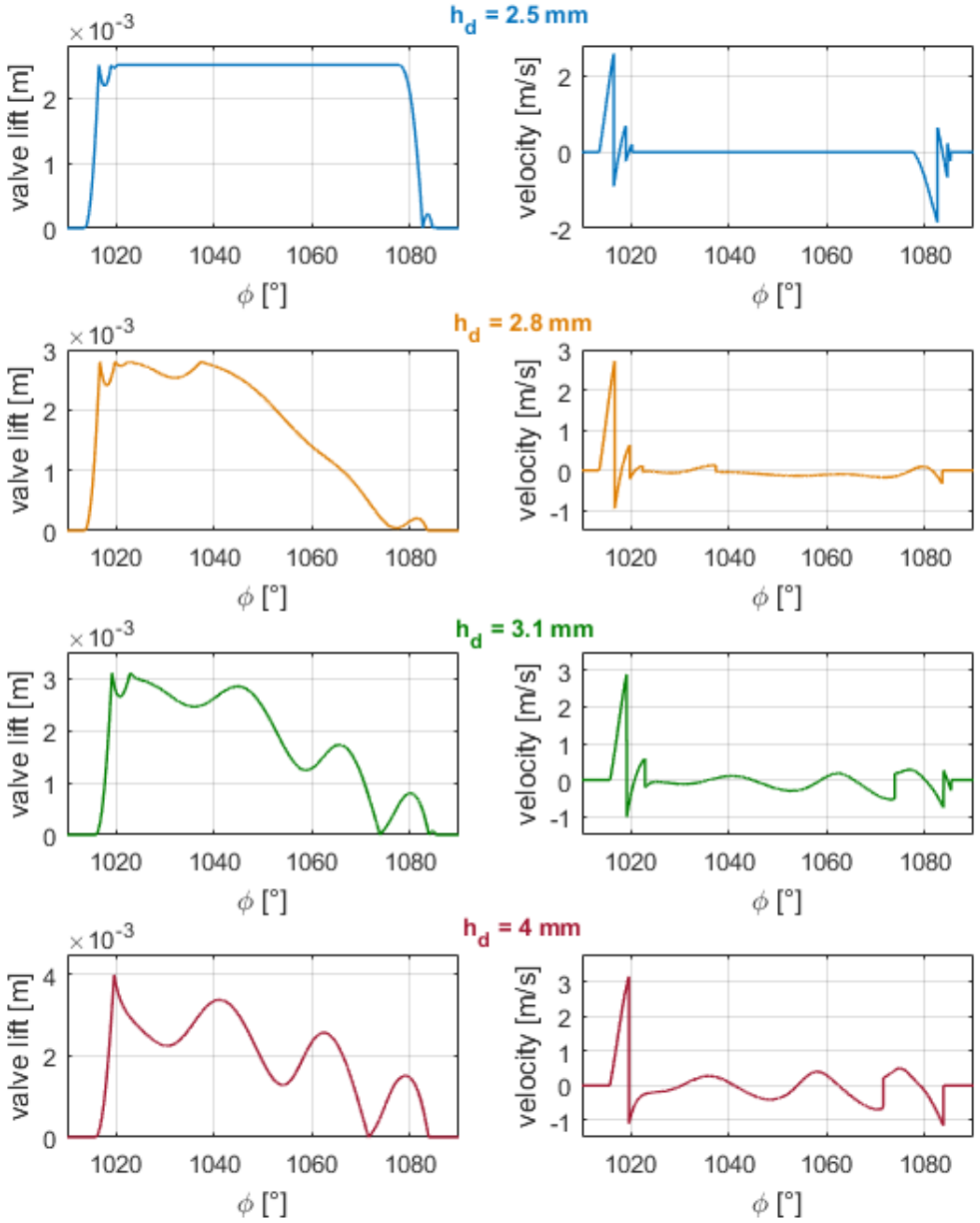

Figure 67 Valve movement under various maximum discharge valve lifts

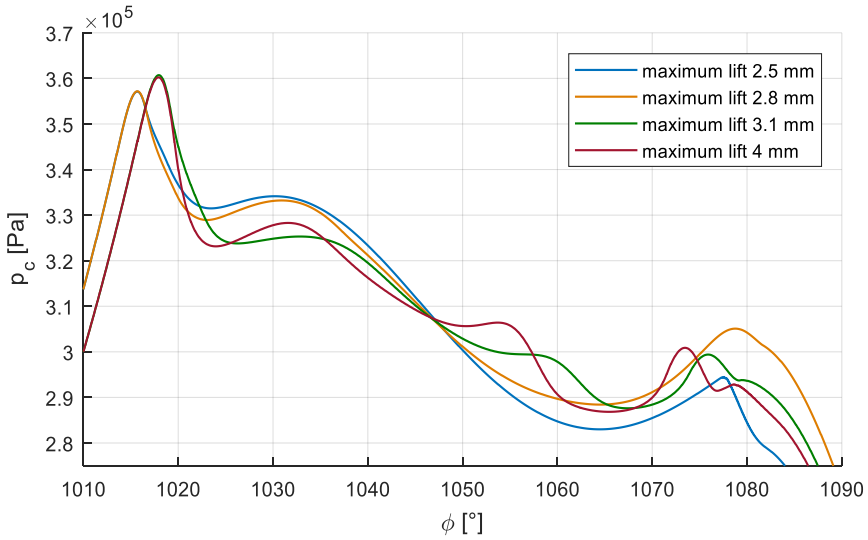

Figure 68 Pressure in the cylinder under various maximum discharge valve lifts – discharge phase

Conclusion

Considering the valves of the reciprocating compressor as a key component highly influencing the reliability as well as the efficiency of this type of compressor, and furthermore given the irreplaceability of these machines in applications throughout various industrial branches, it is imperative that the design of the valves and their behavior is pursued seriously. First and foremost, this thesis has been devoted to providing an elaboration of the phenomena by which the valve dynamics is constituted and the parameters which influence them, whilst the emphasis has been put on their qualitative assessment.

For the purpose of fulfilling the stated goals, a mathematical model describing the motion of compressor valves has been proposed. The introduced simplifying assumptions have been extensively discussed, factoring into their impact on the accuracy of results. This model has been afterwards implemented into a tool in the commercially available software known as MATLAB, utilizing the programming paradigm based on objects to maintain the versatility and customizability of the model. In the final analysis, besides the discussion of valve behavior under various design parameters, a deeper insight has been gained into the dependency of the mathematical model on experimentally-obtained coefficients.

Despite the fact that there are some limitations, mainly due to the restriction of the sealing element dynamics to one-dimension, the assumption of quasi-steady flow, etc. used heretofore, which do not permit, in the aftermath, the study of effects like unparalleled collisions or an extensive study of nonstationary behaviors, the model has the potential to be widely utilized; either in the very early stages of valve design development, or as a valuable tool to predict quantities, which are hard to measure such as impact velocities etc. This is also supported by the satisfactory agreement of the trends of valve plate motion with experimental data borrowed from the cited sources.

The modeling of valve dynamics is still a research subject and thus there are areas, in which further improvement would be welcomed. As an important matter for further study one can consider an alternative to the calculation of mass flow through valves on the basis of a flow coefficient, establishing the variation of the gas force with the flow or by considering unsteady effects at small valve openings.

References

1. ***Kompresory.*** [Online] 2012. [Citace: 12. 11 2016.] http://kke.zcu.cz/export/sites/kke/about/projekty/enazp/projekty/01_Stavba-a-provoz-stroju_1-3/1_IUT/002_Kompresory---Kolarcik-a-kol---P3.pdf.

2. Ninković, Dobrivoje and Taranović, Dragan and Pešić, Radivoje. ***Modelling Valve Dynamics and Flow in Reciprocating Compressors.*** [Online] 2013. [Cited: 11 15, 2016.] http://oaji.net/articles/2014/766-1398015561.pdf.

3. ***Compressor Valves and Unloaders for Reciprocating Compressors.*** [Online] 2002. [Cited: 11 12, 2016.] http://d-rco.com/techpapers/tp015.pdf.

4. Howes, Brian and Long, Bryan. ***Using Simulation of Reciprocating Compressor Valve Dynamics to Improve Economic Performance.*** [Online] [Cited: 2 5, 2017.] http://www.betamachinery.com/assets/pdfs/Technical_Articles/Using_Simulation_of_Reciprocating_Compressor_Valve_Dynamics_to_Improve_Economic_Performance.pdf.

5. Habing, R. A. ***Flow and Plate Motion in Compressor Valves.*** [Online] 2005. [Cited: 10 4, 2016.] http://doc.utwente.nl/50744/1/thesis_Habing.pdf. ISBN 90-365-2179-3.

6. Stetefeld, R. ***Els- und Kalteerzeugungsmaschinen.*** Stuttgart : s.n., 1901.

7. Hirsch, M. ***Die Kaltemaschine.*** Berlin : Springer, 1932.

8. Lanzendörfer, E. ***Strömungsvorgange und Bewegungsverhaltnisse bei Druckventilen schnell-laufender Kompressoren.*** s.l. : Z. VDI 76, 1932.

9. Costagliola, M. ***The theory of spring-Loaded Valve for Reciprocating Compressor.*** s.l. : Journal of Applied Mechanics 17 415-20, 1950.

10. Pereira, Evandro L. L. and Dechamps, Cesar J. and Ribas, Fernando A. ***Numerical Analysis of Heat Transfer inside the Cylinder of Reciprocating Compressors in the Presence of Suction and Discharge Processes.*** [Online] 2010. [Cited: 10 5, 2016.] http://docs.lib.purdue.edu/cgi/viewcontent.cgi?article=2994&context=icec.

11. ***Study of the Effective Flow Area of Compressor Plate Valve .*** [Online] 1994. [Cited: 11 5, 2016.] http://docs.lib.purdue.edu/cgi/viewcontent.cgi?article=1976&context=icec.

12. Touber, Simon. ***A Contribution to the Improvement of Compressor Valve Design.*** [Online] 1976. [Cited: 9 2016, 10.] http://repository.tudelft.nl/islandora/object/uuid:4c12fa64-32c6-4fd5-9ebc-e733621c96ac/datastream/OBJ/view.

13. Böswirth, L. Flow Forces and the Tilting of Spring Loaded Valve Plates - Part I. [Online] 1980. [Cited: 11 8, 2016.] http://docs.lib.purdue.edu/cgi/viewcontent.cgi?article=1329&context=icec.

14. Tuhovcak, Jan and Hejčík, Jiří and Jícha, Miroslav. ***Modelling fluid flow in a reciprocating compressor*** . [Online] 2015. [Cited: 12 5, 2016.] http://www.epj-conferences.org/articles/epjconf/pdf/2015/11/epjconf_efm2014_02100.pdf.

15. ***Experiences with Simulation of Reciprocating Compressor Valve Dynamics.*** **Howes, Brian and Lin, Leonard and Zacharias, Val. Calgary,** Canada : International Pipeline Conference — Volume 2, ASME1996, 1996. IPC1996-1904.

16. Bloch, Heinz P. and Hoefner, John J. ***Reciprocating Compressors: Operation & Maintenance.*** Houston : Gulf Professional Publishing, 1996. ISBN-0080515940, 9780080515946.

17. Tierean, Mircea Horia and Baltes, Liana Sanda. ***Design of Valves Used in Reciprocating Compressors*** . [Online] [Cited: 11 12, 2016.] ISBN: 978-960-474-140-3.

18. Mechanical Engineering Site. ***Reciprocating Compressor basic parts.*** [Online] [Cited: 11 15, 2016.] http://www.mechanicalengineeringsite.com/reciprocating-compressor-basic-parts/.

19. ***Burckhardt Poppet Valve™.*** [Online] Burckhardt Compression AG. [Cited: 2 12, 2017.] http://www.burckhardtcompression.com/service/components/compressor-valves/poppet/

20. Maclaren, J.F. T. and Kerr, S.V. and Tramschek, A. B. and Sanjines, A. ***A Model of a Single Stage Reciprocating Gas Compressor Accounting for Flow Pulsations.*** [Online] [Cited:12,7,2016] http://docs.lib.purdue.edu/cgi/viewcontent.cgi?article=1111&context=icec

21. ***Deviations from Ideal Gas Law Behavior.*** [Online] Bodner Research Web. [Cited: 2 1, 2017.] http://chemed.chem.purdue.edu/genchem/topicreview/bp/ch4/deviation.php.

22. ***Ideal Gas Law*** . [Online] The Engineering ToolBox. [Cited: 2 1, 2017.] http://www.engineeringtoolbox.com/ideal-gas-law-d_157.html.

23. Tuhovcák, Ján and Hejčík, Jiří and Jícha, Miroslav. ***Heat Transfer Analysis in the Cylinder of Reciprocating Compressor.*** [Online] 2016. [Cited: 12 28, 2016.] http://docs.lib.purdue.edu/cgi/viewcontent.cgi?article=3408&context=icec.

24. Thermodynamics and Propulsion. ***Control volume form of the conservation laws .*** [Online] Massachusetts Institute of Technology. [Cited: 10 3, 2016.] http://web.mit.edu/16.unified/www/FALL/thermodynamics/notes/node19.html.

25. ***Mass and Energy Balance of Unsteady-flow Processes.*** [Online] [Cited: 10 25, 2016.] https://ecourses.ou.edu/cgi-bin/ebook.cgi?doc=&topic=th&chap_sec=04.5&page=theory.

26. Anon. ***Simulation of a reciprocating compressor, Application study (PACE analog computer).*** Long Beach, N.J., U.S.A. : Electronic Associates Inc., 1963. 11-4-la.

27. Mechanics Lecture Notes. ***Notes for lecture 9 and 10: Momentum and Impulse.*** [Online] [Cited: 2 8, 2017.] http://www.damtp.cam.ac.uk/user/stcs/courses/mechanics/lecturenotes/L9_L10.pdf.

28. Müllner, Thomas. ***Flow Patterns and Valve Dynamics in Multi-Valve Reciprocating Compressors.*** [Online] 2015. [Cited: 3 2, 2017.] https://publik.tuwien.ac.at/files/PubDat_244144.pdf.

29. Pizarro-Recabarren, Rodrigo Adrian and Barbosa, Jader Jr. and Deschamps, Cesar J. ***Modeling the Stiction Effect in Automatic Compressor Valves.*** [Online] 7 16, 2012. [Cited: 12 5, 2016.] http://docs.lib.purdue.edu/cgi/viewcontent.cgi?article=3043&context=icec.

30. Khalifa, H. E. and Liu, X. ***Analysis of Stiction Effect on the Dynamics of Compressor Suction Valve.*** [Online] 1998. [Cited: 12 28, 2016.] http://docs.lib.purdue.edu/cgi/viewcontent.cgi?article=2220&context=icec.

31. Fleming, J.S. and Tramschek, A.B. and Abdul-Husain, J.M.H. Comparison of Flow and Pressure Distribution in Simple Valves Using Different Computational Methods. [Online] 1988. [Cited: 11 28, 2016.] http://docs.lib.purdue.edu/cgi/viewcontent.cgi?article=1606&context=icec.

32. Bráblík, J. ***Gas pulsations as a factor affecting operation of automatic valves in reciprocating compressors.*** s.l. : International Compressor Conference, Purdue, 1972. p. 188.

33. Olver, J. ***Nonlinear Ordinary Differential Equations.*** [Online] 2012. [Cited: 1 10, 2017.] http://www-users.math.umn.edu/~olver/am_/odz.pdf.

34. ***ode45.*** [Online] [Cited: 12 20, 2016.] https://www.mathworks.com/help/matlab/ref/ode45.html#outputarg_y.

35. ***Ordinary Differential Equation Solvers ODE23 and ODE45.*** [Online] [Cited: 4 15, 2017.] https://blogs.mathworks.com/cleve/2014/05/26/ordinary-differential-equation-solvers-ode23-and-ode45/#a495083d-5d4a-4fac-afbc-768444430751.

36. Ashino, Ryuichi and Nagase, Michihiro and Vaillancourt, Rémi. Behind and Beyond the MATLAB ODE Suite. [Online] Division of Mathematical Sciences, Osaka Kyoiku University, Kashiwara, 1 2000. [Cited: 4 15, 2017.] https://www.wire.tu-bs.de/docs/lehre/veranstaltungen/uebungen/ode1_ws05/MatlabODESuite.pdf.

37. Smith, Eric D. and Szidarovszky, Ferenc and Karnavas, William J. and Bahill, A. Terry. ***Sensitivity Analysis, a Powerful System Validation Technique.*** [Online] [Cited: 12 27, 2016.] http://citeseerx.ist.psu.edu/viewdoc/download?doi=10.1.1.149.4781&rep=rep1&type=pdf

38. ***Special suction lines influencing the volumetric efficiency of reciprocating compressors.*** Jaspers, H. A. Madrid : s.n., 1967. Proc. XII Int. Congr. Refrig. Madrid, paper 3.54.

39. Upfold, R.W. Designing Compressor Valves to Avoid Flutter. [Online] 1972. [Cited: 4 20, 2017.] pp. 400-406..

40. ***Compressor Valves.*** [Online] CPI. [Cited: 11 5, 2016.] http://c-p-i.com/en/compressor-valves/.

41. Guerra, Christopher J. and Kolodziej, Jason R. ***A Data-Driven Approach for Condition Monitoring of Reciprocating Compressor Valves*** . [Online] [Cited: 10 5, 2016.] http://gasturbinespower.asmedigitalcollection.asme.org/article.aspx?articleid=1770088.

42. Affonzo, Luis Octavio Amaral. ***Machinery Failure Analysis Handbook: Sustain Your Operations and Maximize Uptime.*** s.l. : Elsevier, 2013. ISBN-9780127999821.

43. Heat and Mass Transfer Technological Center . ***Fluid Structure interaction .*** [Online] Universitat Politècnica de Catalunya, Barcelona. [Cited: 4 2, 2017.] http://www.cttc.upc.edu/research/node/77.

44. Reciprocating Compressor Valves: Design. [Online] Dott. Ing. Mario Cozzani Srl. [Cited: 4 14, 2017.] http://www.cozzani.com/capabilities/design/.

A Default Compressor Setup

Here we state the default input parameters, with which the simulation tool was tested and which were used in the qualitative comparison of our results with others. Since we did not find the exact parameters needed for our simulator in any of the cited conference proceedings, from which we used the experimental results, we employed data from various other sources to arrive at admissible values.

Ideal gas			
heat capacity ratio	κ	1.4	$[-]$
ideal gas constant	r	287.1	$[Jkg^{-1}K^{-1}]$
Crank mechanism			
connecting rod length	L	0.18	$[m]$
cylinder diameter	D_c	0.12	$[m]$
clearance length	z_0	0.01	$[m]$
angular velocity of the crankshaft	ω	31.4	$[rad\ s^{-1}]$
radius of the crankshaft	R	0.045	$[m]$
Suction valve			
spring preload deflection	$x_{0,s}$	0.01	$[m]$
maximum valve plate lift	h_s	0.00125	$[m]$
spring stiffness	k_s	13	$[Nm^{-1}]$
mass (plate with equivalent of spring)	m_s	0.015	$[kg]$
valve plate diameter	$D_{v,s}$	0.036	$[m]$
valve port diameter	$D_{p,s}$	0.034	$[m]$
coefficient of restitution	$c_{r,s}$	0.5	$[-]$
friction coefficient	$c_{f,s}$	3.2	$[Nsm^{-1}]$
flow coefficient	α_s	0.65	$[-]$
Discharge valve			
spring preload deflection	$x_{0,d}$	0.005	$[m]$
maximum valve plate lift	h_d	0.00125	$[m]$
spring stiffness	k_d	125	$[Nm^{-1}]$
mass (plate with equivalent of spring)	m_d	0.018	$[kg]$
valve plate diameter	$D_{v,d}$	0.038	$[m]$
valve port diameter	$D_{p,d}$	0.036	$[m]$
coefficient of restitution	$c_{r,d}$	0.4	$[-]$
friction coefficient	$c_{f,d}$	2.8	$[Nsm^{-1}]$
flow coefficient	α_d	0.7	$[-]$

Suction piping system			
static pressure in steady-state reservoir	p_{s0}	100000	$[Pa]$
static temperature in the reservoir	T_{s0}	293.15	$[K]$
volume of the suction chamber	V_s	0.0008	$[m^3]$
effective length of the suction pipe	L_s	1	$[m]$
effective cross-sectional area of the pipe	A_s	0.0003	$[m^2]$
loss coefficient in the suction pipe	ξ_s	1	$[-]$
Discharge piping system			
static pressure in steady-state reservoir	p_{d0}	300000	$[Pa]$
static temperature in the reservoir	T_{d0}	350	$[K]$
volume of the discharge chamber	V_d	0.002	$[m^3]$
effective length of the discharge pipe	L_d	1	$[m]$
effective cross-sectional area of the pipe	A_d	0.00035	$[m^2]$
loss coefficient in the discharge pipe	ξ_d	1	$[-]$
Adhesion			
surface tension	γ_{LG}	0.012	$[Nm^{-1}]$
meniscus contact angle	β	7.5	$[°]$
oil film thickness	h_{film}	$5 \cdot 10^{-7}$	$[m]$

The values of the variables pertaining to the suction and discharge piping systems are chosen from the source [12]. The variables relating to adhesion are chosen in accordance with [29]. Regarding the variables, which refer to the crank mechanism and valves, they are mainly chosen according to the source [12]. The clearance length is derived from the source [14]. Among the values, for which we decided to use estimated ones and for which we could not find in any cited source are the preload deflection for the spring and loss coefficients in the pipes.

B Content of the DVD

Folder / File	*Description*
bin	The bin folder contains the files of the developed tool.
defaultParameters.m	This file contains the default input parameters for the compressor model.
ReciprocatingCompressor_app.mlapp	This is the GUI of the application.
ReciprocatingCompressor_class.m	This is the compressor class.
runTool.m	This file can be used to run the simulation without GUI.
GUI_assets	The *GUI_assets* subfolder contains the pictures included in the GUI.
logo_UWB.png	The logo of the University of West Bohemia in Pilsen
Compressor.png	The schematic drawing of the compressor.
Valve.png	The schematic drawing of the compressor valve.
Results	The *Results* subfolder contains the results of performed simulations as well as configuration and parameters of the corresponding compressor.
doc	The *doc* folder contains a copy of this thesis.
Master_Thesis_Michal_Volf.pdf	The *PDF* version of this thesis
Master_Thesis_Michal_Volf.docx	The *DOCX* version of this thesis